

Groundwater Modelling

Table of Contents

11.I.1		1
	11.I.1.1 Background	1
	11.I.1.2 Objective	5
	11.I.1.3 Scope of Work	6
11.1.2	2 HYDROGEOLOGY	6
	11.I.2.1 Surface Terrain and Drainage	7
	11.I.2.2 Geology	7
	11.I.2.2.1 Upland Areas	7
	11.I.2.2.2 Lowland Areas	11
	11.I.2.2.3 Permafrost	11
	11.I.2.3 Groundwater Flow	11
	11.I.2.4 Recharge	19
	11.I.2.5 Hydraulic Conductivity	19
	11.I.2.6 Tunnel	22
	11.I.2.7 Co-Disposal Facility	22
11.1.3	3 CONCEPTUAL MODEL	23
11.I.4	3D NUMERICAL MODEL CONSTRUCTION	25
	11.I.4.1 Model Approach	25
	11.I.4.2 Code Selection and Description	25
	11.I.4.3 Model Grid and Domain	25
	11.I.4.4 Model Layering and Surfaces	28
	11.I.4.5 Groundwater Flow Boundaries	30
	11.I.4.6 Model Parameterization	32
	11.I.4.6.1 Recharge	32
	11.I.4.6.2 Hydraulic Conductivity	32
	11.I.4.6.3 Porosity and Storage	34
11.1.5	5 MODEL CALIBRATION	34
11.I. C	6 PREDICTIVE MODEL (MINING) SIMULATIONS	38

11.I.i





	11.I.6.1 Mi	ne Progression	38
	11.I.6.2 Pr	edictive Model Boundaries	42
	11.I.6.3 Es	timated Mine Inflows and Groundwater Removal	42
	11.I.6.4 Pc	tential Drawdown Due To Active Mining	44
	11.I.6.5 Pc	st-Closure	47
	11.I.6.6 Pc	tential Reduction in Discharge to Waterbodies	47
11.1.7	ASSES	SMENT OF DENSITY DEPENDENT FLOW AND POTENTIAL SALINE UPWELLING	53
	11.I.7.1 Mo	odelling Approach	53
	11.I.7.2 Mo	odel Assumptions	54
	11.I.7.3 Nu	Imerical Cross-Section Location and Mesh Geometry	54
	11.I.7.4 Ma	aterial Properties	57
	11.I.7.5 Bc	undary Conditions	57
	11.I.7.5.1	Flow Boundaries	57
	11.I.7.5.2	Transport Boundaries	61
	11.I.7.6 Ini	tial Conditions	64
	11.I.7.7 Mo	odel Results and Discussion	64
	11.1.7.7.1	2D Model Heads	64
	11.1.7.7.2	TDS Concentration of Groundwater Seepage Entering the Open Pit	64
	11.1.7.7.3	Open Pit Capture Zone	64
	11.1.7.7.4	Density Dependent Flow versus Non-Density Dependent Flow	69
	11.1.7.7.5	Potential Convection Currents	69
11.1.8	B SUMM	ARY	72
11.1.9	REFER	ENCES	73

TABLES

Table 11.I.1-1: Background Data and Key Technical References	4
Table 11.I.2-1: Groundwater Level Data	14
Table 11.I.2-2: Surface Water Flow Data	18
Table 11.I.4-1: Model Assumptions	26
Table 11.I.4-2: Morphometric Data for Lakes	30
Table 11.I.4-3: Summary of 3D Groundwater Model Input Parameters	32



Report No. 09-1373-1004

Table 11.I.5-1: Calibrated Model Groundwater Flow Budget	. 37
Table 11.I.6-1: Simulated Groundwater Removal Due To Mining Operations	. 43
Table 11.I.6-2: Simulated Pre-Mine, Active Mining, and Post-Closure Groundwater Flow Budget	.49

FIGURES

Figure 11.I-1: Study Area	2
Figure 11.I-2: Local Site Detail and Proposed Infrastructure	3
Figure 11.I-3: Topography and Drainage	8
Figure 11.I-4: Bedrock Geology Map	9
Figure 11.I-5: Borehole Locations	
Figure 11.I-6: Inferred Groundwater Elevation	
Figure 11.I-7: Bedrock Hydraulic Conductivity Testing Results	
Figure 11.I-8: Overburden Hydraulic Conductivity Results	21
Figure 11.I-9: Conceptual Model Section	
Figure 11.I-10: Finite Element Mesh and Model Domain	
Figure 11.I-11: Combined Topography and Bathymetry Surface (Top of Layer 1)	
Figure 11.I-12: Model Boundary Conditions	
Figure 11.I-13: Recharge Distribution	
Figure 11.I-14: Simulated Water Table (Calibrated Model)	
Figure 11.I-15: Head Calibration Plot	
Figure 11.I-16: Flow Calibration Plot	
Figure 11.I-17A: Mine Progression – Open Pit	
Figure 11.I-17B: Mine Progression – Underground Workings	
Figure 11.I-18: Simulated Groundwater Removal Due to Mining Operations	
Figure 11.I-19: Simulated Water Table Drawdown Due To Mining	
Figure 11.I-20: Simulated Water Table Post-Closure (Pit Lake at 260 masl)	51
Figure 11.I-21: Simulated Water Table Drawdown Post-Closure (Pit Lake at 260 masl)	
Figure 11.I-22: 2D Section Model Location	
Figure 11.I-23: 2D Model Finite Element Mesh	
Figure 11.I-24: 2D Model Material Properties	
Figure 11.I-25: 2D Model Boundaries	
Figure 11.I-26: Equivalent Freshwater Heads	
Figure 11.I-27: Measured TDS Concentration Profiles	62

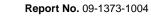


Report No. 09-1373-1004

Figure 11.I-28: 2D Model Transport Boundaries	63
Figure 11.I-29: Groundwater Heads for 2D Model Simulations 1 and 2	65
Figure 11.I-30: TDS Concentration Profiles Following End of Mining Simulation	66
Figure11.I- 31: Simulated Average Concentration of TDS in Groundwater Seepage Entering Pit	67
Figure 11.I-32: Simulated Groundwater Elevations and Capture Zone of Pit at End of Mining	68
Figure 11.I-33: TDS Concentration Profile at 1000 Years Following End of Mining	70
Figure 11.I-34: Head Profile at 1000 Years Following End of Mining	71









11.I.1 INTRODUCTION

11.I.1.1 Background

This report describes the numerical groundwater modelling undertaken for the Fortune Minerals Limited (Fortune) NICO Project site (the site). Fortune proposes to mine a cobalt-gold-bismuth-copper deposit using underground and Open Pit techniques. The site is located about 160 kilometres (km) northwest of Yellowknife in the Northwest Territories (NWT) (see Figure 11.I-11 for study area and Figure 11.I-2 for site detail).

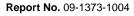
Golder Associates Ltd. (Golder) was retained by Fortune in 2009 to provide an assessment of mining impacts from the proposed NICO Project on groundwater in the NICO area. This includes the compilation of relevant background information for the site, the development of a conceptual hydrogeological model of the NICO area and regional surroundings, and the completion of detailed calculations and modelling to assess the groundwater conditions associated with the proposed mine.

The Mackenzie Valley Review Board (MVRB) has outlined the information required for the NICO Project environmental assessment in a Terms of Reference (MVRB 2009). According to the Terms of Reference, Fortune must predict potential impacts on groundwater flows in the NICO Project area, in particular, the water quality and quantity of final effluent discharged to the environment during all phases of the NICO Project life cycle, incorporating predicted changes over time in the amount or quality of mine water outflows. Furthermore, the Terms of Reference call for a relatively comprehensive understanding of the groundwater flow system, how it relates to the overall water budget and how it may be affected by the proposed mining operations. The following measures of impact are examined in this report: potential drawdown and reduction in discharge to surface waterbodies.

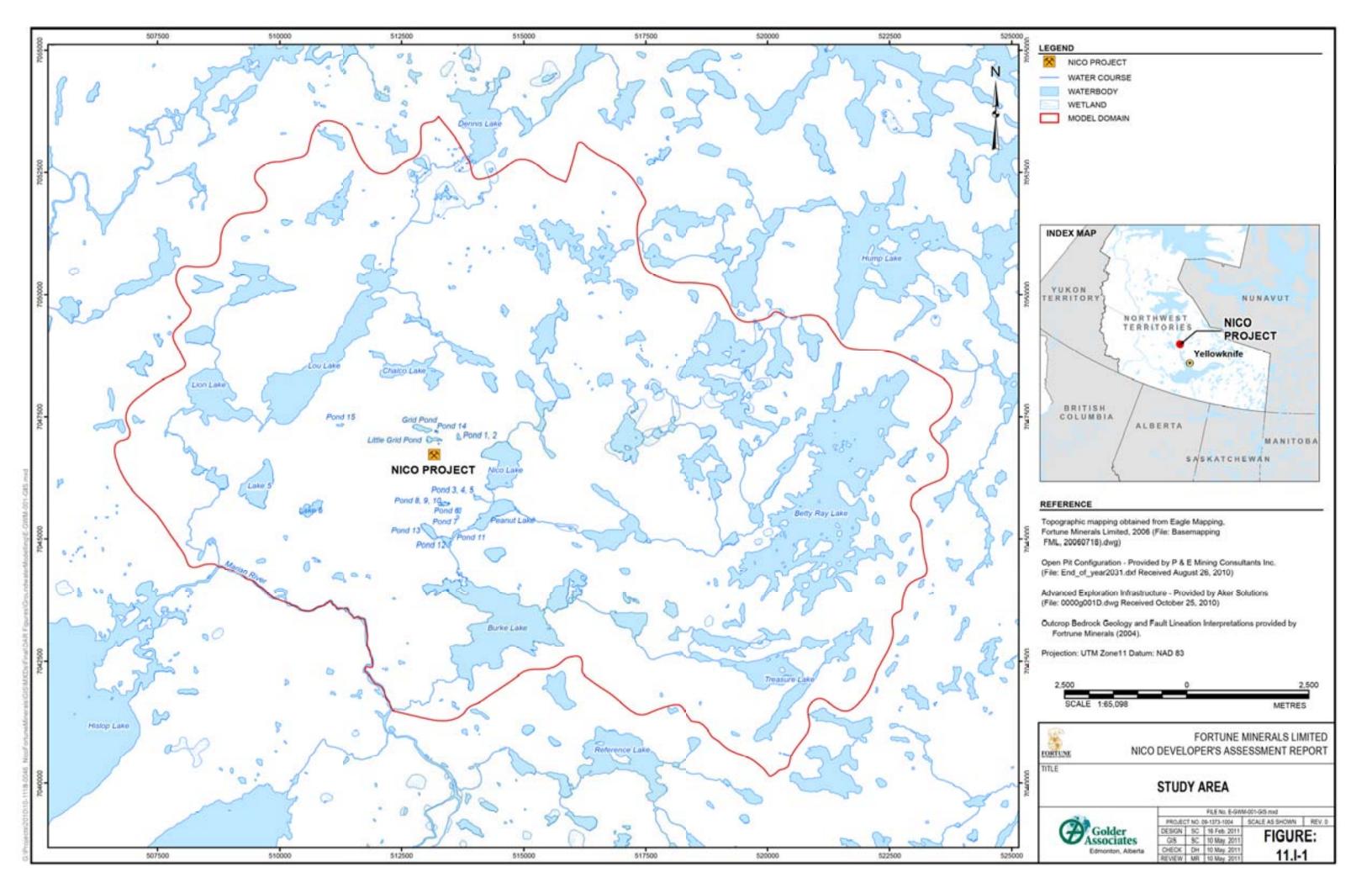
Background data and key references utilized in support of this groundwater modelling project are summarized in Table 11.I.1-1.

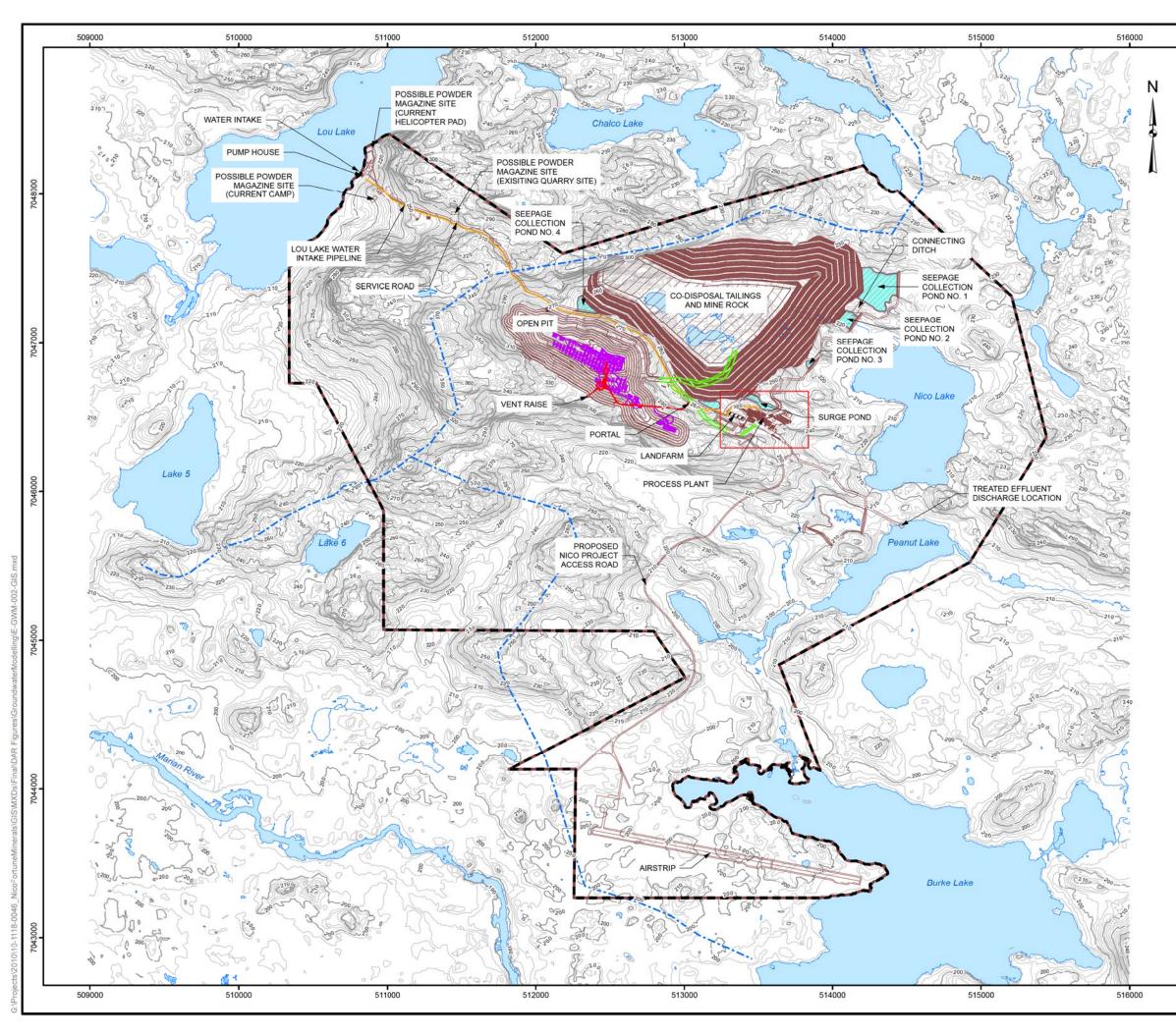












1	LEGEND						
LOU LAKE WATER INTAKE PIPELINE							
	HAUL ROAD						
	SERVICE ROAD						
	SEEPAGE DAM						
	REGIONAL WATERSHED BOUNDARY						
7048000	PROJECT LEASE BOUNDARY						
704	EXISTING PORTAL AND TUNNEL						
	PROPOSED UNDERGROUND WORKINGS						
	WATERCOURSE						
	CONTOUR - (2 m INTERVAL)						
	CONTOUR - (10 m INTERVAL)						
	PROPOSED INFRASTRUCTURE						
7047000							
7047							
SEEPAGE COLLECTION/SURGE POND							
8							
7046000							
0	REFERENCE						
-Topographic mapping obtained from Eagle Mapping, Fortune Minerals Limited, 2006 (File: Basemapping (FML, 20060718).dwg)							
	-Open Pit Configuration - Provided by P & E Mining Consultants Inc.						
	(File: End_of_year2031.dxf Recieved August 26, 2010)						
	-Advaced Exploration Infrastructure - Provided by Aker Solutions (File: 0000g001D.dwg Recieved October 25, 2010)						
	-Projection: UTM Zone11 Datum: NAD 83						
000							
7044000							
	SCALE 1: 25,000 METRES						
	FORTUNE MINERALS LIMITED NICO DEVELOPER'S ASSESSMENT REPORT						
	TITLE						
000	LOCAL SITE DETAIL AND PROPOSED INFRASTRUCTURE						
7043000							
FILE No. E-GWM-002-GIS.mxd PROJECT NO. 09-1373-1004 SCALE AS SHOWN REV. 0							
1	Golder Associates DESIGN SC 16 Feb. 2011 GIS SC 10 May. 2011 FIGURE:						
	Edmonton, Alberta CHECK DH 10 May. 2011 REVIEW MR 10 May. 2011 11.I-2						

Background Data	Source
Regional topographic mapping and site DEM.	Fortune Minerals Limited (2006). File: Basemapping (FML, 20060718).dwg (Eagle Mapping), and Atlas of Canada.
Bathymetric data for Grid Pond, Little Grid Pond, Nico Lake, Peanut Lake, Burke Lake, Reference Lake, and Ponds 8, 9, 10, 11, 12, and 13.	Draft Report On Aquatic Baseline Report for the Proposed NICO Project. 08-1373-0011. 2000. Submitted to Fortune Minerals. September 2010.
66 site borehole logs.	Technical Memorandum – Re: DOC 078 – Groundwater Quality at the NICO Project – Summary of Results of Groundwater Quality Monitoring Conducted in 2004 and 2009. 08-1118-0043 (4360). Submitted to Fortune Minerals. 8 February 2010.
Thermistor data at 9 wells.	Technical Memorandum – Re: Monitoring Update – August 2008, Thermistor Strings and Piezometers NICO Site, North West Territories. 05-1117-032. Submitted to Fortune Minerals. 17 October 2008.
Measured groundwater levels for site wells and potentiometric surface maps.	Factual Report On Geotechnical and Hydrogeological Investigations For The Proposed Open Pit And Underground Mine Workings, NICO Deposit, North West Territories. 03- 1117-029. Submitted to Fortune Minerals Limited. February 2005.
Packer testing data and analysis.	Factual Report On Geotechnical and Hydrogeological Investigations For The Proposed Open Pit And Underground Mine Workings, NICO Deposit, North West Territories. 03- 1117-029. Submitted to Fortune Minerals Limited. February 2005.
Measured surface water flows.	Golder field measurements of seasonal flows 2005 to 2008. Golder (2009). Draft Report On Baseline Hydrology for the Proposed NICO Mine Project. 08-1373-0017.2000. Submitted to Fortune Minerals Ltd. January 2009.
Tunnel inflow.	Rough estimation made in field.
TDS vs. depth data for Canadian Shield.	Hydrogeological Modeling of Mining Operations At The Diavik Diamonds Project. Proceedings of the Sixth International Symposium on Environmental Issues and Waste Management in Energy and Mineral Production, University of Calgary, Calgary, Alberta.
Technical Reference	Relevance to Modelling Work
Mackay, J.R. (1962). Pingos of the Pleistocene Mackenzie Delta Area. Geographic Bulletin, No. 18, p. 21- 63.	Discusses heat conduction beneath northern lakes, and, specifically, provides equations describing the relationship between depth of unfrozen ground beneath the lake and the depth and area of the lake itself. This information was utilized in conceptualizing the presence or absence of permafrost beneath the lakes within the model domain.
Koshinsky, G.D. (1970). The Morphometry of Shield Lakes In Saskatchewan. Limnology and Oceanography, Vol. 15, Issue 5, p. 695-701.	Presents morphometric data for 68 lakes on the Precambrian Shield in Saskatchewan. The area vs. depth relationships discussed in this report informed model assumptions regarding bathymetry of lakes with no depth data.

Table 11.I.1-1: Background Data and Key Technical References





Technical Reference	Relevance to Modelling Work
Kuchling, K., Chorley, D., Zawadski, W. (2000). Hydrogeological Modeling of Mining Operations At The Diavik Diamonds Project. Proceedings of the Sixth International Symposium on Environmental Issues and Waste Management in Energy and Mineral Production, University of Calgary, Calgary, Alberta.	Provides a plot of TDS vs. depth from a number of sources including the Diavik site, Lupin mine, and previously published data (Frape and Fritz, 1987). This data was consulted in constructing the 2D model to determine if saline upwelling would be a significant issue for the NICO mine.
Golder (2005). Factual Report On Geotechnical and Hydrogeological Investigations For The Proposed Open Pit And Underground Mine Workings, NICO Deposit, North West Territories. 03-1117-029. Submitted to Fortune Minerals Limited. February 2005.	Details some of the basic geologic and hydrogeologic conceptualization developed for the model, including major geologic units. The report also contains borehole logs and static water levels for 65 site wells, and summarizes hydraulic conductivity data for rock types based on packer testing at 3 site wells (NICO-03-281, NICO-03-282 and NICO-03-283).
Golder (2007). Report On NICO Tailings Dams and Process Plant Facilities 2006 Geotechnical Site Investigation. 05-1117-032 (9100). Submitted to Fortune Minerals Limited. April 16, 2007. 1117-032. Submitted to Fortune Minerals Limited. April 2007.	Contains borehole logs and grain size analysis for 7 boreholes that encountered overburden in the valley areas; much of the overburden conceptualization utilized in the model was derived from this data. Shallow bedrock hydraulic conductivity data is also presented. Further, initial thermistor data and commentary on permafrost is included.
Golder (2007). Final Summary Report On Open Pit, Underground and Mine Waste, Geotechnical Engineering Studies And Environmental Baseline Data Collection For NICO Project, Fortune Minerals, Northwest Territories. 05- 1117-032. Submitted to Fortune Minerals Limited. April 2007.	Supports much of the conceptualization provided in the February 2005 report mentioned above. The report also presents initial estimates of pit and underground seepage, based on analytical methods. Lastly, the study details mine waste management and tailings facility design.
Golder (2008). Technical Memorandum – Re: Monitoring Update – August 2008, Thermistor Strings and Piezometers NICO Site, North West Territories. 05-1117- 032. Submitted to Fortune Minerals. October 17, 2008.	Asserts the absence of permafrost in the hill areas and the presence of discontinuous permafrost in the low-lying valley areas. Also provides hydrographs of groundwater levels at select wells.
Golder (2009). Draft Report On Baseline Hydrology for the Proposed NICO Mine Project. 08-1373-0017.2000. Submitted to Fortune Minerals Ltd. January 2009.	Provides recharge and surface water flow data.
Golder (2010). Technical Memorandum – Re: DOC 078 – Groundwater Quality at the NICO Project – Summary of Results of Groundwater Quality Monitoring Conducted in 2004 and 2009. 08-1118-0043 (4360). Submitted to Fortune Minerals. February 8, 2010.	Provides 3 detailed cross-sections of the proposed open pit area.
Golder (2010). Draft Report On Aquatic Baseline Report for the Proposed NICO Project. 08-1373-0011. 2000. Submitted to Fortune Minerals. September 2010.	Includes bathymetry mapping for Grid Pond, Little Grid Pond, Nico Lake, Peanut Lake, Burke Lake, Reference Lake, and Ponds 8, 9, 10, 11, 12, and 13. The data used to interpolate these maps is used in the groundwater model surface generation.

Table 11.I.1-1: Background Data and Key Technical References (continued)

11.I.1.2 Objective

This appendix is a technical document for the NICO Project. The objectives of the groundwater modelling assessment are to estimate the proposed NICO Project's effects on the local and regional groundwater flow systems. Specifically, the following items are addressed:

Drawdown: The potential groundwater level drawdown induced from mine dewatering/depressurization over the life of the mine and post-closure is modelled.





- Reduction in Baseflows: The potential decrease in groundwater discharge to waterbodies surrounding the mine is calculated.
- Inflow Rates to the Active Mine: Groundwater inflow estimates over the life of the mine are calculated.
- Evaluate Potential for Upwelling of Deeper Saline Water: The modelling evaluates the potential for saline upwelling during mining.

11.I.1.3 Scope of Work

To meet the above objectives, the following tasks were undertaken:

- 1) A review of groundwater information collected in the NICO Project area. This includes background reports, regional mapping, borehole logs, groundwater levels, packer testing, grain size analysis, thermistor data, surface water flows, and tunnel inflows (see Table 11.I.1-1).
- 2) Development of a conceptual hydrogeological model. The conceptual hydrogeological model synthesizes the knowledge of the site and regional surroundings into a system with specified inflows, outflows, sources, sinks, groundwater flow patterns, major hydrostratigraphic units, and boundaries.
- 3) Selection of modelling software. Based on the key components of the conceptualization and the objectives of the modelling (see above), an appropriate modelling tool was chosen.
- 4) Model construction. A 3-dimensional (3D) numerical model was constructed based on the conceptual model. To assess saline upwelling, a 2-dimensional (2D) model was derived from the 3D construct.
- 5) Model calibration. The 3D model was calibrated to measured groundwater levels, surface water flows, and tunnel inflows.
- 6) Predictive simulations. The 3D model was modified to include the Open Pit and underground workings over the mine life. Transient simulations allow prediction of groundwater levels and inflow rates over time as the mine progresses. In addition, the 2D model assesses the potential for saline upwelling during mining.

This hydrogeological modelling appendix is organized as follows: Section 11.I.2 summarizes hydrogeologic findings for the site and regional surroundings pertinent to the modelling. Section 11.I.3 synthesizes this information into a conceptual model of the hydrogeologic system. Section 11.I.4 details the construction of the 3D model. Section 11.I.5 describes the model calibration to field data. Section 11.I.6 discusses the 3D predictive simulations and results, including an analysis of mine inflows, drawdown, and groundwater baseflow reduction. Section 11.I.7 describes the 2D modelling completed to assess the potential for saline intrusion to the mine. Finally, Section 11.I.8 summarizes the findings of the modelling assessment.

11.I.2 HYDROGEOLOGY

May 2011

This section provides an overview of the pre-mining hydrogeological conditions of the site and regional surroundings. Much of the following information has been presented in previous reporting (see Table 11.I.1-1). However, for completeness, and to provide a basis for the current modelling conceptualization (Section 11.I.3), a brief description is given of key aspects of the hydrogeologic system and important data utilized in model construction/calibration.





11.I.2.1 Surface Terrain and Drainage

The study area topography and drainage is shown on Figure 11.1-3. Ground elevations within the study area range from 190 metres above sea level (masl) to 370 masl. The majority of the study area consists of low-lying, densely wooded swampy terrain with a significant number of small to large lakes and streams ("lowlands areas"). In addition, the landscape features a significant number of distinct hills or "upland" areas. Most of these upland areas, scoured by the action of glaciers, have bedrock at surface, and are sparsely vegetated. The NICO Project lies on one of these upland features.

11.I.2.2 Geology

A bedrock surface geology map of the area is provided on Figure 11.I-4. Subsurface geological data (borehole logs) are generally in the vicinity of the proposed Open Pit area (see borehole locations on Figure 11.I-5). Therefore, much of the geologic interpretation implemented in the model is inferred from site data and applied at a regional scale. To simplify the regional interpretation, the geology within the model domain is divided based on the following distinct topographic settings: 1) upland areas, and 2) lowland areas.

11.I.2.2.1 Upland Areas

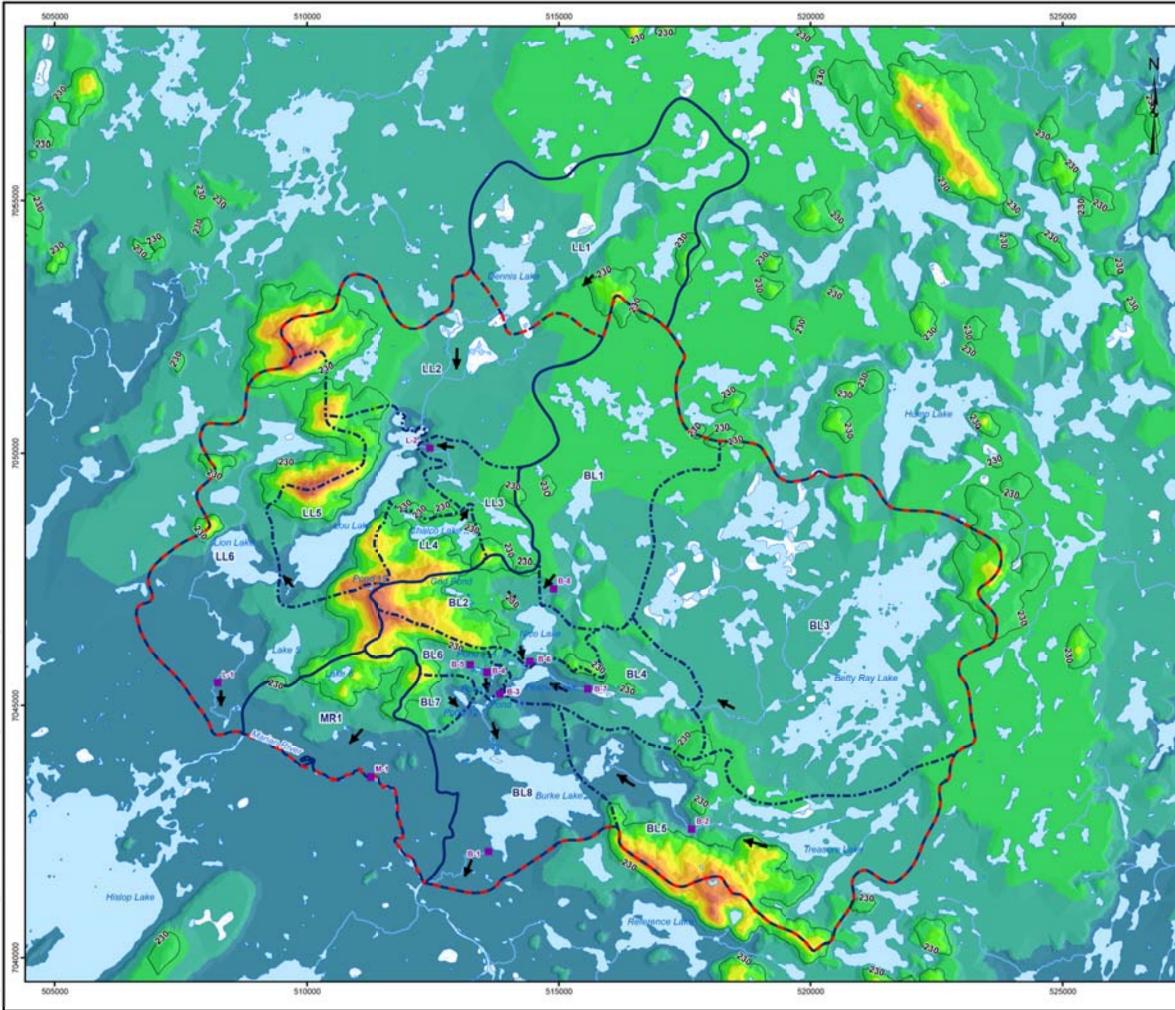
The upland areas (defined as those areas with elevations greater than 230 masl; see Figure 11.I-3), are generally comprised of fractured rock outcrop at surface, low permeability bedrock at depth and an absence of permafrost throughout.

The NICO site is located within an upland area. The NICO deposit is situated in Snare Group meta-sedimentary rocks comprised of siltstone, impure dolomite, subarkosic wacke, and arenite. These strata are interpreted to dip 50° to 80° towards 030°. The sedimentary rocks are overlain by Faber Lake Group volcanic rocks of rhyolitic to rhyodacitic composition. The sedimentary rocks are intruded by quartz-feldspar porphyry and feldspar-porphyry dykes. The ore deposit is found mainly in ironstone sedimentary units that containing iron rich biotite and amphibole, magnetite, hematite, and feldspar with some chlorite and carbonate, referred to as "black rock schist." Geotechnical logging indicates that the site is typically comprised of Good Quality rock, with localized exceptions including Fair and Very Good rock intervals, based on the Q-System (Golder 2005).



May 2011





	G		

	WATERCOURSE
-	MAJOR DRAINAGE BOUNDARY
	SUB-DRAINAGE BOUNDARY
	CONTOUR - 230 MASL (DENOTES UPLANDS VS LOWLAND AREAS)
\rightarrow	SURFACE WATER FLOW DIRECTION
	WATERBODY
1	WETLAND
6.5	MODEL DOMAIN

SURFACE WATER FLOW STATION

ELEVATION (M)

5	360
1.000	340
	320
	300
	280
	260
	240
	220
	200
	180



FORTUNE TITLE

Base data obtained from - NTDB (National Topographic Database)
 1: 50k Topograpic Map Sheets (Map Sheet No. - 085J, 085K, 085N, 085O
 and 086C)

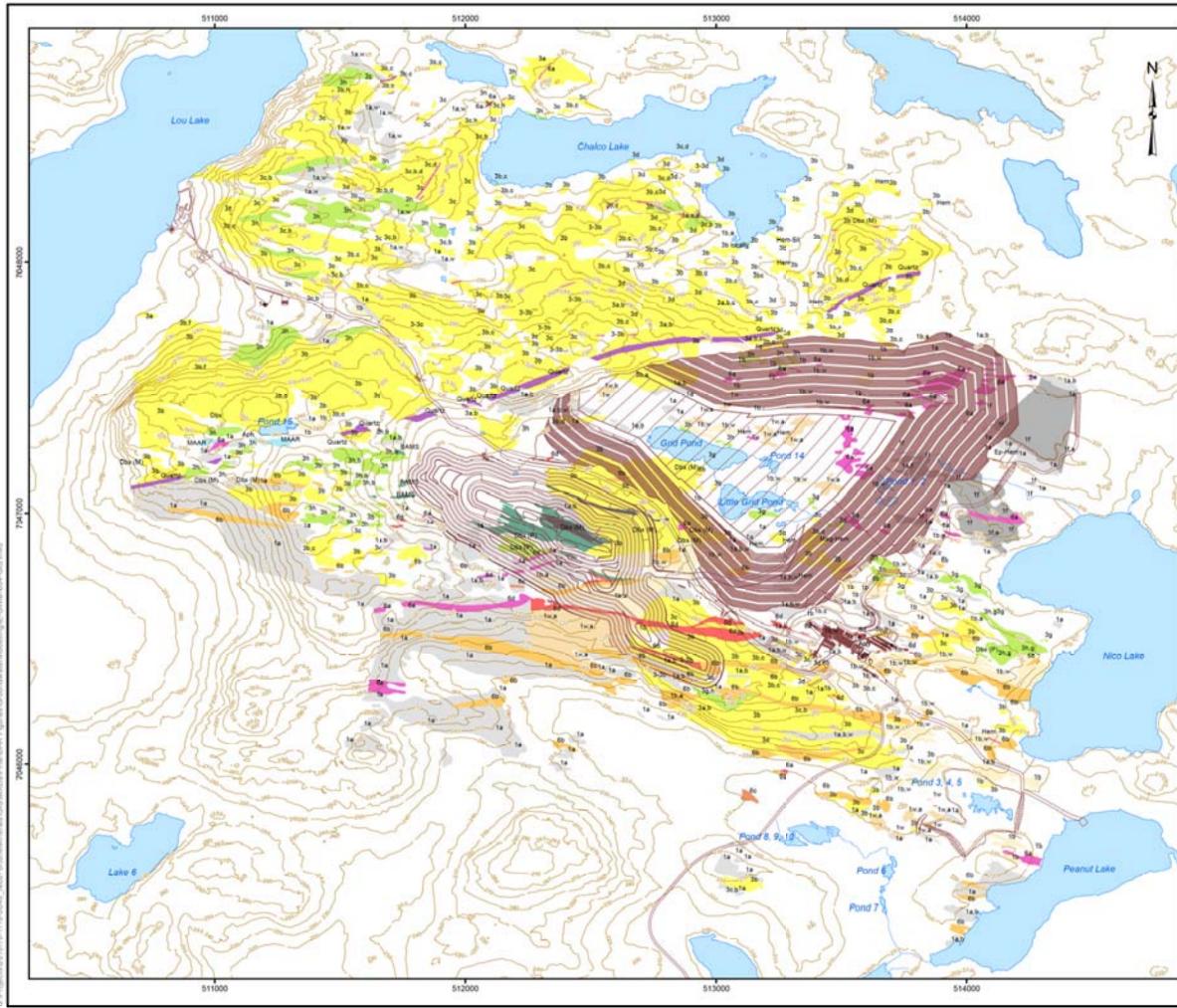
Projection: UTM Zone11 Datum: NAD 83



FORTUNE MINERALS LIMITED NICO DEVELOPER'S ASSESSMENT REPORT

TOPOGRAPHY AND DRAINAGE

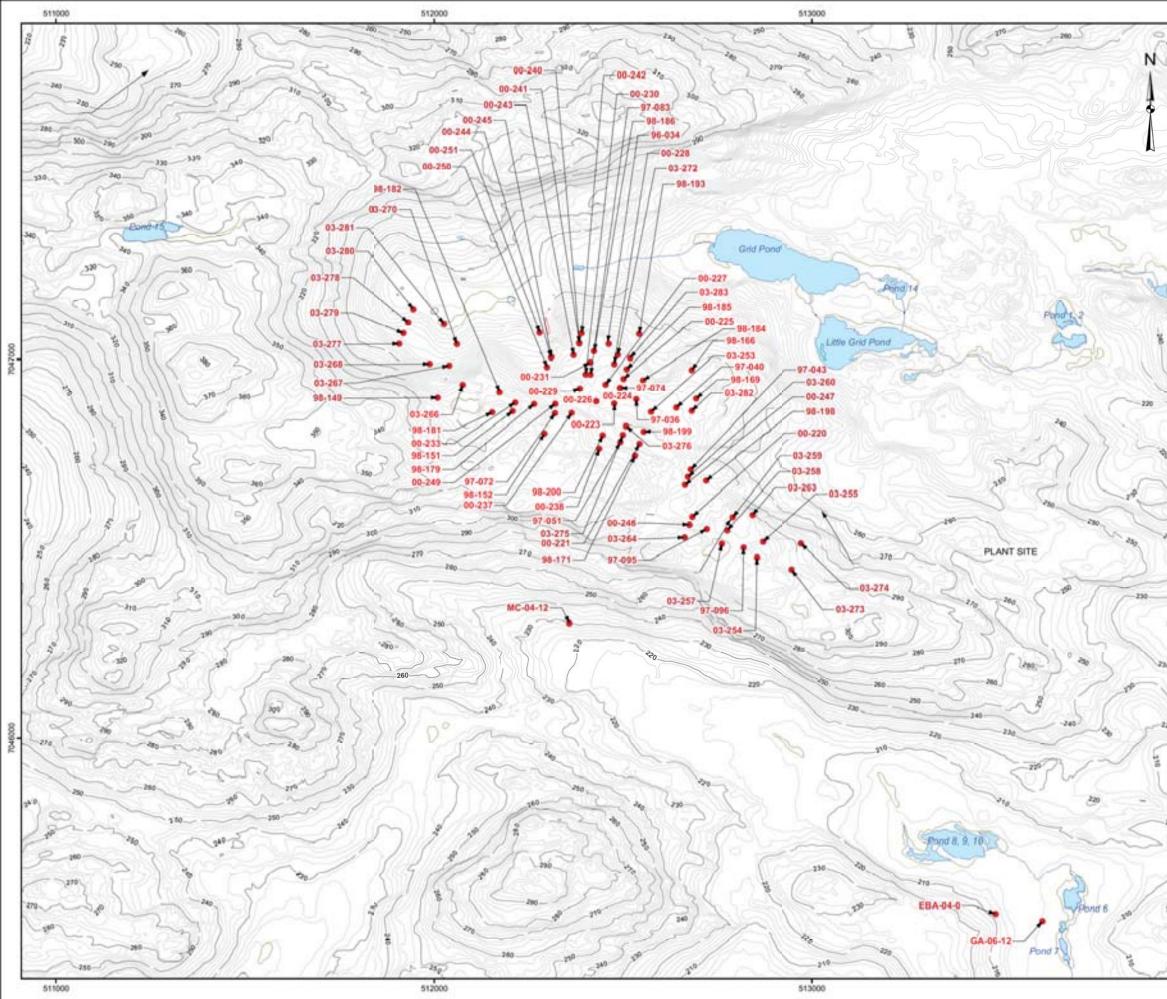
in the second	FILE No. E-GWM-003-GIE med								
0	PROJEC	TNO.	89-1373-1004	SCALE AS SHOWN	REV.0				
Golder	DESIGN	50	16 Feb. 2011	FIGURE:					
Associates	Q5	SC	10 May 2011						
Edmonton, Alberta	CHECK	DH	10 May 2011	4410					
	REVIEW	MR	10 May. 2011	11.1-3					



LEGEND WATERCOURSE CONTOUR - (10 m INTERVAL) WATERBODY GEOLOGY 15 SUBARKOSIC ARENITE 11 CORDIERITE SCHIST 1a SILTSTONE 1w SUBARKOSIC WACKE 3h.g HETEROLITHIC BRECCIAS, DEBRIS FLOW 3a, 3b, 3c, 3d 6a FELDSPAR PORPHYRY 6b QUARTZ-FELDSPAR PORPHYRY 6c QUARTZ PORPHYRY 6d FLEDSPAR-AMPHIBOLE PORPHYRY QUARTZ VEINING BIOTITE-AMPHIBOLE-MAGNETITE SCHIST MAAR MAAR BRECCIA UNKNOWN REFERENCE -Topographic mapping obtained from Eagle Mapping. Fortune Minerals Limited, 2006 (File: Basemapping (FML, 20060718).dwg) - Geology obtained from Fortune Minerals Limited (2005) -Open Pit Configuration - Provided by P & E Mining Consultants Inc. (File: End_of_year2031.dxf Recieved August 26, 2010) -Advaced Exploration Infrastructure - Provided by Aker Solutions (File: 0000g001D.dwg Recieved October 25, 2010) -Projection: UTM Zone11 Datum: NAD 83 SCALE 1:15,000 METRES FORTUNE MINERALS LIMITED 65 NICO DEVELOPER'S ASSESSMENT REPORT FORTUNE TITLE

BEDROCK GEOLOGY MAP

	FILE No. E-GWM-004-GIS mid								
	PROJEC	T NO. (09-1373-1004	SCALE AS SHOWN	REV.0				
Golder	DE5IGN SC 16 Feb. 2011			FIGURE:					
Associates	Q5	SC.	10 May 2011	FIGUR	C :				
Edmonton, Alberta	CHECK	DH	10 May 2011	4414					
22 K C C C C C C C C C C C C C C C C C C	REVIEW	MR	10 May 2011	11.1-	4				



LEGEND

WATERCOURSE CONTOUR - (2M INTERVAL)

CONTOUR - (10M INTERVAL)

WATERBODY

. BOREHOLE LOCATION

NOTE

 Borehole location based on collar; note that the well bore itself may be on an angle, (see Report On NICO Tailings Dams and Process Plant Facilities 2008 Geotechnical Site Investigation (Golder, April 2007) and Factual Report On Geotechnical and Hydrogeological Investigations For The Proposed Open Pit And Underground Mine Workings, NICO Deposit, North West Territories (Golder, February 2005) for borehole log details.

REFERENCE

-32

EORTAINE

 Topographic mapping obtained from Eagle Mapping, Fortune Minerals Limited, 2006 (File: Basemapping (FML, 20060718).dwg)

-Projection: UTM Zone11 Datum: NAD 83



FORTUNE MINERALS LIMITED NICO DEVELOPER'S ASSESSMENT REPORT

BOREHOLE LOCATIONS

	FLENis E-GWM-005-G/B.mat								
()	PROJEC	T NO. 0	9-1373-1004	SCALE AS SHOWN	REV.0				
Golder	DESIGN	SC	16 Feb. 2011	FIGUR	E.				
Associates	GIS	SC	10 May. 2011	FIGUR	E:				
Edmonton, Alberta	CHECK	DH	10 May. 2011	441	-				
and the second second second	REVEW	MR	10 May. 2011	11.1-	D				

11.I.2.2.2 Lowland Areas

The lowland areas are defined as regions with elevations less than 230 masl (see Figure 11.I-3). The defining geologic characteristics of the lowland areas are variable thicknesses of overburden at surface and discontinuous permafrost at depth (where lakes are not present). The overburden consists of peat, topsoil, and organics followed by silty clay to clayey silt, and then glacial till. Measured thicknesses of overburden vary from 0.5 to 9.4 metres (m) (Golder 2007b).

The bedrock geology underlying the overburden in the lowland areas is variable; siltstone, rhyolite and wacke have been identified in the lowland cores near the NICO deposit (Golder 2007b). Regardless of the rock type, the bedrock material is usually described as slightly weathered at shallow depths, becoming increasingly strong to very strong with depth, and containing moderate to widely spaced fractures (Golder 2007b). From a hydraulic perspective, the shallow bedrock in the lowlands is consider to be, in essence, an extension of that found in the upland areas.

11.I.2.2.3 Permafrost

Based on field measurements, significant areas of discontinuous permafrost are inferred to be present in the lowland areas (Golder 2008). Thermistor measurements in 3 lowland wells (EBA-04-05, GA-06-07, and GA-06-11) indicate a permafrost thickness ranging from 29 to 76 m (average of about 50 m) with an active zone in the overburden ranging from 2 to 4 m.

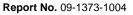
11.I.2.3 Groundwater Flow

Generally, groundwater flows radially outward from the topographic highs (considered recharge zones) to the lowland areas, where shallow groundwater is anticipated to report to streams and lakes (considered discharge zones) (see Figure 11.I-6). Average measured water level data for site wells is provided in Table 11.I.2-1.

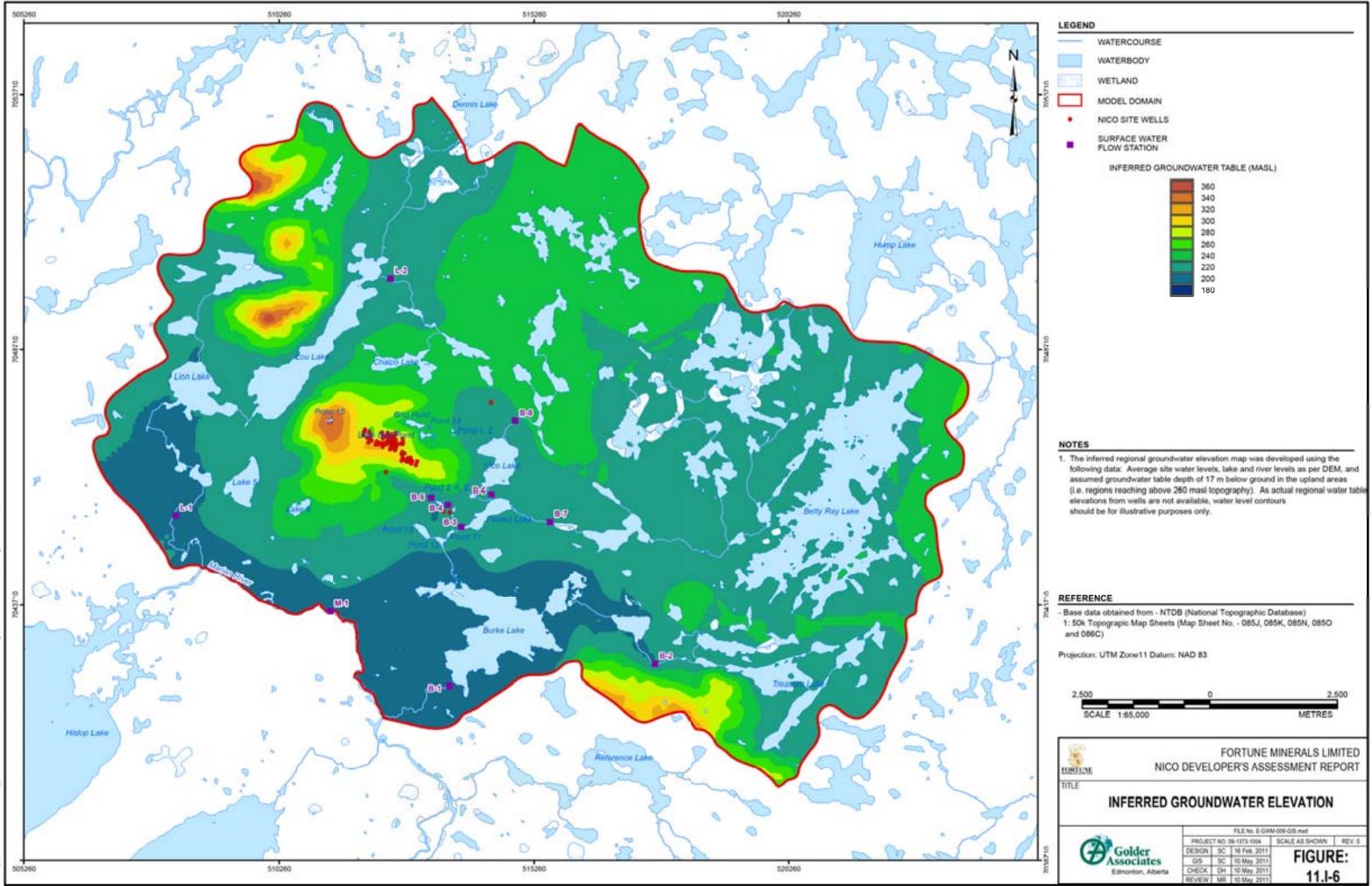
The majority of the measured water levels used to produce the inferred groundwater flow map (Figure 11.I-6) are limited to the NICO Project site. The measured water levels indicated that groundwater levels in the upland area range from 1 to 37 m below ground surface (average 17 m below ground), follow topography, and thus flow is roughly radial from the hill itself. As most of these water levels were measured in open exploratory boreholes, they are considered to be generally indicative of the water table elevation. It should be noted that the upper fractured zone (as defined in Section 11.I.3) is commonly not saturated.

As shown on Figure 11.I-6, groundwater elevations have been extrapolated beyond the existing site data. This extended regional interpretation was based on topographic elevations of the numerous lakes and streams in the lowland areas which are considered to be hydraulically connected to the groundwater system. Topographic maps are considered to provide a reasonable estimation of lake levels. In addition, the groundwater elevations in the remaining off-site upland areas were assigned to be 17 m below ground, based on the average measured water levels at the NICO Project site. Therefore, the water table elevations for the off-site upland areas shown on Figure 11.I-6 are inferred based on a generalized average condition. This should be recognized when examining this figure.









Lakes and streams in the lowland areas around the site are considered locations of groundwater discharge. Groundwater that discharges to waterbodies becoming surface water is referred to as baseflow. Figure 11.I-3 shows the location of lakes within the study area and surface water flow stations. Table 11.I.2-2 provides measured flow data for these stations (this measured flow includes both baseflow and other contributions from other sources such as direct precipitation and runoff).

As mentioned above, groundwater is generally considered to discharge to the lakes and streams within the lowland areas; however, a seep has been observed along the sides of the NICO hill "bowl" areas at elevations of roughly 240 to 250 masl.







Table 11.I.2-1: Groundwater Level Data

FEFLOW ID	Site / MOE ID	X NAD83 (Collar)	Y NAD83 (Collar)	Measuring Point X NAD83 (accounting for borehole angle)	Measuring Point Y NAD83 (accounting for borehole angle)	Average Measured Groundwater Elevation (masl)	Calculated Head (Calibrated Model)	Residual
1	00-220	512,683	7,046,585	512,682	7,046,582	286.5	279.2	-7.3
2	00-221	512,543	7,046,777	512,541	7,046,773	293.2	286.9	-6.3
3	00-244	512,310	7,047,005	512,307	7,046,999	276.5	275.7	-0.8
4	00-245	512,310	7,047,006	512,310	7,047,004	275.9	275.1	-0.9
5	00-249	512,320	7,046,883	512,318	7,046,877	298.2	287.5	-10.7
6	00-250	512,299	7,046,980	512,297	7,046,975	280.6	277.6	-2.9
7	00-251	512,279	7,047,071	512,278	7,047,068	266.7	265.9	-0.9
8	03-255	512,870	7,046,518	512,868	7,046,514	295.1	270.7	-24.4
9	03-257	512,761	7,046,512	512,760	7,046,512	295.6	275.4	-20.2
10	03-258	512,775	7,046,548	512,772	7,046,541	291.0	275.3	-15.6
11	03-266	512,075	7,046,933	512,072	7,046,926	296.3	283.8	-12.5
12	03-268	511,988	7,046,989	511,988	7,046,988	277.4	276.3	-1.1
13	03-274	512,971	7,046,513	512,966	7,046,502	276.5	264.4	-12.1
14	03-275	512,499	7,046,801	512,496	7,046,796	293.1	288.1	-5.1
15	03-277	511,908	7,047,041	511,907	7,047,038	274.6	275.3	0.7
16	03-278	511,931	7,047,098	511,929	7,047,092	265.9	269.6	3.7
17	03-279	511,919	7,047,069	511,918	7,047,066	270.7	271.7	1.0
18	03-280	511,945	7,047,133	511,945	7,047,132	261.7	265.7	3.9
19	03-281	512,026	7,047,094	512,025	7,047,092	261.0	262.9	2.0
20	97-095	512,721	7,046,551	512,718	7,046,543	288.1	277.2	-10.9
21	97-096	512,818	7,046,502	512,817	7,046,499	295.7	273.5	-22.1
22	98-149	512,010	7,046,899	512,009	7,046,897	304.4	289.0	-15.4
23	98-181	512,154	7,046,861	512,150	7,046,850	306.8	291.3	-15.6
24	98-199	512,554	7,046,809	512,554	7,046,809	292.9	285.8	-7.1





FEFLOW ID	Site / MOE ID	X NAD83 (Collar)	Y NAD83 (Collar)	Measuring Point X NAD83 (accounting for borehole angle)	Measuring Point Y NAD83 (accounting for borehole angle)	Average Measured Groundwater Elevation (masl)	Calculated Head (Calibrated Model)	Residual
25	EBA-04-0	513,486	7,045,535	513,486	7,045,535	202.0	204.6	2.6
26	GA-06-08	514,420	7,047,675	513,609	7,045,516	200.9	203.1	2.2
27	MC-04-12	512,358	7,046,304	512,358	7,046,304	227.4	232.2	4.8
28	00-223	512,477	7,046,884	512,473	7,046,873	291.3	285.8	-5.5
29	00-224	512,492	7,046,925	512,485	7,046,909	279.9	283.3	3.4
30	00-225	512,500	7,046,949	512,496	7,046,937	274.3	281.0	6.7
31	00-226	512,429	7,046,890	512,427	7,046,885	291.8	286.0	-5.8
32	00-227	512,454	7,046,934	512,448	7,046,922	278.1	283.1	5.1
33	00-228	512,476	7,046,988	512,472	7,046,978	273.8	277.9	4.1
34	00-229	512,386	7,046,923	512,380	7,046,906	282.8	285.0	2.2
35	00-230	512,401	7,046,961	512,396	7,046,947	278.9	281.5	2.6
36	00-231	512,413	7,046,992	512,409	7,046,982	276.7	278.2	1.6
37	00-233	512,214	7,046,886	512,210	7,046,874	298.7	288.7	-10.1
38	00-237	512,363	7,046,859	512,358	7,046,846	291.0	289.2	-1.8
39	00-238	512,436	7,046,764	512,433	7,046,753	296.4	290.6	-5.9
40	00-240	512,384	7,047,042	512,379	7,047,027	275.3	273.1	-2.2
41	00-241	512,384	7,047,043	512,381	7,047,033	276.4	272.5	-3.9
42	00-242	512,390	7,047,069	512,386	7,047,058	263.3	269.6	6.3
43	00-243	512,369	7,047,012	512,363	7,046,996	276.4	276.5	0.1
44	00-246	512,675	7,046,563	512,672	7,046,553	284.3	278.7	-5.5
45	00-247	512,663	7,046,669	512,655	7,046,651	277.1	281.2	4.2
46	03-253	512,574	7,046,862	512,573	7,046,860	277.0	283.3	6.3
47	03-254	512,854	7,046,476	512,843	7,046,455	276.9	272.7	-4.2
48	03-259	512,790	7,046,583	512,782	7,046,562	273.3	274.7	1.4
49	03-260	512,671	7,046,690	512,665	7,046,679	273.8	280.8	7.0

Table 11.I.2-1: Groundwater Level Data (continued)





FEFLOW ID	Site / MOE ID	X NAD83 (Collar)	Y NAD83 (Collar)	Measuring Point X NAD83 (accounting for borehole angle)	Measuring Point Y NAD83 (accounting for borehole angle)	Average Measured Groundwater Elevation (masl)	Calculated Head (Calibrated Model)	Residual
50	03-263	512,842	7,046,590	512,834	7,046,572	275.1	271.1	-4.0
51	03-264	512,662	7,046,530	512,656	7,046,515	285.4	277.0	-8.4
52	03-267	512,040	7,046,984	512,039	7,046,981	277.2	276.1	-1.1
53	03-270	512,060	7,047,041	512,059	7,047,038	265.5	267.7	2.1
54	03-272	512,485	7,047,011	512,482	7,047,003	275.9	275.1	-0.7
55	03-273	512,946	7,046,445	512,942	7,046,435	282.4	269.8	-12.6
56	03-276	512,508	7,046,824	512,507	7,046,822	290.7	287.0	-3.7
57	03-282	512,681	7,046,864	512,675	7,046,850	282.4	278.9	-3.5
58	03-283	512,518	7,047,003	512,514	7,046,996	273.0	275.1	2.1
59	96-034	512,462	7,047,041	512,471	7,047,066	266.2	268.3	2.1
60	97-036	512,535	7,046,896	512,531	7,046,885	277.4	283.6	6.2
61	97-040	512,641	7,046,873	512,641	7,046,873	276.1	279.9	3.9
62	97-043	512,679	7,046,710	512,679	7,046,710	277.7	279.9	2.2
63	97-072	512,320	7,046,858	512,314	7,046,844	294.4	289.8	-4.6
64	97-074	512,492	7,046,925	512,489	7,046,914	278.2	282.9	4.7
65	97-083	512,414	7,046,960	512,411	7,046,948	275.9	281.4	5.4
66	98-151	512,208	7,046,864	512,204	7,046,853	303.9	290.4	-13.5
67	98-152	512,292	7,046,805	512,288	7,046,795	306.5	293.0	-13.6
68	98-166	512,681	7,046,972	512,674	7,046,958	275.3	273.2	-2.0
69	98-169	512,693	7,046,897	512,690	7,046,888	276.5	276.7	0.2
70	98-171	512,532	7,046,746	512,527	7,046,731	290.2	287.6	-2.6
71	98-179	512,265	7,046,882	512,260	7,046,870	298.5	288.5	-10.0
72	98-182	512,174	7,046,914	512,170	7,046,903	299.1	285.9	-13.2
73	98-184	512,553	7,046,945	512,550	7,046,936	273.1	279.5	6.4
74	98-185	512,509	7,046,974	512,506	7,046,965	275.4	278.3	2.9

Table 11.I.2-1: Groundwater Level Data (continued)





FEFLOW ID	Site / MOE ID	X NAD83 (Collar)	Y NAD83 (Collar)	Measuring Point X NAD83 (accounting for borehole angle)	Measuring Point Y NAD83 (accounting for borehole angle)	Average Measured Groundwater Elevation (masl)	Calculated Head (Calibrated Model)	Residual
75	98-186	512,423	7,047,022	512,420	7,047,012	276.4	275.0	-1.3
76	98-193	512,542	7,047,068	512,539	7,047,060	258.5	267.1	8.6
77	98-198	512,719	7,046,680	512,715	7,046,670	273.9	277.5	3.6
78	98-200	512,446	7,046,800	512,442	7,046,790	290.8	289.8	-1.0
79	97-051	512,492	7,046,782	512,485	7,046,759	253.5	254.0	0.5
80	GA-06-12	513,609	7,045,516	514,420	7,047,675	213.9	229.6	15.8
81	10-291 (~80 mbgs)	512,051	7,047,177	512,022	7,047,168	255.5	260.9	5.4
82	10-291 (~177 mbgs)	512,051	7,047,177	511,990	7,047,156	248.7	266.7	18.1

Table 11.I.2-1: Groundwater Level Data (continued)

masl = metres above sea level; mbgs = metres below ground surface



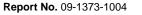




Table 11.I.2-2: Surface Water Flow Data

S	urface Water Flow Ga	auge Station	Info		Measured Field Data									Model Output			
Station	Description	Easting (NAD83)	Northing (NAD83)	Spring 2005 (m³/d)	Summer 2005 (m³/d)	Fall 2005 (m³/d)	Spring 2006 (m³/d)	Summer 2006 (m³/d)	Fall 2006 (m ³ /d)	Spring 2007 (m³/d)	Summer 2007 (m ³ /d)	Fall 2007 (m³/d)	Winter 2008 (m ³ /d)	Spring 2008 (m³/d)	Measured Minimum (m ³ /d)	Measured Maximum (m³/d)	Calibrated Model Simulated GW Baseflow (m ³ /d)
B-8	Nico Lake Inflow	514,890	7,047,313	3,223	415	613	9,677	233	276	657	432	78	NM	579	78	9,677	152
B-6	Nico Creek	514,426	7,045,878	9,858	2,618	691	15,094	924	760	5,944	2,359	354	NM	1,728	354	15,094	252
B-7	Peanut Lake Inflow	515,572	7,045,333	6,592	2,195	2,860	68,705	3,776	4,389	5,357	5,651	1,590	NM	769	769	68,705	353
B-3	Peanut Creek	513,832	7,045,233	21,686	5,858	5,651	72,032	7,880	4,968	16,295	13,556	2,912	3,102	4,441	2,912	72,032	536
B-4	Pond 8 Outlet	513,574	7,045,667	786	156	1,477	1,426	760	873	268	60	52	NM	43	43	1,477	157
B-5	Pond 10 Inlet	513,242	7,045,810	363	NM	769	1,192	328	320	251	225	9	NM	69	9	1,192	146
B-2	Burke Lake Inflow	517,630	7,042,551	11,284	328	631	13,824	130	3,344	302	389	17	NM	95	17	13,824	425
B-1	Burke Creek	513,607	7,042,119	55,642	804	4,977	119,595	6,074	6,601	1,598	19,570	1,331	5,797	2,635	804	119,595	1,355
L-2	Lou Lake Inflow	512,441	7,050,101	5,098	415	389	8,916	302	432	613	769	86	NM	1,866	86	8,916	139
L-1	Lou Creek	508,229	7,045,459	41,429	337	2,532	79,894	363	1,849	9,435	4,432	674	NM	12,191	337	79,894	623
M-1	Marian River	511,263	7,043,583	993,946	572,054	458,784	3,710,534	1,203,898	1,050,192	896,486	600,739	248,573	235,872	550,714	235,872	3,710,534	N/A ^a

Notes: See Figure 11.I-3 of report for flow gauge stations, catchment areas, and lake locations.

B-series and L-series stations listed in order of up to down gradient location where possible (see Figure 11.I-3).

"Baseflow" means groundwater discharge to a surface water receptor. The simulated baseflow listed in the table above corresponds to the simulated discharge at the station in question.

The **measured** field data flows may take into account a variety of sources including: direct precipitation, runoff, groundwater baseflow, evaporation etc., and may reflect variation caused by seasonal conditions (freeze, melt etc.). The **modelled** flows only account for groundwater baseflow over an averaged condition.

Baseflow separation from the measured field data was not possible due to complications caused by extensive beaver dams throughout the study area. Hence the low end of measured flows were considered as rough targets in the calibration process (see report Section 11.I.5). ^a The model only contains a small portion of the Marian River, as such simulated discharge was not compared to actual flow measurements during calibration (note the measured flows account for flow upstream of the model).

NM = not measured; GW = groundwater; m^3/d = cubic metres per day





11.I.2.4 Recharge

Meteorological data have been collected at the site from October 2004 to August 2008; however, the monitoring does not provide winter precipitation data. Consequently, regional data have been used to assess the precipitation conditions at the NICO Project. The closest meteorological station to the site is at Yellowknife. Average annual precipitation in the Yellowknife area is about 281 millimetres per year (mm/yr) (Annex G). Based on the precipitation inputs recorded at Yellowknife and based on the sufficial soils in the NICO study area, it is estimated that about 10 to 50 mm/yr infiltrates the ground and reaches the water table (Annex G).

11.I.2.5 Hydraulic Conductivity

Figure 11.I-7 and Figure 11.I-8 summarize hydraulic conductivity testing results completed at the NICO Project, including packer testing in the bedrock and grain size analysis results for overburden samples using Shepherd's Method (Shepherd 1989).

In general, the bedrock is relatively low hydraulic conductivity material, ranging from approximately 5E-6 metres per second (m/s) to 1E-10 m/s with a geometric mean of test results of 3E-8 m/s. While the correlation between hydraulic conductivity and test interval is not particularly strong, there does appear to be some decrease in permeability with depth.

The overburden material is generally silty till with occasional pockets of sand. Shepherd's Method has been used to estimate the hydraulic conductivity of the overburden based on available grain size curves (Golder 2007a) as follows:

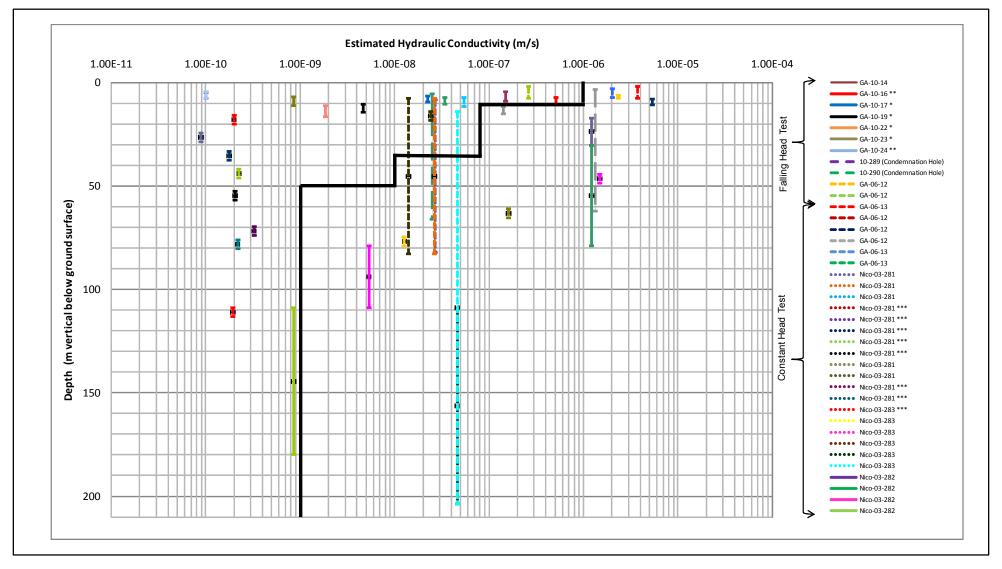
$$K = a(D_{50})^b$$

where D_{50} is the diameter of the 50 percentile grain size in mm, and a and b are empirical constants based on the soil type, considered to be 100 (feet per day) and 1.5, respectively, for this analysis. Based on an analysis of the grain size curves the hydraulic conductivity of the overburden ranges from 5E-4 m/s to 3E-8 m/s, with a geometric mean of 3E-6 m/s. [Note: sample MC-06-23 SA1 underwent analysis using Hazen's Formula due to its larger D50 (> 10 mm)].



May 2011



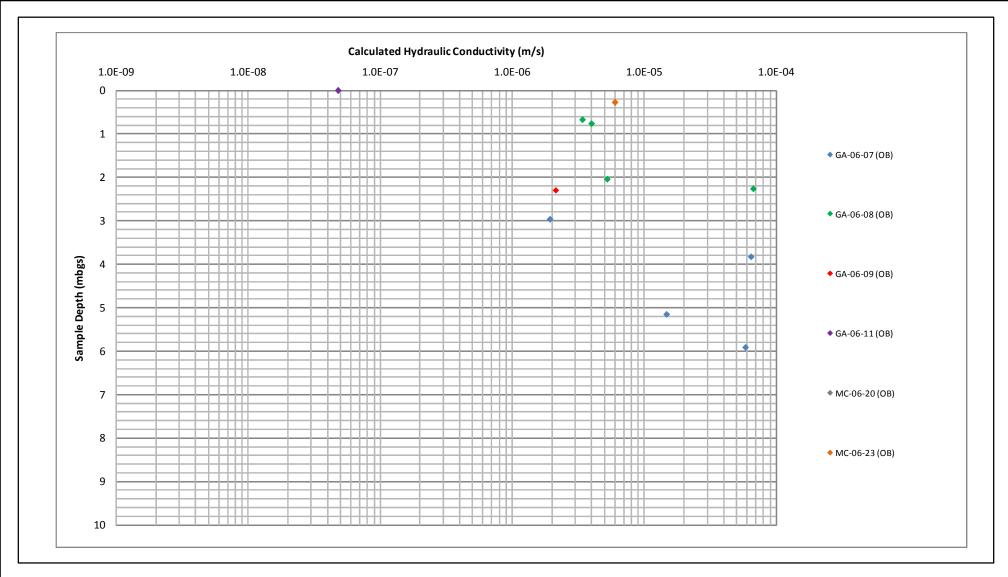


NOTE

- 2. ** The interval is either very tight rock or very tight rock and frozen. Result is not representative.
- 3. *** Value presented is an estimated Upper Bound on permeability.
- 4. Collar elevations and top of bedrock elevations vary considerably over the site due to hilly terrain. For example, the GA drillholes in the valley are collared at elevations considerably lower (70m or more lower) than the collars of Nico 03-282 and Nico-03-283 on the hill.
- 5. Thick black line represents hydraulic conductivity distribution in model



^{1. *} The test interval may occur in frozen rock, and result may not be representative.



NOTE

1. Hydraulic conductivity results derived from applying Sheperd's method to grain size analysis.



11.I.2.6 Tunnel

In 2006 and 2007 Fortune obtained a bulk sample from underground by excavating a decline tunnel with portal elevation at 253.5 masl to a final depth of about 105 masl (see Figure 11.I-2 for location of the as-built tunnel). The total length was approximately 1700 m, with a 5 m x 5 m cross-sectional dimension. The tunnel was actively dewatered during excavation (May to October 2006 and March to August 2007). Dewatering ranged from roughly <5 to 60 cubic metres per day (m^3/d), depending on the season (i.e., flows are highest during the freshet, and zero during frozen periods). Groundwater seepage to the tunnel was crudely estimated between 4 to 6 m^3/d during winter months. However, during the freshets in both 2006 and 2007, flows increased by about one order of magnitude, with crude estimates of inflow on the order of 50 m^3/d . The surge is attributed to surface water directed into the tunnel through the overlying fractured zone and/or through ungrouted drill holes.

Between the 2 mining periods and subsequent to mining, the tunnel was not dewatered. As a result, the water level in the tunnel rose between the 2 periods of mining then was pumped out before the second period of mining. Subsequent to discontinuation of mining in August 2007, the water level in the underground workings and decline tunnel rose to surface at the portal by July 2009, a period of just under 2 years. In August and September 2009, the water was pumped periodically from the portal area to control discharge flows while monitoring the quality of the water to be discharged. Since all of the monitoring results indicated that the water quality met discharge criteria, the mining inspector agreed that mine water could drain freely from the portal provided regular monitoring continued to demonstrate acceptable water quality. In May 2010, water was freely discharging from the portal in response to the spring freshet, but by June 2010 this had stopped and the water level was about 2 to 3 m below the point at which water would freely flow from the portal area.

Due to the lack of observed response in nearby boreholes, and the tight rock through which much of the tunnel is bored, the tunnel dewatering causes only a localized drawdown response. Only 1 borehole (97-051) has had water level similar to that of the underground workings, which is controlled by the portal discharge at about 260 m. Borehole 97-051, estimated to be within about 10 m of the underground workings, is considered to be in direct hydraulic connection with the underground workings, likely via a fracture.

11.I.2.7 Co-Disposal Facility

The Co-Disposal Facility (CDF), which will be comprised of Mine Rock and thickened tailings placed in layers and cells, will be located in the catchment area labelled BL2 on Figure 11.I-3.

For purpose of assessing the influence of Open Pit and underground mining on groundwater in the surrounding areas, and potential for reduction of base flow to nearby lakes and streams, the need to include the CDF was carefully considered as part of the conceptualization of the site hydrogeology. It was concluded that it was not necessary to include this facility in the 3-D hydrogeological model for the following reasons:

- the catchment basin will receive the same amount of recharge through infiltration with or without the CDF;
- surface diversion of runoff is not material to this model;
- the bottom of the CDF will lie on native materials; and
- the tailings will be thickened to the point that they will not bleed water prior to deposition.





The conclusion was that the CDF would not materially affect the hydrogeology of BL2 for purpose of the numerical model.

11.I.3 CONCEPTUAL MODEL

The conceptual model is the synthesis of the hydrogeologic information provided above, and forms the generalized framework behind the construction of the numerical model. Figure 11.I-9 shows a pictorial representation of the conceptual model, pre-mining.

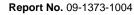
The model conceptualization has been divided into 2 main areas: 1) upland and 2) lowland. In summary, water recharges the system in the upland area and flows outward to the lowland areas where it may exit from seeps in the hillside, travel farther and discharge into lakes or streams, or continue in a deeper flow system and discharge at another lake or stream further downgradient. The recharge rates utilized in the model are derived from the climate data discussed in Section 11.I.2.4, and fine-tuned during calibration (discussed in Section 11.I.5).

The geology in the upland area consists of relatively high permeability fractured rock at surface and increasingly lower permeability rock with depth. No attempt has been made to differentiate among the different rock types in the model conceptualization and, ultimately, the numerical model because, in general, the bedrock hydraulic conductivity testing results do not appear to be related to geology. The hydraulic conductivity assignments of the rock layering with depth are derived from the testing data (see Section 11.I.2.5) and fine-tuned during calibration (discussed in Section 11.I.5).

The geology in the lowland area consists of relatively high permeability silt till at surface underlain by permafrost, which, in turn, is underlain by relatively low hydraulic conductivity bedrock. The lowland bedrock is considered an extension of the bedrock material found in the upland areas (see Figure 11.I-9). The majority of the overburden is frozen; however, there is an active zone through which groundwater flow is seasonally possible.

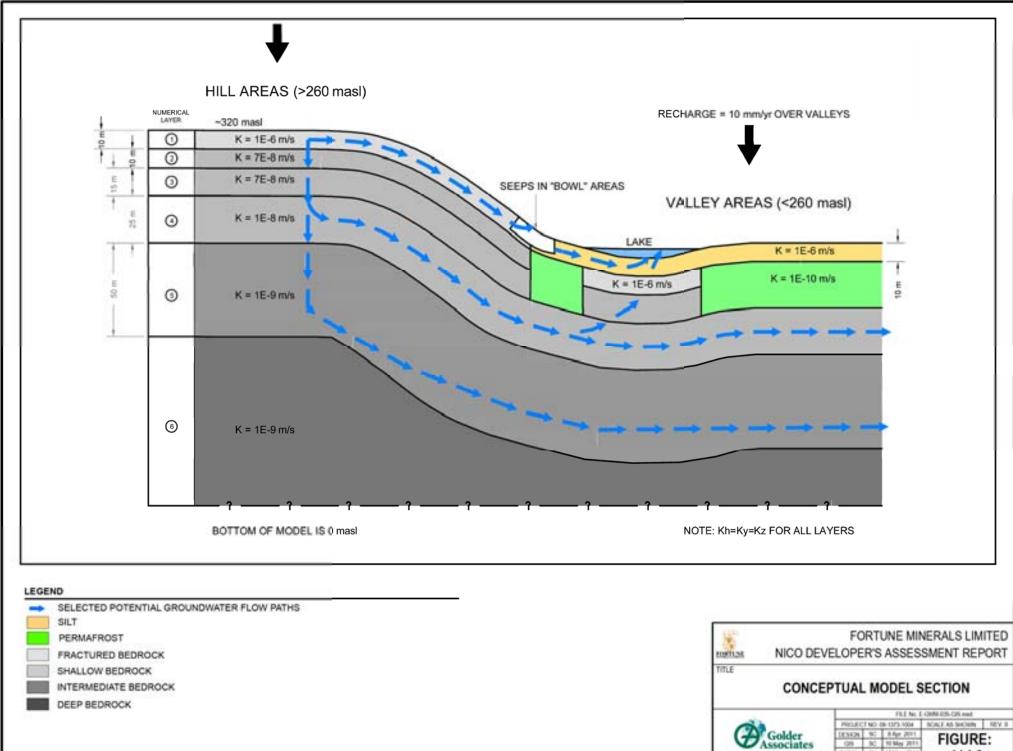
Exceptions to the configuration described above are lowland areas overlain by lakes. Here permafrost is not considered to exist because of thermal convection currents emanating from the lake itself. Mackay (1962) has developed a series of analytical equations that relate lake radius to depth of unfrozen material below the lake. For a lake of radius 200 m or greater (over 80% of waterbodies within the model domain are greater than this dimension), a ground temperature of -10 °C (twice as cold as the average air temperature at Yellowknife), a lake temperature of 2 °C and geothermal gradient of about 1 °C per 50 m, permafrost would be absent to depths of greater than 50 m (the ultimate depth of permafrost in the model).







```
0. Projects/2010/10-1118-0046_NooForuneMinerals/GIS/MXDvFinal/DAR Figures/GroundwaterModelling/E-GVM-035-GIS.mvd
```



CHECK (N 19 May 201

And in the local data

Edmonton, Alberte

11.1-9

11.I.4 3D NUMERICAL MODEL CONSTRUCTION

11.I.4.1 Model Approach

As described in Section 11.I.1.2, the objective of the current modelling assessment was to estimate the proposed NICO Project's effects on the groundwater flow system. The approach to the modelling was to initially construct and calibrate a 3D steady state numerical groundwater flow model to measured field data. Subsequent to calibration, the model was modified to account for the progression of the mine, and was simulated in a transient manner to model the effects of mining over time.

A summary of the assumptions used in this approach are provided in Table 11.I.4-1.

11.I.4.2 Code Selection and Description

The numerical finite element code FEFLOW (version 5.413, May 2010), was used to simulate the 3D groundwater flow of the NICO study area. FEFLOW is a multi-purpose 3D groundwater flow code developed by WASY GmbH, Berlin, Germany (Diersch 2002). The code is verified, well documented, and has been widely used for simulating regional groundwater flow systems.

FEFLOW was chosen for its ability to accomplish the following:

- efficiently discretize a large model domain;
- closely conform the model mesh to hydrologic features such as watershed boundaries, rivers, and the mine footprint;
- run a relatively seamless and more "realistic" simulation of the Open Pit geometry through time using unique time-variable boundary conditions at each node representing the mine; and
- easily produce 2D cross-sectional models from the 3D numerical model (as will be discussed in Section 11.I.7).

11.I.4.3 Model Grid and Domain

The model mesh and domain is shown on Figure 11.I-10. The extent of the model domain was based on watershed boundaries, as shown on Figure 11.I-3. Furthermore, the model was decidedly regional in scale in order to address the Terms of Reference requirements as described in Section 11.I.1. The advantage to having a model domain at this large scale is the avoidance of potential boundary effects caused by drawdown from the Open Pit dewatering.

The dimensions of the mesh elements vary in size from about 500 m at the model boundaries to 10 m around the Open Pit area. The model consists of 272 952 elements, 160 545 nodes, and 6 layers (7 "slices"/surfaces). The total area of the model domain is about 143 square kilometres (km²).



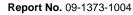




Table 11.I.4-1: Model Assumptions

The groundwater flow system can be simulated using an equivalent porous medium approach. This is considered reasonable provided the scale of observation (in this case the extent of dewatering) is much greater than the scale of the individual fractures.

Flow is laminar and is governed by Darcy's Law, as such, groundwater flow is controlled by hydraulic gradient and the hydraulic conductivity of the saturated material.

The calibrated model (i.e., pre-mining scenario) was conducted at steady-state conditions. Using this approach the model reflects long-term conditions based on average or historical yearly data.

Transient modelling was utilized during predictive simulations. However, the time-scale of mining operations as provided were yearly, thus the model time steps progress in a yearly fashion. Time-dependent variables, such as recharge and mine progression, were based on yearly intervals and did not take into account short-term, seasonal, or unusual events.

The hydrogeology of the area can be classed into 2 main groupings based on physiographic region: 1) upland areas; and 2) lowland areas. Upland areas are defined as regions at and surpassing 230 masl, lowland areas are those below 230 masl. The hydrogeology of the 2, though linked, is distinct. In summary, the upland areas are considered recharge zones whereas the lowlands are considered discharge zones.

Permafrost is absent underneath upland areas but present in the lowlands, except under lakes where thermal plumes emanating from the lakes themselves prevent the formation of permafrost.

Lakes and rivers in the model are considered discharge features.

Topographic elevations are considered to be adequately reflective of average lake water levels.

Bathymetric data was used for lakes where available. The following lakes have bathymetry data: Grid Pond, Little Grid Pond, Nico Lake, Peanut Lake, Burke Lake, Reference Lake, and Ponds 8, 9, 10, 11, 12, and 13. In the absence of data, the following was assumed:

1) lakes with a surface area of less than 60 000 m^2 have a depth of 1 m; and

2) all remaining lakes (greater than 60 000 m²) have a depth of 4.3 m.

Based on the data presented in Table 11.I.4-2, the following assumptions were made regarding lakes with no depth measurements:

1) lakes with a surface area of less than 60 000 m² have a depth of 1 m; and

2) all remaining lakes (greater than 60 000 m²) have a depth of 4.3 m (the average depth of the larger lakes listed in Table 11.I.4-2).

The hydraulic conductivity (K) of rock in the model utilized a "bulk" approach, and varies solely based on depth (K decreases with depth). Hydraulic conductivities of particular rock types versus others (for example igneous intrusive versus metasedimentary) was not considered significant when compared to the depth correlation.

The orientation of bedrock units (i.e. strike, dip, etc.) was not considered significant from a groundwater flow perspective. Each layer in the model is uniform thickness (with the exception of the final layer, which ends at 0 masl). Each material property is isotropic (that is horizontal K is equivalent to vertical K).

The hydraulic conductivity of the overburden also utilized a "bulk" approach. Individual overburden samples revealed a range of material types – from sand to clay. However, on the whole, the overburden is considered to behave hydraulically as a silt-type unit.

The overburden is considered to allow flow (active) through at least part of its thickness. Within the model, an active overburden thickness of 4 m was assumed based on the observed range of active thickness observed in the field.

Mine inflow due to discrete fractures has not been considered. However, if a significant fracture were encountered, it could increase mine inflow considerably.

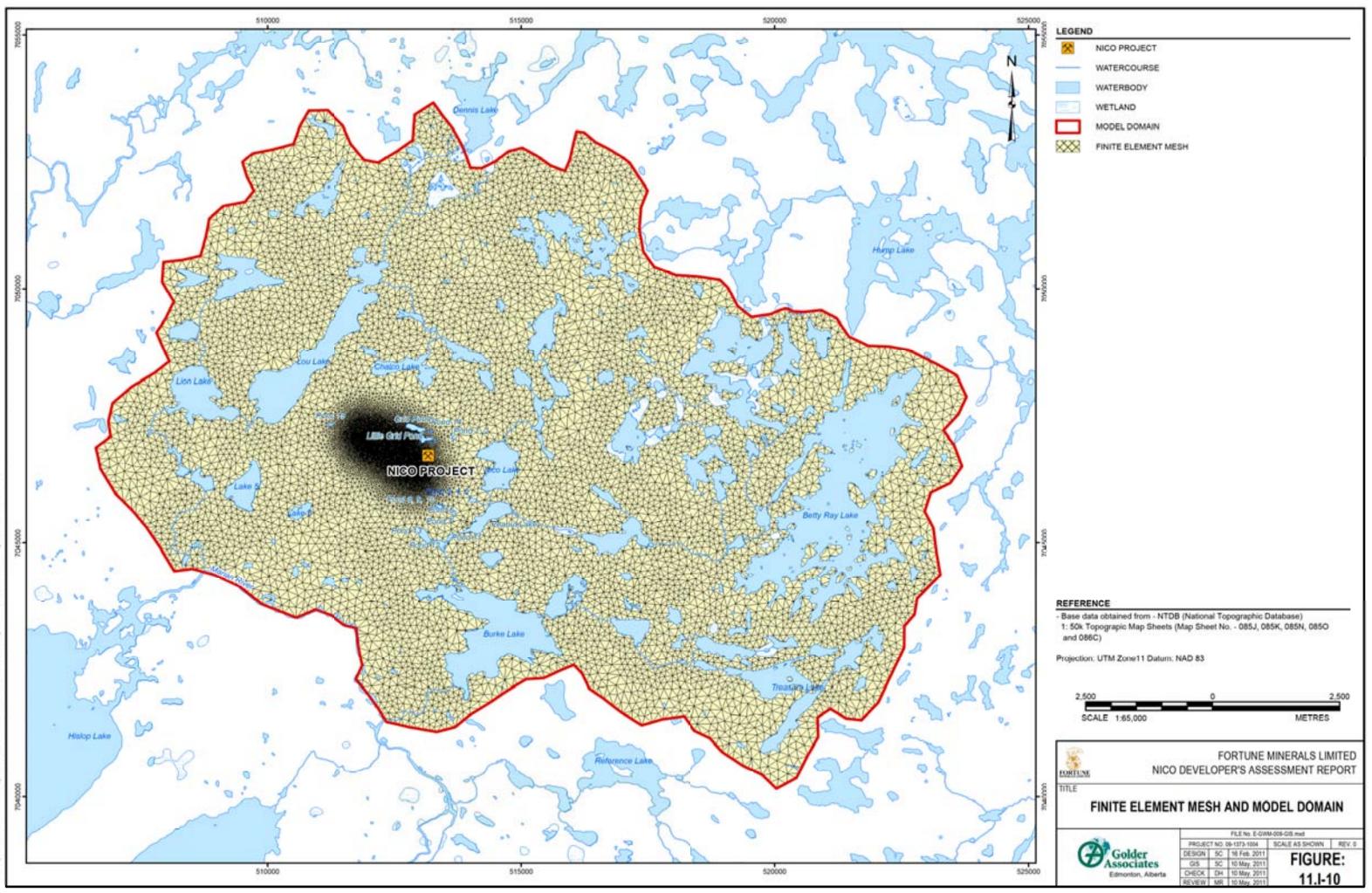
Density dependent flow is not a factor in this hydrogeologic system (this consideration was tested and verified as described in Section 11.I.7).

masl = metres above sea level; m2 = square metres

May 2011







G Projects/2010/10-1118-0048_NocFortuneMinerals/GISMXDvFnarIDAR Figures/GroundwaterMoosterg/E/GWM-009

11.I.4.4 Model Layering and Surfaces

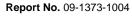
Figure 11.I-9 provides a pictorial representation of the model layers. A description of each is provided below. Note that the terms "shallow", "intermediate" and "deep" bedrock utilized below are arbitrary; these terms simply allow grouping of bedrock intervals sharing the same hydraulic properties in the model.

- Layer 1, Fractured Cap Rock (Upland Areas)/Silty Overburden (Lowland Areas): Layer 1 hosts the fractured cap rock in the upland areas and silty overburden in the lowland areas. This layer is bound by a combined topography and bathymetry surface on top (see Figure 11.I-11) and has a 10 m thickness in the upland areas (i.e., 10 m of fractured rock) and 4 m in the lowland areas (i.e., 4 m of overburden, the upper measured thickness of active overburden flow in the study area). This surface merges data from 2 sources: 1) a 5 m x 5 m Digital Elevation Model (DEM) (Fortune 2006); and 2) bathymetric data collected by Golder (Golder 2010b). The following lakes have bathymetric data utilized in this study: Grid Pond, Little Grid Pond, Nico Lake, Peanut Lake, Burke Lake, Reference Lake, and Ponds 8, 9, 10, 11, 12, and 13. Table 11.I.4-2 displays some morphometric parameters of these lakes. The remaining lakes within the model domain do not have depth data. However, based on the data presented in Table 11.I.4-2, the following assumptions were made regarding lakes with no depth measurements: 1) lakes with a surface area of less than 60 000 m² have a depth of 1 m; and 2) all remaining lakes (greater than 60 000 m²) have a depth of 4.3 m (the average depth of the larger lakes listed in Table 11.I.4-2). These depths were subtracted from the DEM surface as appropriate. This layer was interpolated onto the FEFLOW mesh using a nearest-neighbour routine.
- Layer 2, Shallow Bedrock (Upland Areas)/Permafrost and Shallow Bedrock (Lowland Areas): Layer 2 hosts shallow bedrock material in the upland areas and permafrost or shallow rock (underneath lakes only) in the lowland areas. This layer has a uniform thickness of 10 m below the bottom of Layer 1.
- Layer 3, Shallow Bedrock (Upland Areas)/Permafrost and Shallow Bedrock (Lowland Areas): Layer 3 hosts shallow bedrock material in the upland areas and permafrost or shallow bedrock (underneath lakes only) in the lowland areas. This layer has a uniform thickness of 15 m. (Note that although Layer 2 and 3 share the same properties, they were divided to allow for vertical "discretization" in the model.)
- Layer 4, Shallow Bedrock (Upland Areas)/Permafrost and Shallow Bedrock (Lowland Areas): Layer 4 hosts shallow bedrock in the upland areas and permafrost or shallow bedrock (underneath the lakes only) in the lowland areas. This layer has a uniform thickness of 25 m. Note that the combined permafrost thickness between Layers 2, 3, and 4 is 50 m, the average measured permafrost thickness in the study area.
- Layer 5, Intermediate Bedrock: Layer 5 contains intermediate bedrock, with a uniform thickness of 50 m. Notably, the material comprising Layer 5 is the same underneath the upland areas as it is underneath the lowlands.
- Layer 6, Deep Bedrock: Layer 6 hosts deep bedrock. This layer extends to the bottom of the model, arbitrarily "cut-off" at 0 masl. The thickness of this layer ranges from 263 m (underneath the uplands) to 71 m (in the lowlands).

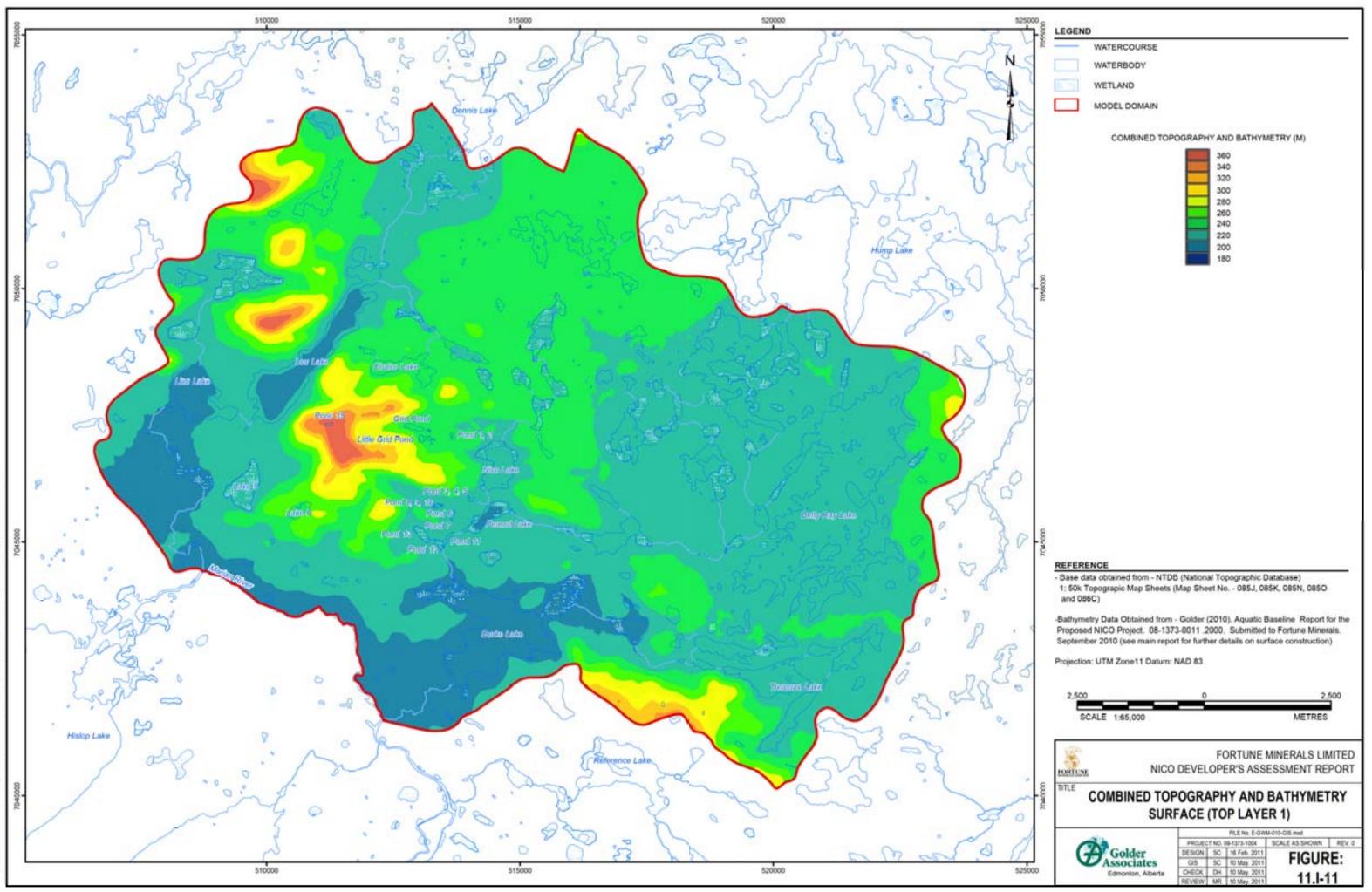
11.1.28











Lake	Volume (m³)	Surface Area (m²)	Average Depth (m)	Maximum Depth (m)
Burke	3 415 770	2 340 495	1.5	8.7
Grid	32 406	33 189	1.0	2.2
Lion	5 759 160	843 153	6.8	20.3
Little Grid	10 150	18 683	0.5	1.5
Lou	13 409 708	1 879 069	7.1	23.3
Nico	1 566 126	507 188	3.1	6.6
P12-13	58 198	58 198	1.0	1.8
Peanut	824 524	231 697	3.6	11.4
Pond 8-9	6 331	9 054	0.7	2.1
Reference	4 099 256	1 188 221	3.4	14.0
Summit	349 596	80 335	4.4	8.4

Table 11.I.4-2: Morphometric Data for Lakes

m = metre; m^2 = square metre; m^3 = cubic metre

11.I.4.5 Groundwater Flow Boundaries

The following section describes the groundwater flow boundaries in the model (see Figure 11.I-12).

The edges of the model domain are bounded by watershed boundaries (see Figure 11.I-3); as no regional groundwater elevation data was available, surface water and groundwater divides are assumed to coincide. The extreme edges of the model domain may be considered "no-flow" boundaries, in other words, groundwater is neither gained nor lost through these boundaries. The one exception is along the southwest of the model, where the Marian River forms a constant head boundary.

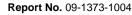
Internal to the model, all major lakes and streams are implemented in the model as constant head nodes set at topographic elevation. The nodes are constrained such that only groundwater is removed from the system; this assignment, in effect, implies that the waterbodies serve as groundwater discharge zones only within the model. These surface water features exist only in Layer 1.

Around the NICO Project site, seepage face nodes were implemented at DEM elevations in the "bowl" areas of the model to simulate seeps along the sides of the hill. As a seepage face, these nodes allow discharge from the model at a head equivalent to topography, but do not contribute water to the system.

The existing tunnel was implemented in the model as a series of constant head nodes ranging from 253.5 masl at the portal to 100 masl at the terminus of the tunnel. These nodes were constrained so that they could only remove water from the system. Note that the tunnel nodes appear in Layers 1 to 6.

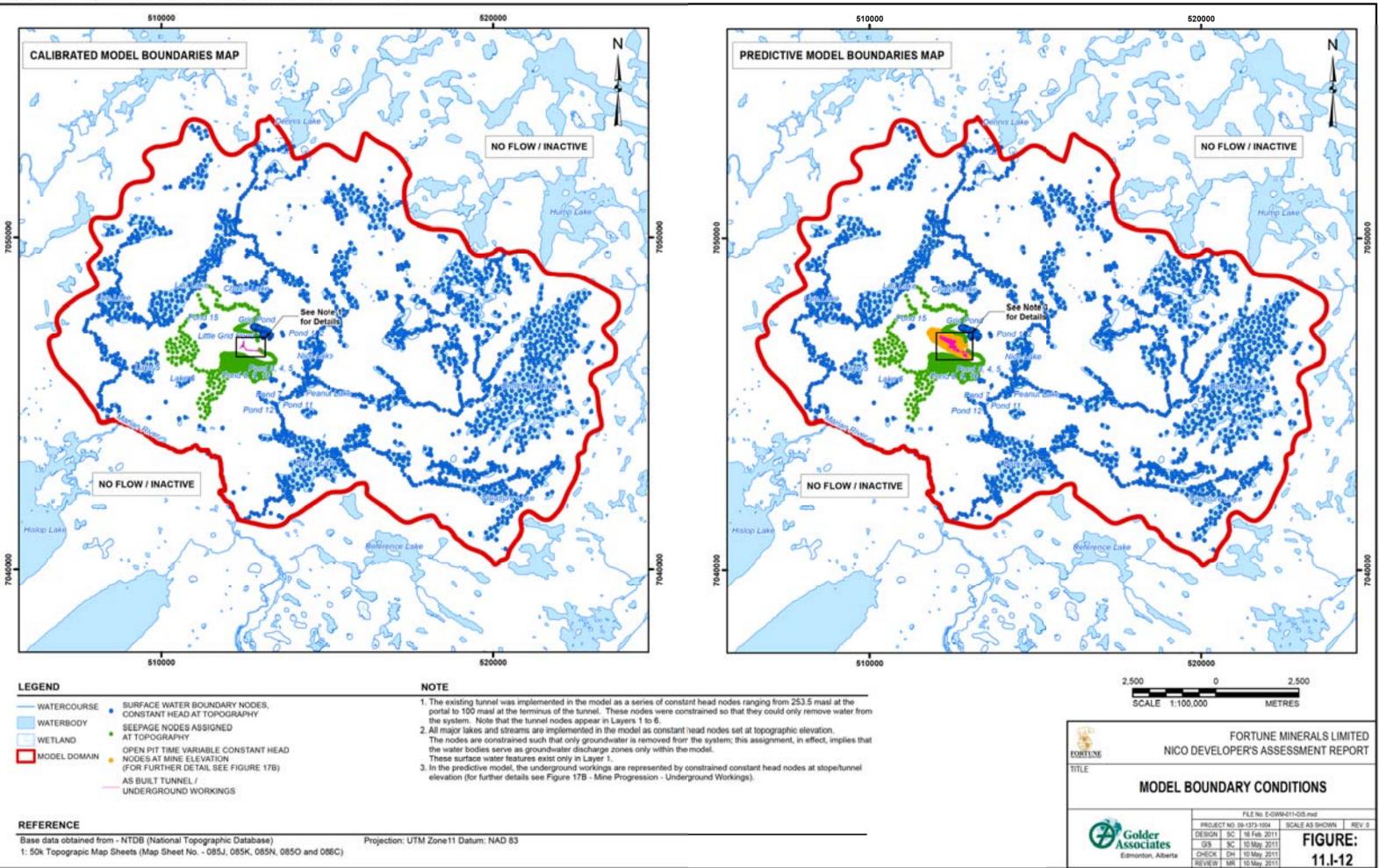
Vertically, the model is bound by topography/bathymetry at surface and a no flow boundary at depth (0 masl).







G-Projects/2010/10-1118-0546_NicoFortuneMinerate/GISMXDs/Final/DAR Figures/GroundwaterModeling/E-GWM-011-GIS.mxd



11.I.4.6 Model Parameterization

The model parameters are described in detail below; Table 11.I.4-3 provides a summary.

Basic Model Constructi	on - FEFLOV	N Me	esh Details			
Number of Elements:		272	,592			
Number of Nodes:			,545			
Number of Layers:		6				
Model Top:		188	- 375 masl (as defin	ed by topograp	ohy and bathyme	etry)
Model Bottom:		0 m	asl			
Hydraulic Properties of	Model Hydr	ostra	atigraphic Units			
	Hydrauli Conductiv K _h = K _v (m	vity	Total Assumed Thickness (m)	Porosity	Specific Yield	Specific Storage (1/m)
Overburden (Silt Till)	1E-06		4	0.4	0.18	1E-06
Fractured Bedrock (top of bedrock veneer)	1E-06		10	0.002	0.002	1E-06
Shallow Bedrock	7E-8 to 1E-	8	50	0.00034	0.00034	1E-06
Intermediate Bedrock	1E-09		50	0.00034	0.00034	1E-06
Deep Bedrock	1E-09		variable	0.00034	0.00034	1E-06
Model Recharge Rates						
Upland areas: 30 mm/yr,	lowland area	s: 10) mm/yr			

masl = metres above sea level; m/s = metres per second; mm/yr = millimetres per year

11.I.4.6.1 Recharge

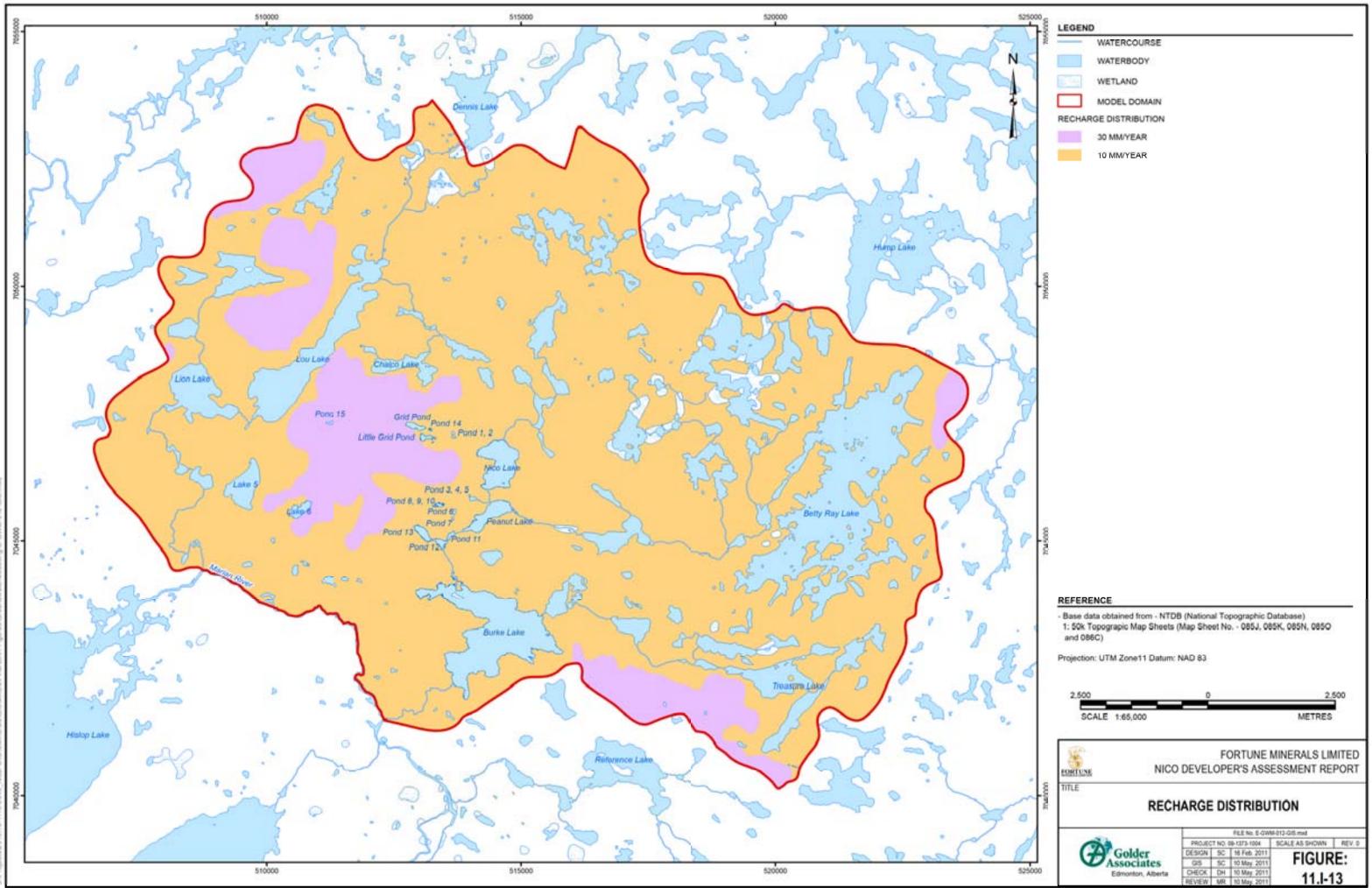
The recharge distribution applied in the model is shown on Figure 11.I-13. The simulated recharge is higher in the upland areas (30 mm/yr) than the lowland areas (10 mm/yr), in agreement with the model conceptualization described in Section 11.I.3. In addition, the recharge values utilized in the model fall within the range of measured values as discussed in Section 11.I.2.4. The final values arrived at in the model were "fine-tuned" during the calibration process, as described below in Section 11.I.5. Note that areal recharge is the only source or "input" of water to the groundwater model; lakes and streams, considered discharge zones, do not contribute groundwater to the system.

11.I.4.6.2 Hydraulic Conductivity

May 2011

The hydraulic conductivity distribution of each model layer is shown on Figure 11.I-6. The hydraulic conductivities utilized in overburden and bedrock fall within the range of measured values presented in Section 11.I.2.5, and were fine-tuned during the calibration process, as described in Section 11.I.5. The highest hydraulic conductivity layers are the upper fractured rock in the upland areas and the silts in the lowlands (1E-6 m/s); from these shallow zones the hydraulic conductivity decreases with depth (1E-9 m/s in the deep bedrock). Permafrost, in reality essentially "impermeable", is modelled as a relatively low hydraulic conductivity material at 1E-10 m/s.





11.I.4.6.3 Porosity and Storage

A porosity of 0.4 and a storativity of 0.18 were used for the overburden material. These values are considered typical for silt till (Freeze and Cherry 1979; Johnson 1967)

The bedrock porosity was derived by analyzing packer testing data in combination with rock characterization descriptions for boreholes 03-281, 03-282 and 03-283. Using the "Osnes Extraction from Fixed-Interval-Length Effective Transmissivities" (OxFilet) method (Lim and Dershowitz, 2010), a mean effective porosity of 3.4E-4 was calculated, with an upper end of 0.002 and a standard deviation of 2.4E-4. An effective porosity of 0.002 was used for the fractured rock at surface. The mean porosity of 3.4E-4 was used in the model elsewhere in the rock. Specific yield in the bedrock was considered to be equivalent to porosity. Specific storage was assigned as 1E-6/m.

11.I.5 MODEL CALIBRATION

The model was calibrated through a "trial-and-error" process by varying the recharge and hydraulic conductivity of the hydrostratigraphic units within the model until simulated groundwater elevations, flow directions and stream discharge compared reasonably well with observed conditions. Calibration targets included (see Figure 11.I-14 for locations):

- average static water levels measured at NICO wells;
- low flow measurements at stream flow gauges; and

May 2011

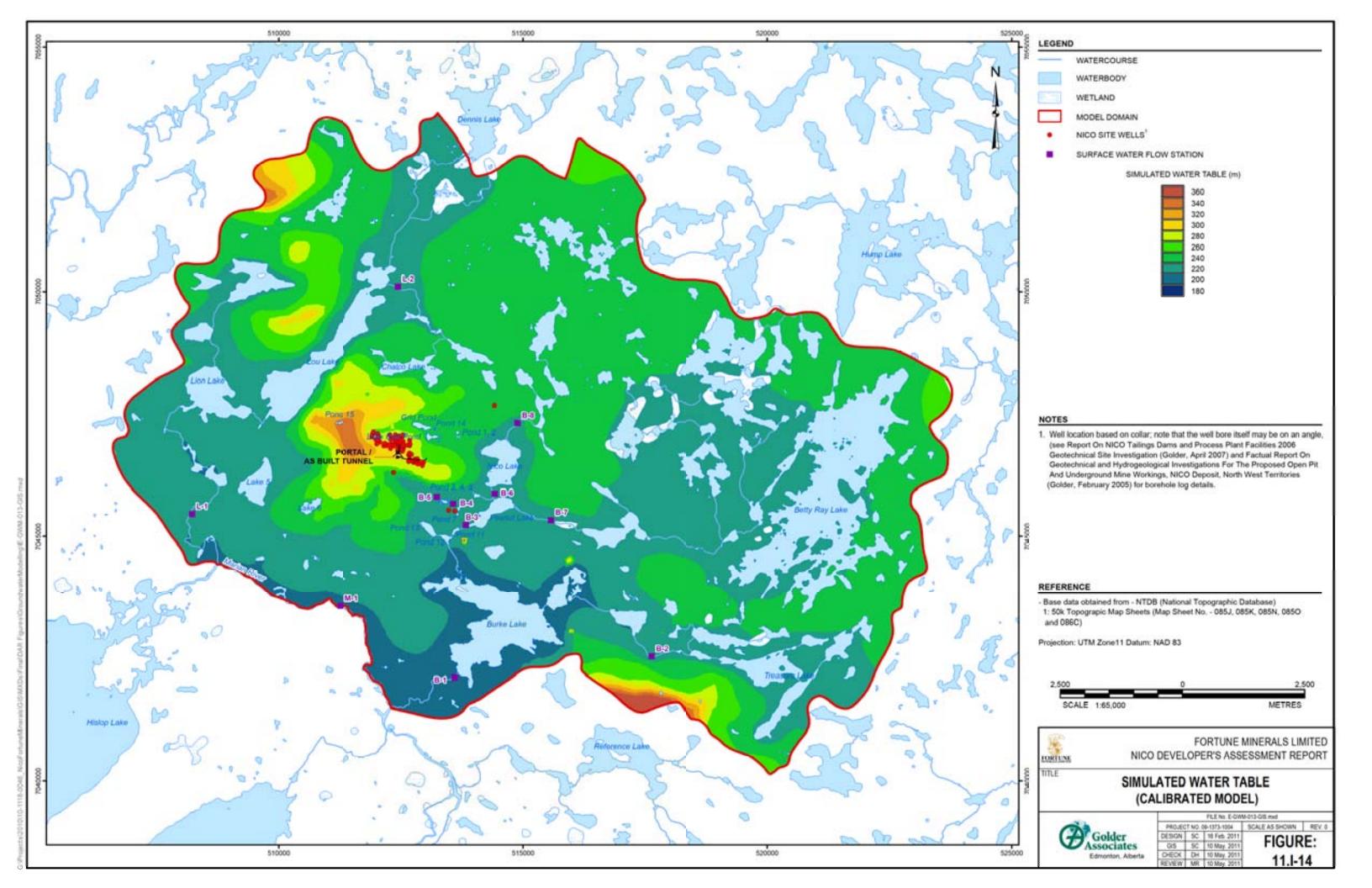
measured discharge from the flooded tunnel through the portal opening.

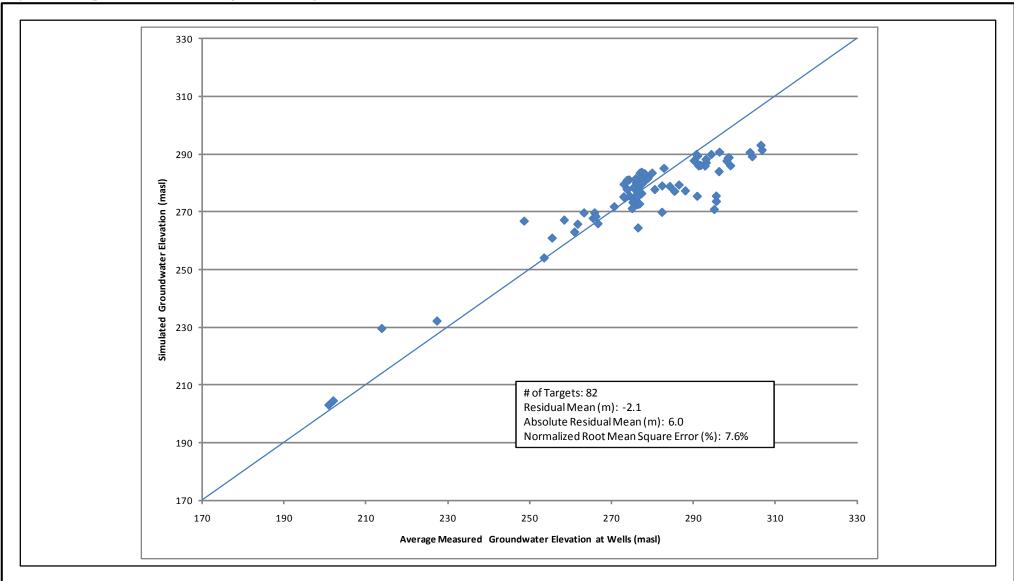
Figure 11.I-14 shows the simulated water table elevation of the calibrated model. The simulated groundwater elevations indicate radial flow from the upland areas out to the lowlands. The groundwater flow gradient is relatively high in the uplands, and dramatically decreases in the flat lowland areas, where groundwater elevation is strongly influenced by the "flattening" presence of numerous lakes and streams. Notably, the simulated flow patterns compare well with the inferred groundwater table presented on Figure 11.I-4.

Average static water levels measured in 82 boreholes at the NICO Project were used in the steady-state model calibration. Figure 11.I-15 shows a head calibration plot for the model (simulated water levels at wells versus average measured water levels at well locations in the model), and also provides selected calibration statistics. Generally, the simulated groundwater levels compare reasonably well with the measured groundwater levels. Following the "trial-and-error" calibration process, the residual mean was -2.1 m, the absolute residual mean was 6.0 m and the normalized RMS error was 7.6%. Table 11.I.2-1 provides the head calibration data utilized in the model, the simulated head at each well, and the residual.











Low-flow measurements from 10 stream flow gauges were also used in the steady-state model calibration (see Table 11.I.2-2). The flow measurements were taken roughly spring/summer/fall from 2005 to 2008. Figure 11.I-16 shows a flow calibration plot for the model. Simulated groundwater discharge at surface waterbodies (baseflow) was compared to the measured flows. In general, the simulated baseflows are below or within the measured low-flows at the gauges. Note that the model can only simulate groundwater baseflow contribution to surface waterbodies; input/output from precipitation, runoff, evaporation, etc. is not accounted for in the model. The measured data, however, even at low flow, may comprise all these components, in addition to groundwater baseflow. However, as baseflow separation was not possible at these gauges (mainly due to interference from beaver dams), a modelled flow below or between the measured low-flow range is considered a reasonable match as part of the current calibration.

A groundwater budget for the calibrated model is provided in Table 11.I.5-1. Note that the only source of water to the model is areal recharge. All discharge in the calibrated model is to surface waterbodies. Table 11.I.5-1 has been organized to reflect discharge on a sub-basin level and does not take into account cumulative flows from one sub-basin to the next.

Source / Sink	Inflow / Recharge (m³/d)	Outflow / Discharge (m ³ /d)
Areal recharge	5,254	-
LL2	-	426
LL3	-	139
LL4 [incl. Chalco Lake]	-	129
LL5 [incl. Lou Lake]	-	460
LL6 [incl. Lion Lake]	-	719
BL1	-	466
BL2 [incl. Nico Lake]	-	172
BL3 [incl. Betty Ray Lake]	-	1,092
BL4 [incl. Peanut Lake]	-	202
BL5 [incl. Treasure Lake]	-	672
BL6 [incl. Pond 8,9,10]	-	157
BL7 [incl. Pond 13]	-	28
BL8 [incl. Burke Lake]	-	304
Marian ^a	-	288
SUM:	5,254	5,254

 Table 11.I.5-1: Calibrated Model Groundwater Flow Budget

Notes: The only source of inflow to the model is recharge.

The only sinks in the calibrated model are surface waterbodies within the sub-basins listed above. The outflow portion of the flow budget is analyzed on a sub-basin basis.

See Figure 11.I-3 of the report for sub-basin locations.

Outflow / Discharge may also be considered as baseflow and means groundwater discharge to a surface water receptor within the sub-basin.

^a The model only contains a small portion of the Marian River basin.

Through the calibration process recharge rates, hydraulic conductivities of the geologic units and simulated flow patterns were found in good agreement with available field data. The calibrated model values are, therefore,





considered to represent reasonable estimates for use in developing the predictive model simulations where the mine is implemented and potential impacts on the hydrogeologic system are assessed.

11.I.6 PREDICTIVE MODEL (MINING) SIMULATIONS

11.I.6.1 Mine Progression

The proposed mine phasing is approximately as follows (Sharpe 2010):

- Phase 1 A: Year 1 to Q2 Year 4 (note that underground mining will occur from Year 1 to Year 3);
- Phase 1: Year 1 to end of Year 8;
- Phase 2: Year 2 (stripping upper benches), end Q3 Year 4 to beginning of Year 13;
- Phase 3: Year 11 to Year 19; and
- Post-closure.

The proposed Open Pit geometry for every year of active mining from Year 1 to Year 19 was provided to Golder by P&E Mining Consultants Inc. (Sharpe 2010) as 3D DXFs. Figure 11.I-17A shows a "snapshot" of the mine progression for a sample year in each of the phases listed above, namely: Year 2/Phase 1 A, Year 6/Phase 1), Year 11/Phase 2, Year 19/Phase 3, Ultimate Pit). In addition, Figure 11.I-17B shows the proposed underground workings.

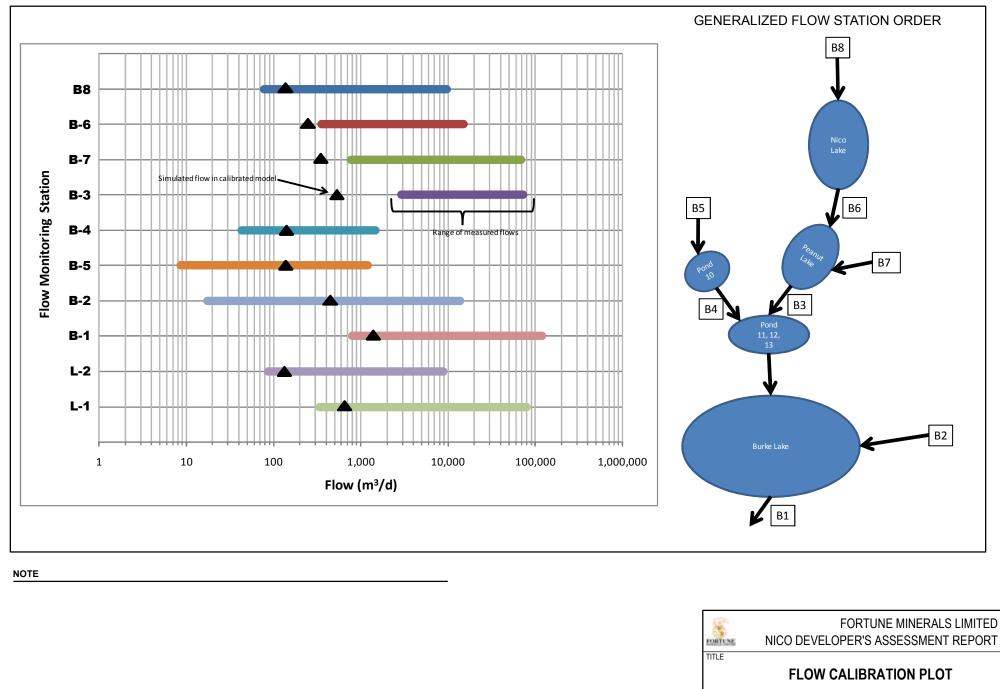
Extracting xyz data from the DXFs provided by P&E Mining Consultants Inc., the Open Pit geometry over time was imported into FEFLOW as time-variable functions applied at nodes comprising the proposed Open Pit. The Open Pit was represented by almost 1000 imported boundary functions in the area of the mine, and over 10 000 interpolated functions surrounding these nodes (see Figure 11.I-12).

Post-closure the Open Pit will fill with water and become a lake with a low point (potential outlet) at about 260 masl.









FILE No. E-GWM-015-GIS.mxd PROJECT NO. 09-1373-1004 SCALE AS SHOWN REV. 0

FIGURE:

11.I-16

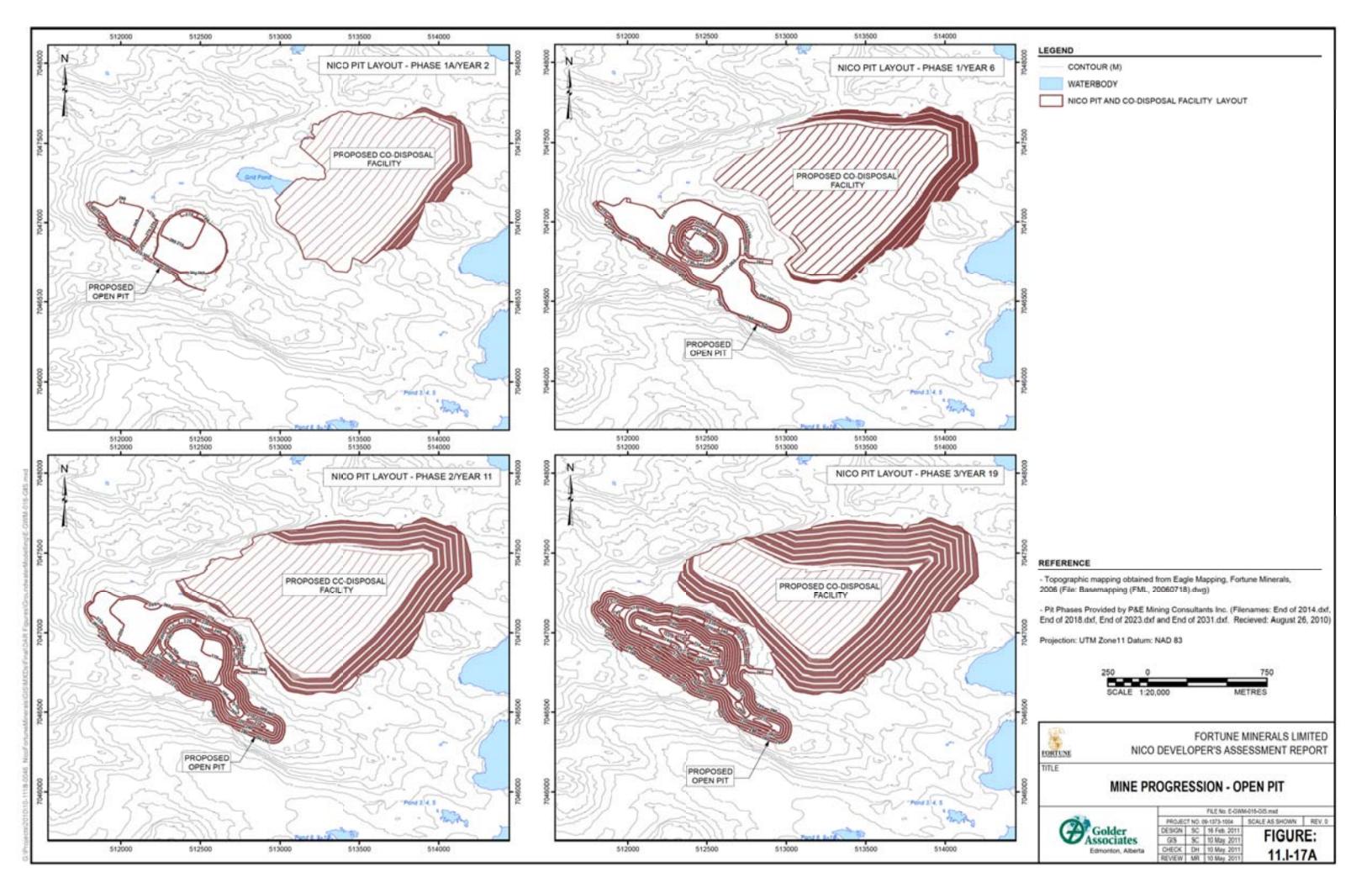
DESIGN SC 8 Apr. 2011

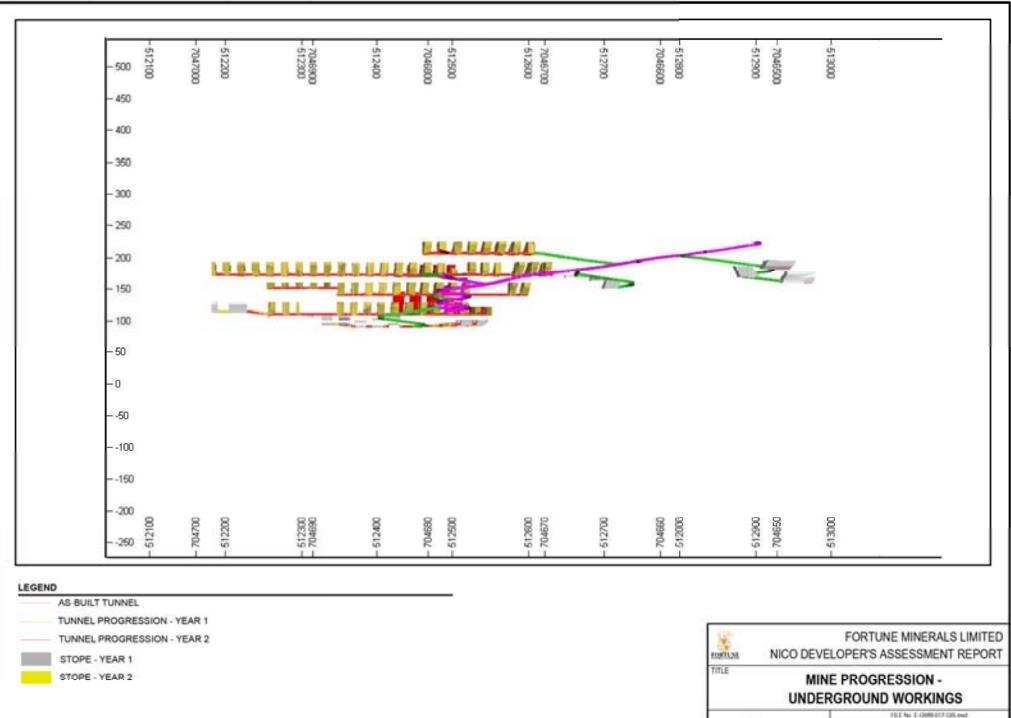
GIS SC 10 May. 2011 CHECK DH 10 May. 2011

REVIEW MR 10 May. 2011

Golder

Edmonton, Alberta





PROJECT NO 48-1373-1004 BOALE AS SHOWN REV II

FIGURE: 11.I-17B

 (E340)
 %
 8 Apr (01)

 01
 SC
 10 May (01)

 0460X
 04
 10 May (01)

 0450X
 04
 10 May (01)

 REVEW
 MIL
 10 May (01)

Golder

Edmonton, Alberte

11.I.6.2 Predictive Model Boundaries

The boundaries used in the predictive modelling were generally the same as in the calibrated model (see Section 11.I.4.5) with the following exceptions:

- The Open Pit, absent in the calibrated model, is implemented as a group of unique time-variable head function nodes over the extent of the mine (see Figure 11.I-12 and also Figure 11.I-17A). As the Open Pit expands (both vertically and horizontally) through time, the head in these nodes decrease accordingly to allow smooth progression of the Open Pit excavation from year to year of the simulation (the estimated operational mine life is 19 years).
- Underground (U/G) workings are proposed to occur during the first 2 years of mine life (see Figure 11.I-12 and also Figure 11.I-17B). The underground workings were dealt with in a separate "stand-alone" 2-year transient model without the pit. With respect to estimating inflows, this is considered a conservative approach as the inflows to both the Open Pit (with U/G workings absent) and tunnel would be greater due to the increased depressurization required to obtain the dewatered condition. With respect to total drawdown, an estimate was derived by superimposing the drawdown of each model (see Section 11.I.6.4). The U/G workings were implemented in a similar fashion to the as-built tunnel (the tunnel was also dewatered in the U/G model as part of the active mining process in the first 2 years) utilizing constrained constant head nodes prescribed at an elevation in accordance with the tunnel network or stope bottom elevation. The U/G progression was divided into 2 years (see Figure 11.I-17B) such that the boundary nodes for Year 2 were not implemented until the appropriate time.
- Post-closure, the Open Pit will fill with water to a presumed elevation of 260 masl. To model this condition, a series of constant head cells within the 260 masl Open Pit contour set at elevation 260 masl were implemented.

The CDF will progress with active mining (see Figure 11.I-17A). The amount of infiltration through the CDF is considered similar to the existing applied recharge within its footprint (10 mm/yr); thus, no modifications were made to the predictive model in this area.

11.I.6.3 Estimated Mine Inflows and Groundwater Removal

Dewatering of groundwater seepage will be required as the underground workings and Open Pit progress. Figure 11.I-18 shows the simulated groundwater removal due to mining operations (these results are also tabulated in Table 11.I.6-1). There are 3 components considered in this analysis: 1) discharge to the underground workings; 2) discharge to the Open Pit; and 3) areal recharge that is now diverted as surface water. The summation of these components is also shown on Figure 11.I-18. The following is noted:

The underground mining begins at time "zero", resulting in a simulated inflow to the underground workings of 61 m³/d by the end of Year 1. By the end of Year 2, the underground openings have expanded to their final layout, resulting in a total inflow of 93 m³/d. After Year 2, dewatering of the underground workings ceases; however, there is still some inflow due to storage (i.e., openings) in the workings. This inflow gradually decreases as water levels in the underground mine recover. By Year 15 the water level in the underground mine intersects that of the Open Pit; from this point onward all inflow to the mine operations is seepage to the Open Pit. Note that these estimates do not account for surface water seepage or "interflow" (water which infiltrates the ground through the upper fractured zone but does not reach the groundwater

11.1.42



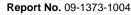




table) which may constitute a significant amount of inflow to the underground workings during the freshet period.

- Groundwater inflow to the Open Pit begins in Year 1 and gradually increases as the mine expands to a maximum of 54 m³/d by the end of mining.
- The greatest amount of groundwater dewatering required during mine operations occurs at Year 2, where the summation of underground and Open Pit dewatering results in a withdrawal of 130 m³/d.
- The estimated groundwater recharge over the pre-mine footprint is 30 mm/yr. The recharge rate over the footprint of the active mine Open Pit is nil as all water is considered diverted/collected. Thus, as the Open Pit expands, the amount of water available for groundwater recharge decreases, as potential infiltration is now collected and removed during dewatering. As shown on Figure 11.I-18, the amount of areal recharge diverted increases as the Open Pit expands (note that some years the surface area of the Open Pit remains the same, hence the amount of diverted recharge remains constant).
- Total groundwater removed due to mining operations peaks at the end of Year 2 at a value of about 152 m³/d. The majority of this initial peak is due to dewatering of the underground workings. After Year 2, the total groundwater removed is relatively consistent; on the order of 100 m³/d.
- The estimates described above pertain exclusively to groundwater. The amount of dewatering required due to direct precipitation, runoff and interflow are not considered (with the exception of the consideration that some of that surface water, once destined to become groundwater recharge, is now diverted as described above).
- Mine inflow due to discrete fractures has not been considered. However, if a significant fracture were encountered, it could increase mine inflow considerably.

Mining Life Year	Underground Workings (m³/d)	Open Pit (m ³ /d)	Areal Recharge Removed (m ³ /d)	Total Groundwater Removed From System (m ³ /d)
0	0	0	0	0
1	61	31	17	109
2	93	37	22	152
3	29	39	27	95
4	22	39	34	95
5	19	39	36	94
6	18	39	36	93
7	16	45	36	97
8	15	49	36	100
9	15	49	36	100
10	14	49	41	104
11	12	49	41	102
12	10	51	41	102

Table 11.I.6-1: Simulated Groundwater Removal Due To Mining Operations





Mining Life Year	Underground Workings (m³/d)	Open Pit (m³/d)	Areal Recharge Removed (m ³ /d)	Total Groundwater Removed From System (m³/d)
13	8	51	41	100
14	6	51	41	98
15	0	51	41	92
16	0	51	41	92
17	0	53	41	94
18	0	53	41	94
19	0	54	41	95

Table 11.I.6-1: Simulated Groundwater Removal Due To Mining Operations (continued)

 m^3/d = cubic metres per day

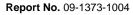
11.I.6.4 Potential Drawdown Due To Active Mining

The simulated water table drawdowns for select years during active mine operations are shown on Figure 11.I-19. The following is noted:

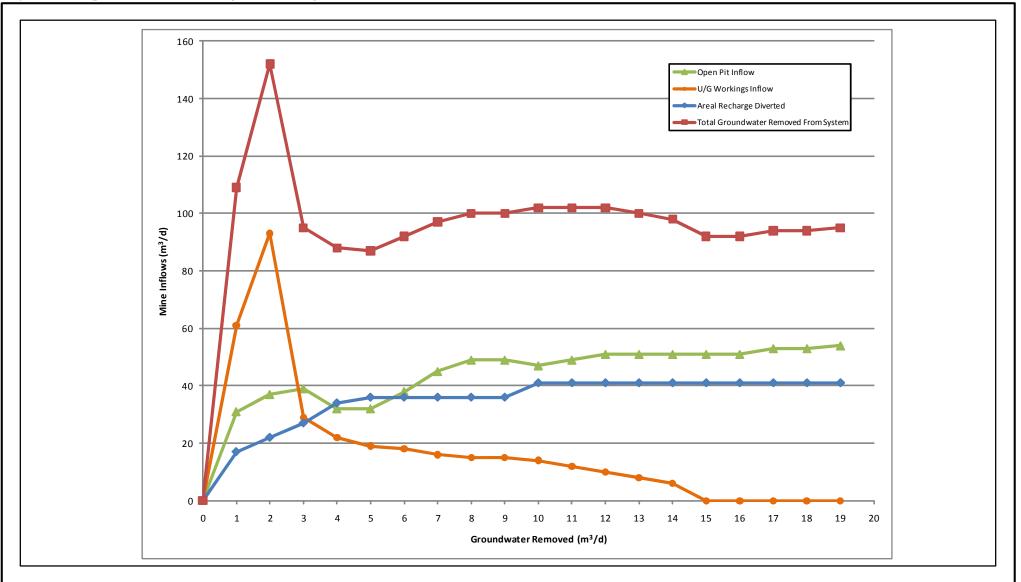
- Drawdown due to underground workings and Open Pit mining were assessed in separate models and combined for this analysis through superposition.
- The shape of the drawdown cone roughly reflects the progression of the Open Pit.
- The maximum drawdown simulated occurs at 19 years. At this time the Open Pit has reached its maximum dimension. Vertically, the drawdown reaches 180 m in the central portion of the Open Pit. Laterally, the 1 m drawdown contour is predicted to be 100 to 510 m from the Open Pit.
- While maximum water taking during the life of the mine occurs during Year 2, the drawdown induced by underground working dewatering has not fully propagated to the water table by Year 2 and is never fully "realized", as active underground dewatering is discontinued after Year 2.



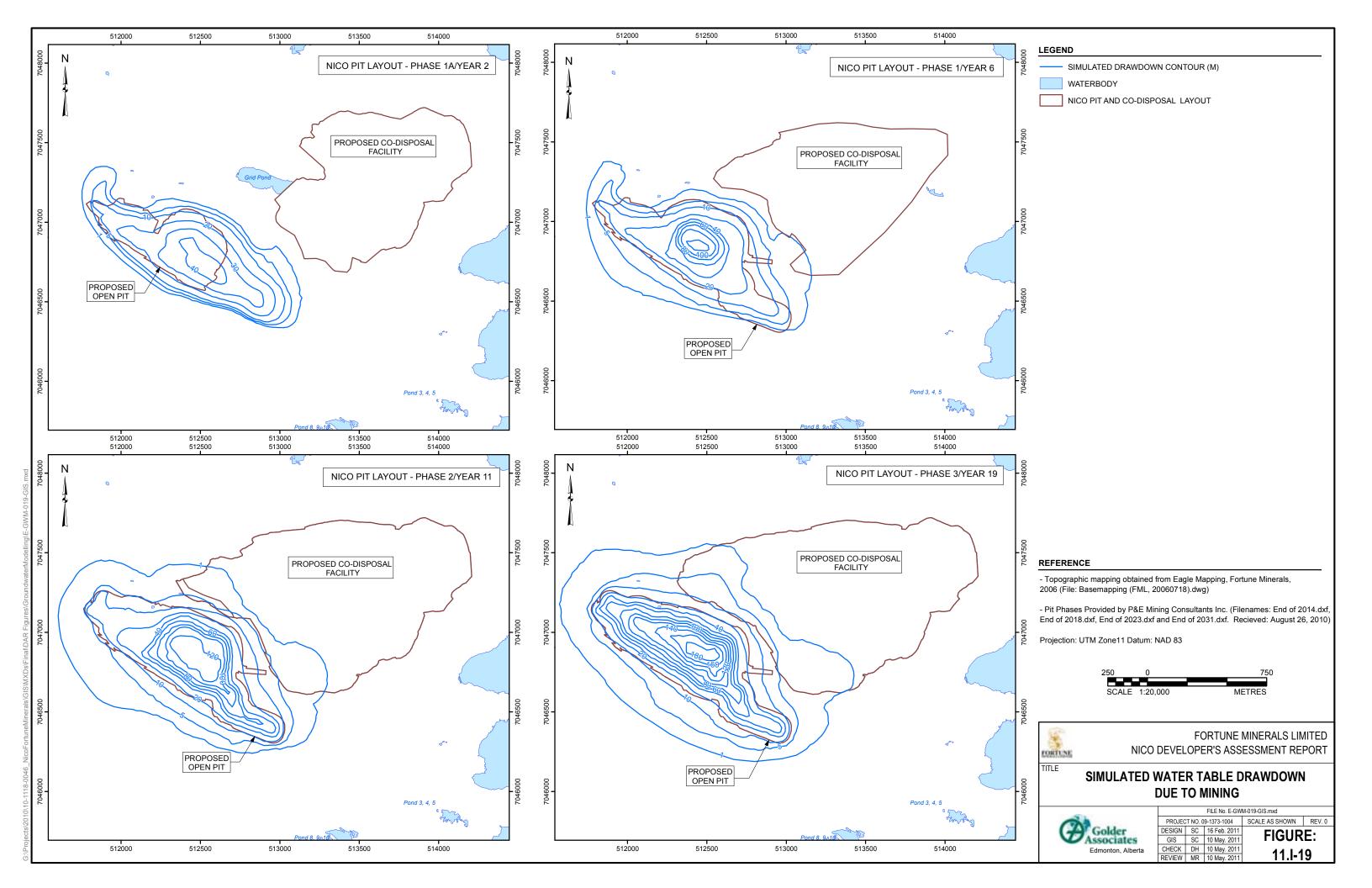
11.I.44











11.I.6.5 Post-Closure

After mining has ceased the Open Pit will fill through naturally occurring surface water and groundwater level inputs to a presumed water level elevation of approximately 260 masl. This is the approximate elevation of the following 3 pit outlet features with lowest elevations, and which will therefore control the ultimate Flooded Open Pit level:

- the portal to the underground workings;
- the natural topographic low point relative to the Open Pit; and
- the exit elevation of the ramp on the ultimate Open Pit.

Figure 11.I-20 illustrates the simulated post-closure water table with the Flooded Open Pit at 260 masl. Figure 11.I-21 shows the simulated drawdown caused by the post-closure condition compared to the pre-mine condition. A maximum drawdown of greater than 30 m is induced in the southwestern area of the Flooded Open Pit (compared to pre-open pit simulated water levels). The 1 m drawdown contour generally extends 50 to 500 m from the Flooded Open Pit, although in an area to the north there is no drawdown as the pre-mine water level was at approximately 260 masl in this area.

The recovery time required for the Flooded Open Pit to reach an elevation of 260 masl will depend primarily on surface water inputs (which will form a far greater percentage of the flow budget for the recovering pit). This recovery process is addressed in Appendix 11.IV.

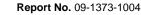
11.I.6.6 Potential Reduction in Discharge to Waterbodies

The groundwater removed during mining operations may result in a decrease in groundwater discharge elsewhere in the system, specifically at lakes and streams (i.e., dewatering may cause a decrease in groundwater baseflow at these waterbodies). Table 11.I.6-2 displays the simulated groundwater budget for the model pre-mine, yearly during active mining, and post-closure, and examines baseflow loss on a sub-basin level (refer to Figure 11.I-3 for the location of each sub-basin). Note that all discharge in the sub-basins is considered reflective of baseflow to waterbodies within these sub-basins (a proportion of some of the discharge within some sub-basins may be due to seeps; however, this water is still considered here as groundwater contribution to surface water receptors). The following is noted with respect to Table 11.I.6-2:

- Rows 1 through 4 (as listed in Table 11.I.6-2) document the amount of groundwater removed from the system due to mining operations over time (as per Table 11.I.6-1).
- Rows 5 through 18 list the amount of groundwater discharge (baseflow) to each sub-basin within the study area for the pre-mine condition and all 19 years of active mining. Row 19 is the summation of this discharge. Note that these results present the discrete discharge for each sub-basin and do not take into account additive or cumulative baseflow contributions (these are discussed below).
- As shown in Row 19, the total amount of discharge to the sub-basin waterbodies decreases in accordance with the amount of groundwater removed due to mining operations (see Row 4).
- Rows 20 through 33 list the simulated reduction in discharge in cubic metres per day for each discrete subbasin during each year of mining. Row 34 lists the total reduction for all sub-basins combined; note that this number is the same as the amount of groundwater removed from the system due to mining (see Row 4).

11.1.47







Congruently, the greatest amount discharge loss occurs during Year 2 of mining, when a total 152 m³/d of groundwater is removed from the system. The magnitude of discharge removal is largely a function of the location of the sub-basins relative to the mine. For instance, sub-basin BL2, encompassing the majority of the mine footprint, has the largest decrease in flow amongst the sub-basins, while BL6, just south of the Open Pit, has the second largest decrease in flow.

- Rows 35 to 48 tabulate the cumulative flows for each sub-basin for pre- and active mining scenarios. The Pre-Mine column for rows 35 through 48 reflects the "base case" by which subsequent baseflow loss due to mining is evaluated (see below). This analysis takes into account the cumulative nature of groundwater flow within the system. For example, total baseflow in sub-basin BL8 is not solely a function of discharge within BL8; rather, the baseflow in this sub-basin is the summation of its own discrete discharge plus the baseflow of the sub-basins upstream of BL8 (namely, BL1, BL2, BL3, BL4, BL5, BL6, and BL7). To see the upstream to downstream progression of baseflow from one sub-basin to the next the reader is referred to Figure 11.I-3.
- Rows 49 to 62 tabulate the estimated baseflow loss on a percentage basis for each sub-basin during active mining. The largest baseflow loss occurs in sub-basin BL6, where a baseflow decrease of 20% to 36% is simulated. Sub-basins BL2 and LL4 have a maximum simulated baseflow loss of under 10%, while LL3, LL5, LL6, BL4, BL8, and Marian have a maximum loss of under 5%. The remaining sub-basins, LL2, BL1, BL3, and BL7 do not have any simulated baseflow loss.

Post-closure some long-term baseflow loss to the surrounding sub-basins will occur due to the presence of the post-closure lake. The maximum percent baseflow loss occurs at sub-basin BL6, where 11% loss is simulated. The remaining sub-basins have zero to 3% baseflow loss. It is important to note that the results described above only account for the groundwater component of the flow budget. Direct precipitation, interflow (water that enters the ground but does not reach the water table), runoff, discharge from mining operations, and upgradient surface water flow contributions are not considered in this analysis.





Table 11.I.6-2: Simulated Pre-Mine, Active Mining, and Post-Closure Groundwater Flow Budget

	imulated Pre-Mine, Active Min	ing, and	FUSI-CI	USUIE GI	ounuwat			N4:									Antino	Min in 11					Post-
							Pre-	Mine									Active	Mining					Closure
		Row	Year 0	Year 1	Year 2	Year 3	Year 4	Year 5	Year 6	Year 7	Year 8	Year 9	Year 10	Year 11	Year 12	Year 13	Year 14	Year 15	Year 16	Year 17	Year 18	Year 19	Final Lake
	U/G Workings	1	0	61	93	29	22	19	18	16	15	15	14	12	10	8	6	0	0	0	0	0	0
Groundwater	Open Pit	2	0	31	37	39	39	39	39	45	49	49	49	49	51	51	51	51	51	53	53	54	11
Inflow To Mine	Recharge Removed	3		17	22	27	34	36	36	36	36	36	41	41	41	41	41	41	41	41	41	41	39
(m ³ /d)	Total Flow Removed From Groundwater System	4	0	109	152	95	95	94	93	97	100	100	104	102	102	100	98	92	92	94	94	95	50
	LL2	5	426	426	426	426	426	426	426	426	426	426	426	426	426	426	426	426	426	426	426	426	426
	LL3	6	139	139	139	139	139	139	139	139	139	139	139	139	139	139	139	139	139	139	139	139	139
	LL4 [incl. Chalco Lake]	7	129	122	120	122	122	122	122	122	122	122	122	121	121	121	121	121	121	121	121	121	126
	LL5 [incl. Lou Lake]	8	460	453	451	454	454	454	454	454	454	454	454	454	454	454	454	454	454	454	454	454	457
	LL6 [incl. Lion Lake]	9	719	714	713	714	714	714	714	714	714	714	714	714	714	714	714	714	714	713	713	713	717
Groundwater	BL1	10	466	466	466	466	466	466	466	466	466	466	466	466	466	466	466	466	466	466	466	466	466
Discharge To	BL2 [incl. Nico Lake]	11	172	129	112	133	133	134	135	132	132	132	130	131	131	132	133	137	137	136	136	136	152
Sub-Basin	BL3 [incl. Betty Ray Lake]	12	1,092	1,092	1,092	1,092	1,092	1,092	1,092	1,092	1,092	1,092	1,092	1,092	1,092	1,092	1,092	1,092	1,092	1,092	1,092	1,092	1092
(m³/d)	BL4 [incl. Peanut Lake]	13	202	202	202	202	202	202	202	202	202	202	202	202	202	202	202	202	202	202	202	202	202
	BL5 [incl. Treasure Lake]	14	672	672	672	672	672	672	672	672	672	672	672	672	672	672	672	672	672	672	672	672	672
	BL6 [incl. Pond 8,9,10]	15	157	116	100	125	125	125	125	123	121	121	119	121	121	122	123	125	125	125	125	124	139
	BL7 [incl. Pond 13]	16	28	28	28	28	28	28	28	28	28	28	28	28	28	28	28	28	28	28	28	28	28
	BL8 [incl. Burke Lake]	17	304	304	304	304	304	304	304	304	304	304	304	304	304	304	304	304	304	304	304	304	304
	MR1 (Marian)	18	288	281	279	282	282	282	282	283	282	282	282	282	282	282	282	282	282	282	282	282	285
Total Discharge	e (m³/d)	19	5,254	5,145	5,102	5,159	5,159	5,160	5,161	5,157	5,154	5,154	5,150	5,152	5,152	5,154	5,156	5,162	5,162	5,160	5,160	5,159	5,204
	LL2	20	0	0	0	0	0	0	0	0	0	0	0	0	0	0	0	0	0	0	0	0	0
	LL3	21	0	0	0	0	0	0	0	0	0	0	0	0	0	0	0	0	0	0	0	0	0
	LL4 [incl. Chalco Lake]	22	0	7	10	7	7	7	7	7	7	7	7	8	8	8	8	8	8	8	8	8	3.5
	LL5 [incl. Lou Lake]	23	0	7	10	6	6	6	6	6	6	6	6	6	6	6	6	6	6	6	6	6	3
	LL6 [incl. Lion Lake]	24	0	5	6	5	5	5	5	5	5	5	5	5	5	5	5	5	5	6	6	6	2.5
Reduction in	BL1	25	0	0	0	0	0	0	0	0	0	0	0	0	0	0	0	0	0	0	0	0	0
Groundwater Discharge To	BL2 [incl. Nico Lake]	26	0	43	60	39	39	38	37	40	40	40	42	41	41	40	39	35	35	36	36	36	20
Sub-Basin	BL3 [incl. Betty Ray Lake]	27	0	0	0	0	0	0	0	0	0	0	0	0	0	0	0	0	0	0	0	0	0
(m ³ /d)	BL4 [incl. Peanut Lake]	28	0	0	0	0	0	0	0	0	0	0	0	0	0	0	0	0	0	0	0	0	0
	BL5 [incl. Treasure Lake]	29	0	0	0	0	0	0	0	0	0	0	0	0	0	0	0	0	0	0	0	0	0
	BL6 [incl. Pond 8,9,10]	30	0	41	57	32	32	32	32	34	36	36	38	36	36	35	34	32	32	32	32	33	18
	BL7 [incl. Pond 13]	31	0	0	0	0	0	0	0	0	0	0	0	0	0	0	0	0	0	0	0	0	0
	BL8 [incl. Burke Lake]	32	0	0	0	0	0	0	0	0	0	0	0	0	0	0	0	0	0	0	0	0	0
	MR1 (Marian)	33	0	7	10	6	6	6	6	5	6	6	6	6	6	6	6	6	6	6	6	6	3





				Pre-Mine								Active Mining								Post- Closure			
		Row	Year 0	Year 1	Year 2	Year 3	Year 4	Year 5	Year 6	Year 7	Year 8	Year 9	Year 10	Year 11	Year 12	Year 13	Year 14	Year 15	Year 16	Year 17	Year 18	Year 19	Final Lake
Total Reduction	n (m3/d)	34	0	109	152	95	95	94	93	97	100	100	104	102	102	100	98	92	92	94	94	95	50
	LL2	35	426	426	426	426	426	426	426	426	426	426	426	426	426	426	426	426	426	426	426	426	426
	LL3	36	268	261	259	261	261	261	261	261	261	261	261	260	260	260	260	260	260	260	260	260	265
	LL4 [incl. Chalco Lake]	37	129	122	120	122	122	122	122	122	122	122	122	121	121	121	121	121	121	121	121	121	126
	LL5 [incl. Lou Lake]	38	1,154	1,140	1,135	1,141	1,141	1,141	1,141	1,141	1,141	1,141	1,141	1,140	1,140	1,140	1,140	1,140	1,140	1,140	1,140	1,140	1,148
	LL6 [incl. Lion Lake]	39	1,873	1,855	1,848	1,855	1,855	1,855	1,855	1,855	1,855	1,855	1,855	1,854	1,854	1,854	1,854	1,854	1,854	1,853	1,853	1,853	1,864
Cumulative	BL1	40	466	466	466	466	466	466	466	466	466	466	466	466	466	466	466	466	466	466	466	466	466
Groundwater Discharge To	BL2 [incl. Nico Lake]	41	638	595	578	599	599	600	601	598	598	598	596	597	597	598	599	603	603	602	602	602	618
Sub-Basins	BL3 [incl. Betty Ray Lake]	42	1,092	1,092	1,092	1,092	1,092	1,092	1,092	1,092	1,092	1,092	1,092	1,092	1,092	1,092	1,092	1,092	1,092	1,092	1,092	1,092	1,092
(m ³ /d)	BL4 [incl. Peanut Lake]	43	1,932	1,889	1,872	1,893	1,893	1,894	1,895	1,892	1,892	1,892	1,890	1,891	1,891	1,892	1,893	1,897	1,897	1,896	1,896	1,896	1,912
	BL5 [incl. Treasure Lake]	44	672	672	672	672	672	672	672	672	672	672	672	672	672	672	672	672	672	672	672	672	672
	BL6 [incl. Pond 8,9,10]	45	157	116	100	125	125	125	125	123	121	121	119	121	121	122	123	125	125	125	125	124	139
	BL7 [incl. Pond 13]	46	28	28	28	28	28	28	28	28	28	28	28	28	28	28	28	28	28	28	28	28	28
	BL8 [incl. Burke Lake]	47	3,093	3,009	2,976	3,022	3,022	3,023	3,024	3,019	3,017	3,017	3,013	3,016	3,016	3,018	3,020	3,026	3,026	3,025	3,025	3,024	3,055
	MR1 (Marian)	48	5,254	5,145	5,102	5,159	5,159	5,160	5,161	5,157	5,154	5,154	5,150	5,152	5,152	5,154	5,156	5,162	5,162	5,160	5,160	5,159	5,204
	LL2	49	0	0	0	0	0	0	0	0	0	0	0	0	0	0	0	0	0	0	0	0	0
	LL3	50	0	3	4	3	3	3	3	3	3	3	3	3	3	3	3	3	3	3	3	3	1
	LL4 [incl. Chalco Lake]	51	0	5	7	5	5	5	5	5	5	5	5	6	6	6	6	6	6	6	6	6	3
	LL5 [incl. Lou Lake]	52	0	1	2	1	1	1	1	1	1	1	1	1	1	1	1	1	1	1	1	1	1
% Reduction in	LL6 [incl. Lion Lake]	53	0	1	1	1	1	1	1	1	1	1	1	1	1	1	1	1	1	1	1	1	0
Groundwater	BL1	54	0	0	0	0	0	0	0	0	0	0	0	0	0	0	0	0	0	0	0	0	0
Discharge To Sub-Basin	BL2 [incl. Nico Lake]	55	0	7	9	6	6	6	6	6	6	6	7	6	6	6	6	5	5	6	6	6	3
Based on	BL3 [incl. Betty Ray Lake]	56	0	0	0	0	0	0	0	0	0	0	0	0	0	0	0	0	0	0	0	0	0
Cumulative	BL4 [incl. Peanut Lake]	57	0	2	3	2	2	2	2	2	2	2	2	2	2	2	2	2	2	2	2	2	1
Baseflows	BL5 [incl. Treasure Lake]	58	0	0	0	0	0	0	0	0	0	0	0	0	0	0	0	0	0	0	0	0	0
	BL6 [incl. Pond 8,9,10]	59	0	26	36	20	20	20	20	22	23	23	24	23	23	22	22	20	20	20	20	21	11
	BL7 [incl. Pond 13]	60	0	0	0	0	0	0	0	0	0	0	0	0	0	0	0	0	0	0	0	0	0
	BL8 [incl. Burke Lake]	61	0	3	4	2	2	2	2	2	2	2	3	2	2	2	2	2	2	2	2	2	1
	MR1 (Marian)	62	0	2	3	2	2	2	2	2	2	2	2	2	2	2	2	2	2	2	2	2	1

Table 11.I.6-2: Simulated Pre-Mine, Active Mining, and Post-Closure Groundwater Flow Budget (continued)

Notes: Refer to Figure 11.I-3 for location of sub-basins and direction of surface water flow through sub-basins.

Simulated sub-basin flows refer to groundwater discharge to surface waterbodies within the sub-basin ("baseflow").

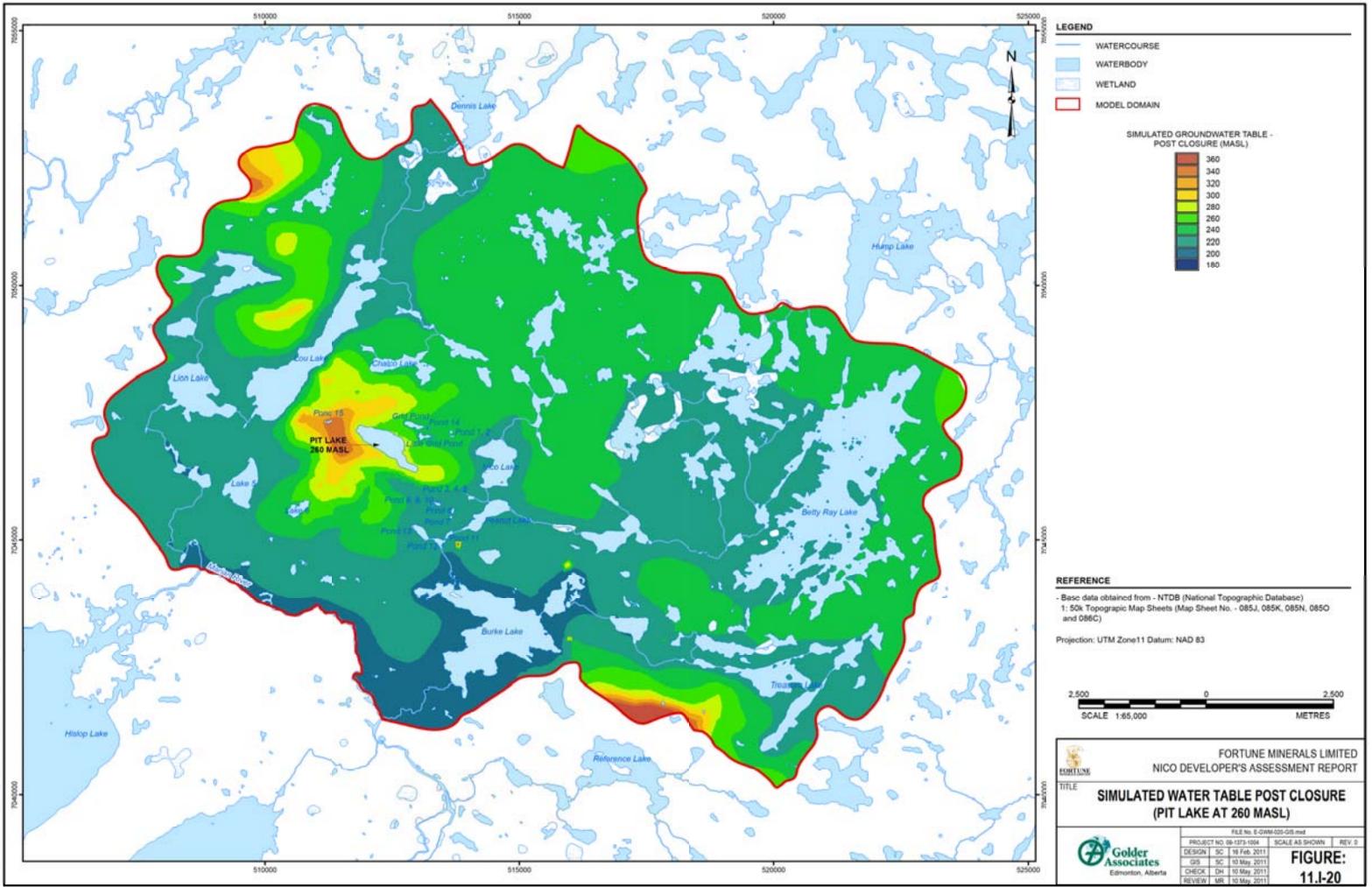
Only groundwater contributions are accounted for. Direct precipitation, interflow (water that enters the ground but does not reach the water table), runoff and upgradient surface water flow contributions not accounted for. Cumulative groundwater discharge summations recognize that many of the sub-basins are interconnected and provide baseflow from one to another. For example, sub-basin BL8 receives flow from BL1 through B7 (refer to Figure 3). Areal recharge pre-mine (30 mm/yr) no longer recharges the mine footprint (this water is removed as surface water); the table notes this flow component.

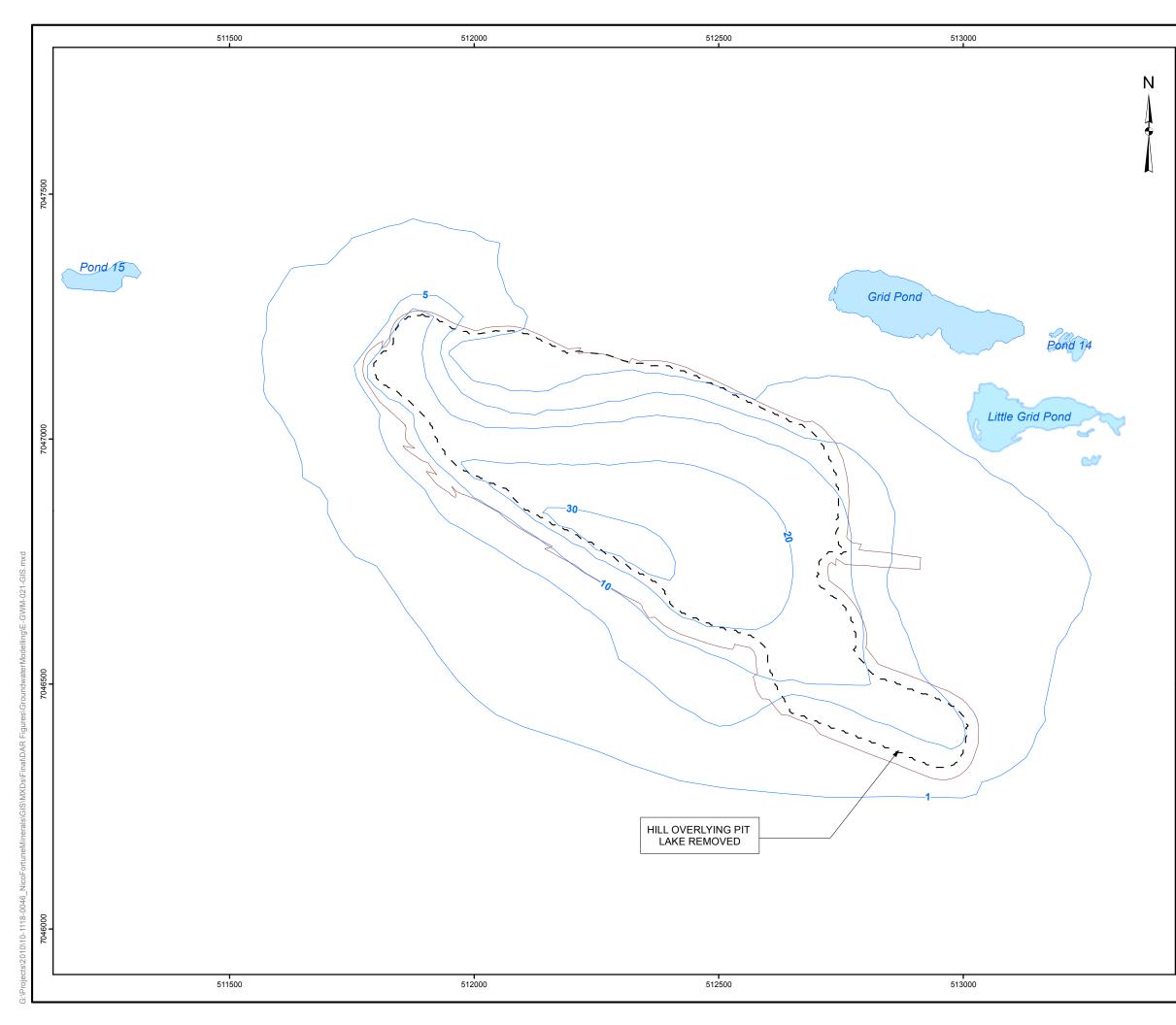
The subwatershed names "BL-" are not to be confused with the stream gauge IDs "B-". The two are unrelated in nomenclature.

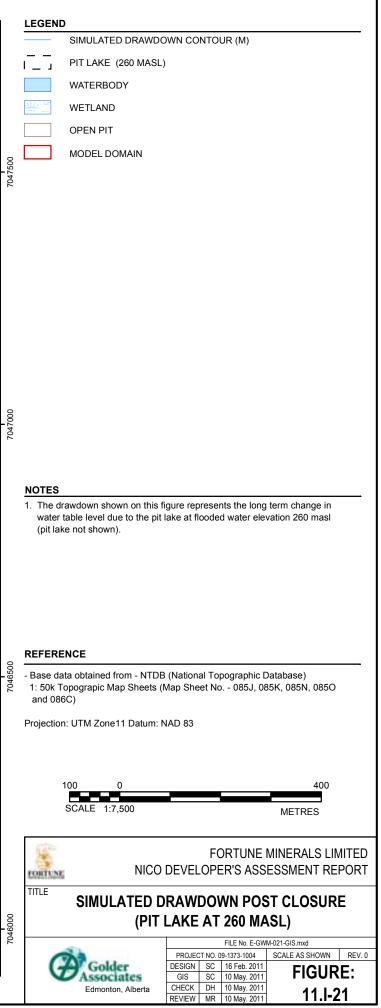
Only a partial subcatchment of the Marian River is simulated in the groundwater model. Total baseflow to the Marian watershed is higher than listed above.











11.I.7 ASSESSMENT OF DENSITY DEPENDENT FLOW AND POTENTIAL SALINE UPWELLING

Groundwater containing high concentrations of total dissolved solids (TDS) may affect the general onsite water distribution and usage, based on Golder's experience with large open-pit mines near the study area (Kuchling et al. 2000). The potential for the upwelling of deep seated brackish water can be a cause for concern with respect to water quality issues. Furthermore, TDS concentrations increase with depth such that adjustments to groundwater flow field calculations may be necessary to account for the density-dependent nature of high TDS groundwater encountered at depths occasionally reached by open-pit mines. To address these concerns, and their potential relevance to the proposed NICO Project, a 2D cross-sectional FEFLOW model was developed. The specific objectives of this aspect of the numerical modelling were as follows:

- evaluate the potential effects of density-dependent gradients on groundwater flow and mass loading at the site;
- provide an indication of potential TDS loadings to the Open Pit over the life of the mine;
- estimate the ultimate depth of groundwater capture into the Open Pit; and
- evaluate the behaviour of high TDS concentrations in groundwater following closure with respect to buoyancy issues (i.e., potential development of convection currents).

The 2D model is a derivative of the 3D model described previously in this appendix. However, it is a stand-alone model with its own particular specifics regarding construction, boundary conditions and parameterization. The approach to the 2D modelling, its construction and parameterization, and the findings of this assessment with respect to density dependent flow and the potential for saline upwelling are provided in the following sections.

11.I.7.1 Modelling Approach

A 2D cross-sectional ("cut-out") FEFLOW model was constructed from the 3D FEFLOW model described above. The approach of using a 2D cut-out model was selected to simplify and more efficiently demonstrate the determination of density effects and solute transport results.

The following modelling simulations were used to achieve the objectives listed above:

- Simulation 1 Density-dependent flow is neglected (non-DDF), and using the appropriate initial conditions (defined below), the model is run transiently for 19 years (expected mine life);
- Simulation 2 Density dependent flow (DDF) is applied, and using the appropriate initial conditions, the model is run transiently for 19 years; and
- Simulation 3 Using the density-dependent model results at a simulation time of 19 years (i.e., the expected mine life) as an initial condition, a new 1000-year simulation is completed where seepage into the Open Pit is discontinued, and the groundwater elevation rebounds to a "natural" level.

Comparison between Simulation 1 and Simulation 2 provides the basis for assessing whether or not densitydependent flow could be significant. The simulations are compared by evaluating the groundwater inflow, TDS loading to the Open Pit, and capture zone for each scenario. Simulations 1 and 2 also allow estimates of TDS loadings to the Open Pit from groundwater seepage over the life of the mine.





Using the results of Simulation 1 and 2, the depth of capture is compared by simulating groundwater flow particles around the perimeter of the Open Pit, backwards-tracking their position based on the groundwater gradients and noting the overall extent of their migration. The output of this simulation allows further evaluation of the potential for high-TDS water upwelling.

Evaluation of Simulation 3 provides the basis for determining whether or not buoyancy issues should be considered further (note that this simulation is not intended to simulate post-closure head conditions; this simulation is detailed in Section 11.1.6.5).

11.I.7.2 Model Assumptions

As the 2D model is derived from the 3D model described earlier, many of the assumptions for the 3D model also apply to the 2D cross-sectional model developed for this evaluation (see Table 11.I.4-1). Additional considerations include:

- The Open Pit is conservatively modelled at full development throughout the 19 year simulation period (represented by seepage nodes that lower the groundwater to the final Open Pit elevation at the beginning of the simulation).
- Underground workings were not considered in this assessment as their ultimate depth is similar to that of the ultimate Open Pit (85 to 95 masl).
- The water table was simplified to be 230 masl along the top of the model; except in areas of the mine, where the water table elevation follows the mine elevation. This consideration is described in more detail below.

11.I.7.3 Numerical Cross-Section Location and Mesh Geometry

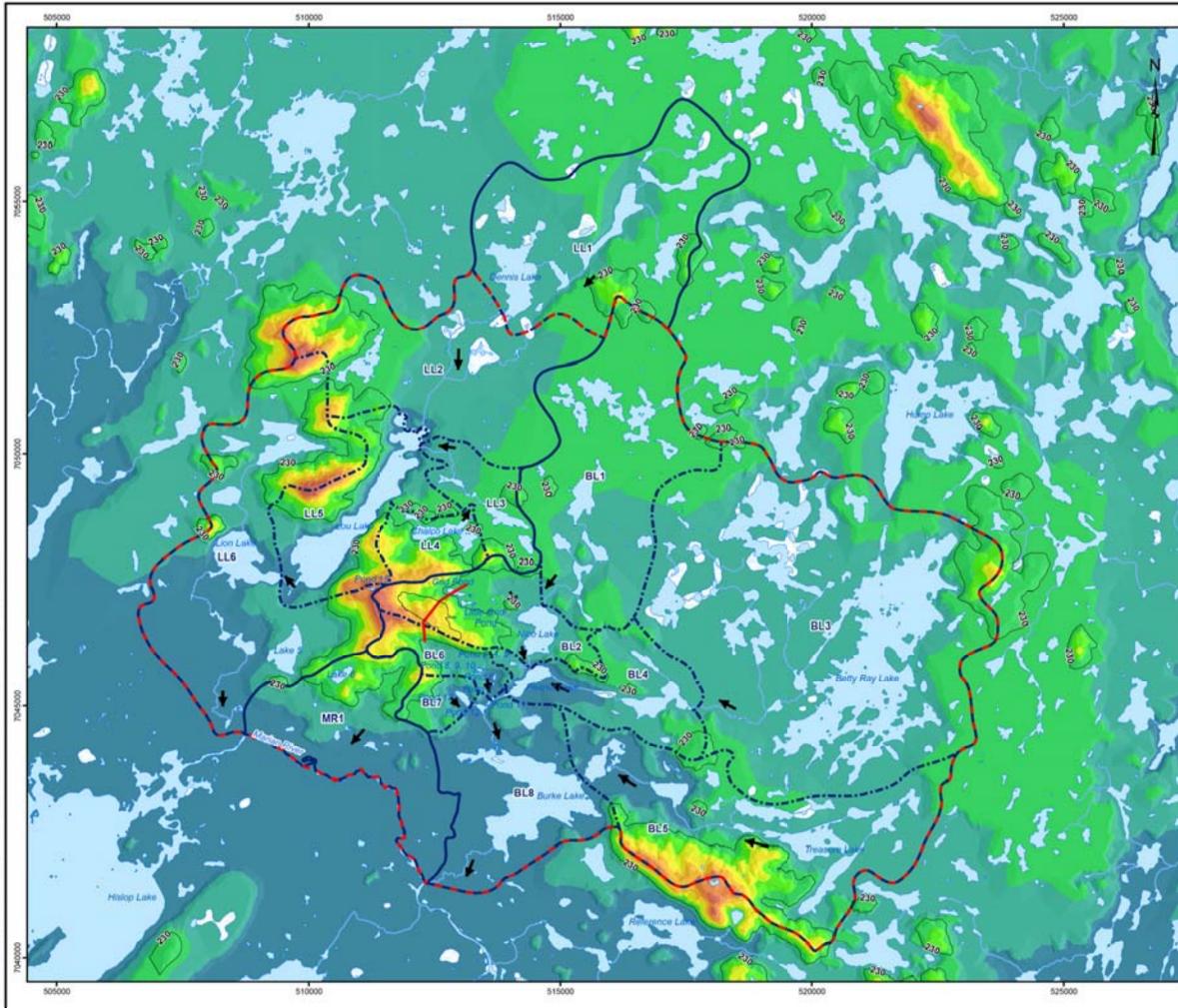
The location of the 2D section model with respect to the 3D model is illustrated on Figure 11.I-22. This location was selected to traverse the deepest area of the Open Pit and to be roughly parallel to the flow path at the end of mining. The ends of the section correspond to the 230 masl uplands versus lowlands demarcation.

The model mesh (see Figure 11.I-23) was constructed using FEFLOW, and extends from a high of 230 to 1000 mbsl. The length of the model is about 1520 m. In the area of the Open Pit, the top of the model ranges from 230 masl down to the Open Pit floor elevation of approximately 95 masl. The upper surface of the mesh is an approximation of the simulated groundwater table at end of mining in the 3D model. It is recognized that the water table is occasionally higher than 230 masl along the section. However, the application of a fixed water table at 230 masl in the model is conservative with respect to maximizing the potential for upwelling. Model layering defined in the 3D model was preserved internally within the 2D model so that material properties could be readily assigned to the appropriate zones.

The model elements vary in dimension from about 5 m around the Open Pit to 20 m at the boundary of the model. The 2D model is comprised of 19 052 triangular elements and 9779 nodes.







		D

_

-	WATERCOURSE

MAJOR DRAINAGE BOUNDARY

SUB-DRAINAGE BOUNDARY

CONTOUR - 230 MASL (DENOTES UPLANDS VS LOWLAND AREAS)

SURFACE WATER FLOW DIRECTION

WATERBODY

WETLAND

2D MODEL SECTION LOCATION

3D MODEL DOMAIN

OPEN PIT

ELEVATION (M)

100	360
100	340
	320
	300
	280
	260
	240
	220
	200
	180



65

EDRTUNE

Base data obtained from - NTDB (National Topographic Database)
 1: 50k Topograpic Map Sheets (Map Sheet No. - 085J, 085K, 085N, 085O
 and 086C)

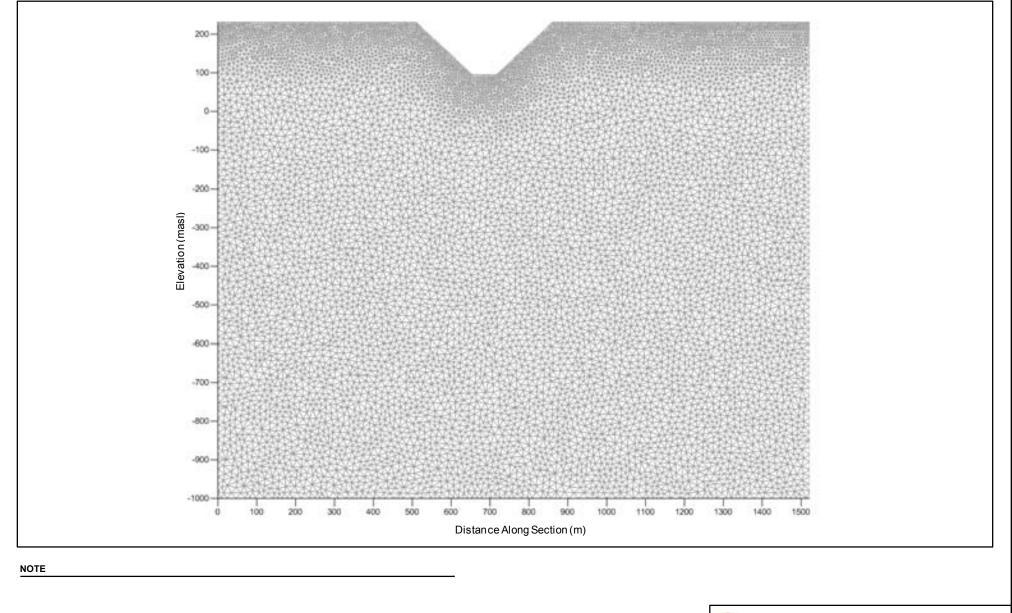
Projection: UTM Zone11 Datum: NAD 83



FORTUNE MINERALS LIMITED NICO DEVELOPER'S ASSESSMENT REPORT

2D SECTION MODEL LOCATION

Г				FILE No. E-OW	9-022-GIS mid	
0		PROJEC	T NO.	10-1373-1004	SCALE AS SHOWN	REV.0
	Golder	DESIGN	SC	16 Feb. 2011	FIGURE:	
	Associates	GS	SC	10 May 2011	FIGUR	C :
	Edmonton, Alberta	CHECK	DH	10 May 2011	11.1-22	
	22 ACC 12 (2012) 202	REVIEW	MR	10 May 2011	11.1-2	2





11.I.7.4 Material Properties

The material (flow) properties assigned to the 2D model are shown on Figure 11.I-24, and summarized further below:

- The model is comprised of the following layers (from shallowest to deepest): fractured rock, shallow rock, intermediate rock, and deep rock.
- The hydraulic conductivity, porosity and storativity assignments are the same as in the 3D model for each unit (see Section 11.I.4.6).
- For the simulations where density-dependent flow was considered, a density ratio of 0.0129 was specified throughout the model. This value was specified as zero for the simulations where density-dependent flow was neglected. The density ratio was determined by taking the difference between the maximum water density within the model domain (1012.89 kg/m³ at 1000 mbsl, and 16 252 mg/L TDS) and the freshwater density (1000.0 kg/m³), and dividing by the freshwater density.
- Longitudinal dispersivity was selected based on data from other sites presented by Shulz-Mackuch (2005). This paper presents field or laboratory derived longitudinal dispersivity versus scale of measurement for a variety of hydrogeologic settings. Based on the size of the model (roughly 1.5 km x 1.2 km), a longitudinal dispersivity of 10 was selected after review of comparable site data. The ratio of longitudinal to transverse dispersivity was assumed to be 10:1.

11.I.7.5 Boundary Conditions

May 2011

11.I.7.5.1 Flow Boundaries

The groundwater flow boundaries specified in the 2D model are illustrated on Figure 11.I-25. Two adaptations of the boundary conditions were specified for this modelling exercise: one set of boundaries was specified for simulations where density-dependent flow is neglected, and one set was specified where density dependent flow is considered.

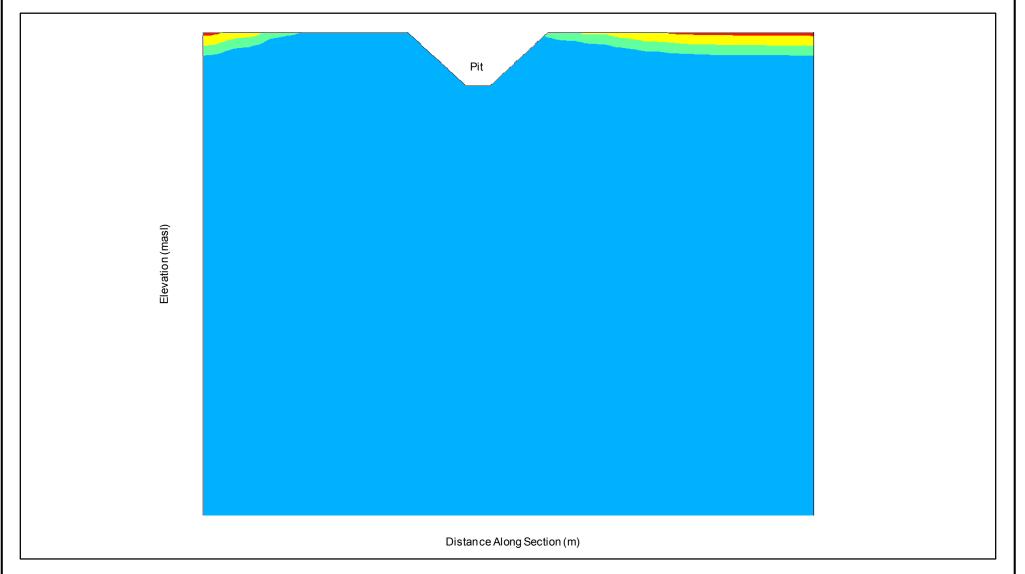
For the case where density-dependent flow is neglected (Simulation 1) the model flow boundaries consisted of constant head nodes at 230 masl along the entire model domain, except in the area of the Open Pit where seepage node boundaries equivalent to the Open Pit elevation are applied.

Where density-dependent flow is considered (Simulations 2 and 3) flow boundaries must account for the additional weight of dissolved solids in the groundwater, and are therefore specified in terms of their equivalent freshwater head. The equivalent freshwater heads are calculated based on the density ratio of groundwater containing a given concentration of dissolved solids to groundwater containing no dissolved solids. This results in an increase in head values with depth, with 230 masl specified at ground surface and approximately 233 masl specified at the base of the model (see Figure 11.I-26).

In Simulation 3 the Open Pit nodes are removed and groundwater is allowed to rebound to "pre-mine" levels. With respect to the 2D model, this is equivalent to 230 masl.

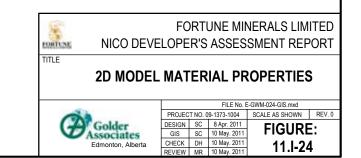


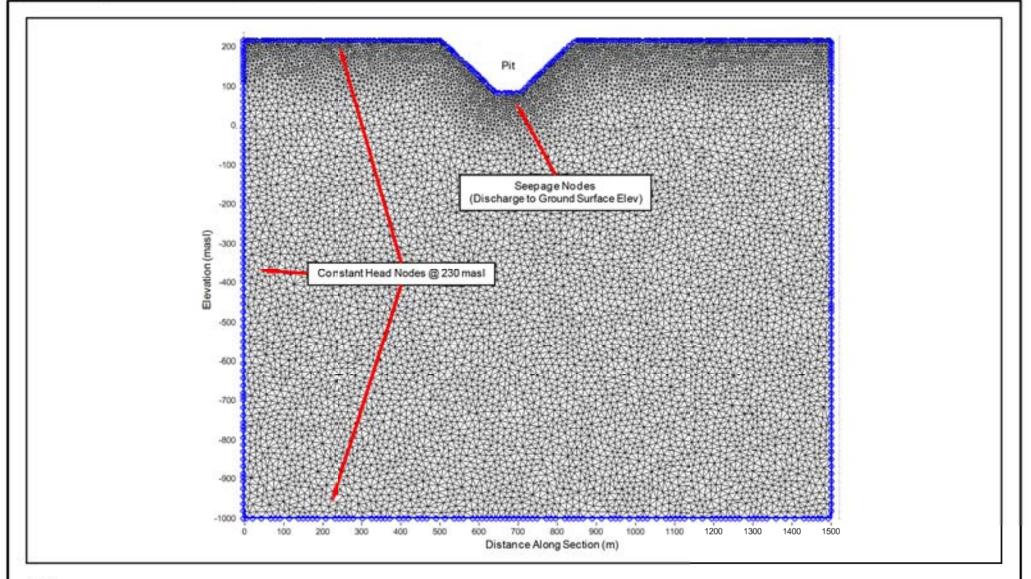




LEGEND

Unit	Description	K (m/s)	Porosity	Sy
	Fractured Rock	1E-06	2E-03	2E-03
	ShallowRock	7E-08	3.4E-04	3.4E-04
	Int. Rock	1E-08	3.4E-04	3.4E-04
	Deep Rock	1E-09	3.4E-04	3.4E-04

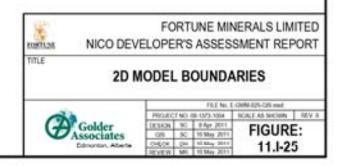


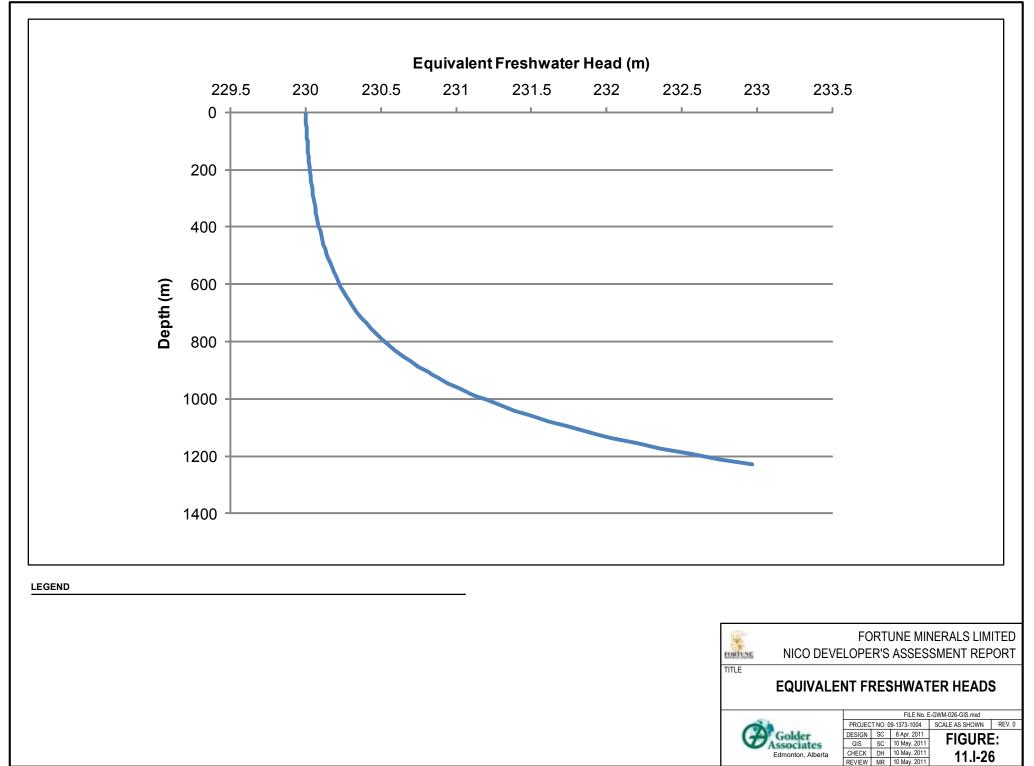


Constant head nodes are specified at 230 masl for the case where density effects are not considered. These boundaries are specified according to the curve in Figure 11.I- 26 for the case where density effects are considered;

The finite element mesh is shown in grey outlines;

The seepage nodes defining the pit range from 230 masl to 95 masl at the bottom of the pit.





11.I.7.5.2 Transport Boundaries

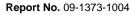
To establish the TDS versus depth profile for the NICO Project site, and thereby assign boundary conditions for the transport simulations, several relatively nearby (Diavik and Lupin sites) data sources were reviewed, as shown on Figure 11.I-27 and summarized below:

- The NICO Project site data was collected from wells 03-281, 03-282, 03-283, and 3 different depth intervals from 10-291. This data is relatively shallow compared to the overall vertical scale of the model and was therefore supplemented with additional deeper regional data datasets.
- Based on a review of the data presented in Kuchling et al., 2000, TDS versus depth data for the Diavik and Lupin mine sites were deemed a reasonable extension of the NICO Project site data at depth. These data (shown on Figure 11.I-27) were combined with the NICO Project data points to establish a TDS profile at depth for use in the model.
- Based on the combination of the NICO Project, Diavik, and Lupin data, a TDS versus depth curve and equation was developed. The equation of this curve is given by:

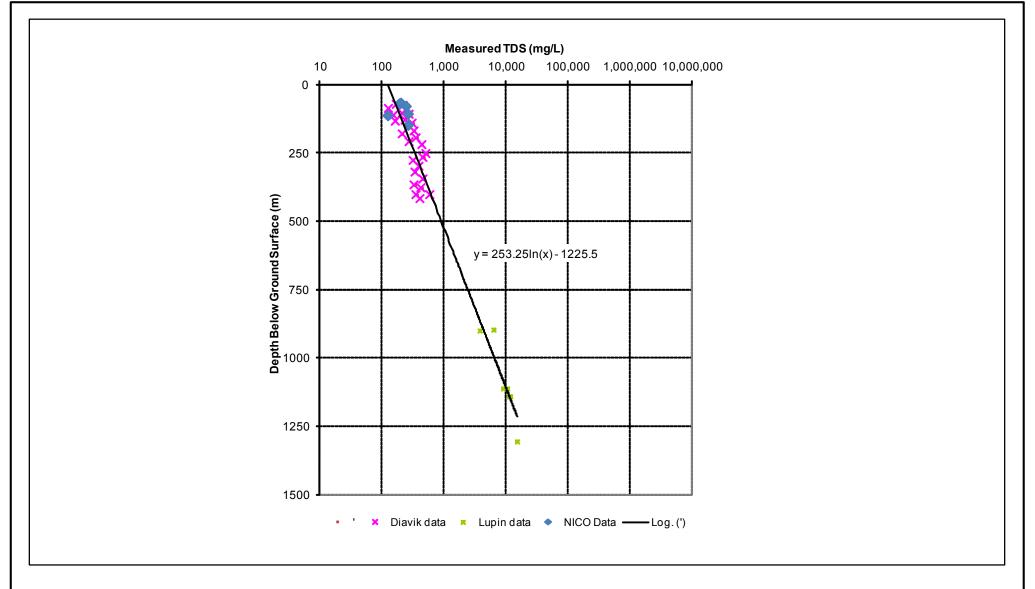
where Depth is depth below ground in metres and TDS is total dissolved solids concentration in mg/L.

Transport boundaries (see Figure 11.I-28) are specified within the model on a node-by-node basis using the equation above.





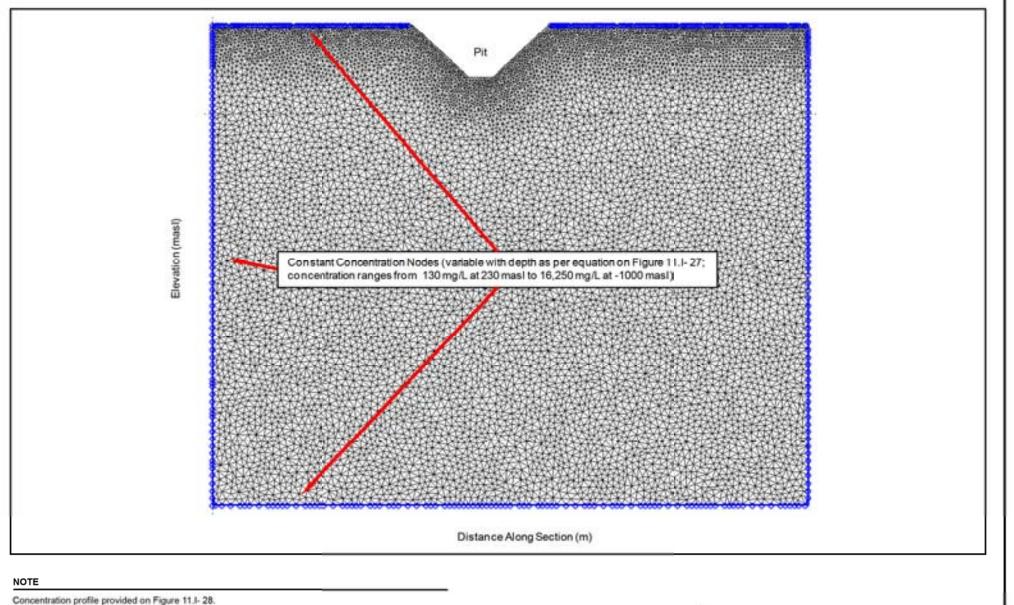






REFERENCE

Diavik and Lupin data taken from: Kuchling, K., Chorley, D., Zawadski, W. (2000). Hydrogeological Modeling of Mining Operations At The Diavik Diamonds Project. Proceedings of the Sixth International Symposium on Environmental Issues and Waste Management in Energy and Mineral Production, University of Calgary, Calgary, Alberta.



The finite element mesh is shown in grey outlines;



11.I.7.6 Initial Conditions

Initial groundwater elevation conditions are defined based on the groundwater flow boundaries described above. For the case where density-dependent flow is neglected, an initial groundwater elevation of 230 masl is specified over the model domain. For the case where density-dependent flow is considered the head profile with depth specified at each end of the model is extrapolated over the entire length of the model section and interpolated at each node to define the initial head condition.

In both cases the initial TDS concentration with depth is interpolated at each node using the TDS versus depth profile (Figure 11.I-27).

11.I.7.7 Model Results and Discussion

11.I.7.7.1 2D Model Heads

The groundwater heads for Simulation 1 (non-DDF) and Simulation 2 (DDF) are shown on Figure 11.I-29. In both simulations, the presence of the Open Pit causes a considerable upward gradient towards the Open Pit itself. The head profiles for both simulations are similar, particularly in the area around the Open Pit. Deeper in the model section the heads diverge slightly.

11.I.7.7.2 TDS Concentration of Groundwater Seepage Entering the Open Pit

The TDS concentrations for both Simulation 1 (non-DDF) and Simulation 2 (DDF) at the end of the 19 year simulation period are shown on Figure 11.I-30. The contour plots in the area of the Open Pit are approximately equivalent, otherwise there is a slight variance between the two results toward the bottom of the model.

The simulated average TDS concentration in groundwater entering the Open Pit over the life of mine for Simulation 1 and Simulation 2 are shown on Figure 11.I-31. The difference between non-DDF and DDF results are minor, generally varying only a few mg/L for a given time period. Note that these concentration curves are an average that divides the total mass loading into Open Pit (i.e., the product of the concentration and discharge at each node along the Open Pit face) by the total seepage. The concentration ranges from about 190 mg/L in Year 1 to 330 mg/L at Year 19. Note that these concentration estimates do not account for dilution from surface water sources also entering the Open Pit. That is, the concentration of TDS in water being pumped from the Open Pit for dewatering is expected to be lower than these estimates due to surface water collection.

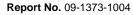
It is important to note that subsequent to Year 19, the mine will begin filling with water from surface water and groundwater seepage. This will reduce the upward hydraulic gradient from depth, as well as contribute dilution to the system. As such, the maximum TDS concentration of groundwater entering the Open Pit is expected to occur at the end of mining.

11.I.7.7.3 Open Pit Capture Zone

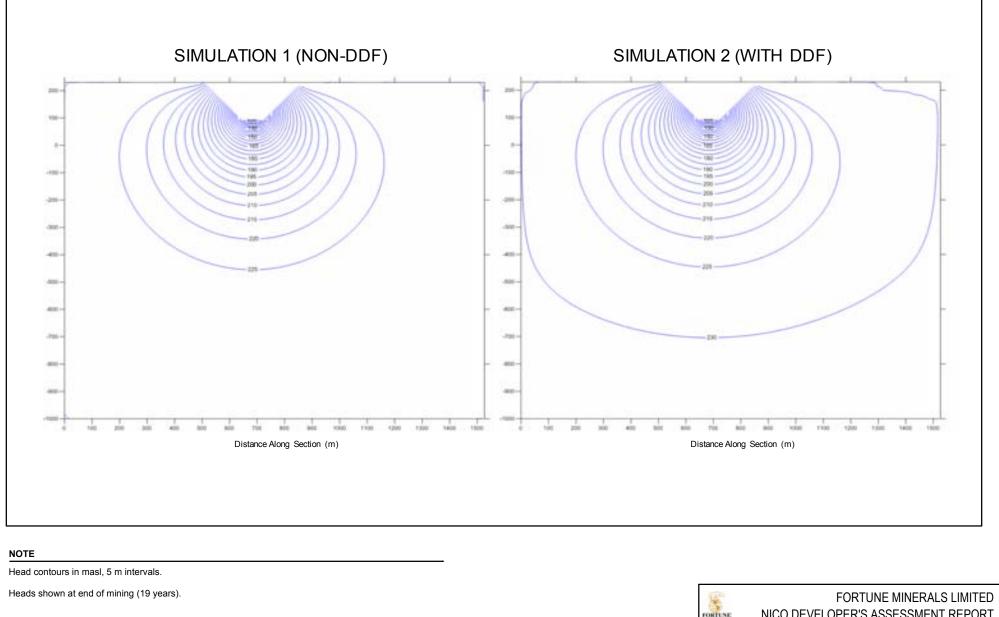
The Open Pit capture zone was derived using reverse particle tracking in FEFLOW. The Open Pit capture zones at end of mining for both Simulation 1 and Simulation 2 are illustrated on Figure 11.I-32. The 2 are practically identical. The capture zone is "bulb" shaped and reaches a maximum depth of 330 m below the bottom of the Open Pit (225 mbsl). At this depth of capture, the associated TDS is estimated to be approximately 760 mg/L according to TDS versus depth profile provide on Figure 11.I-27.

11.I.64

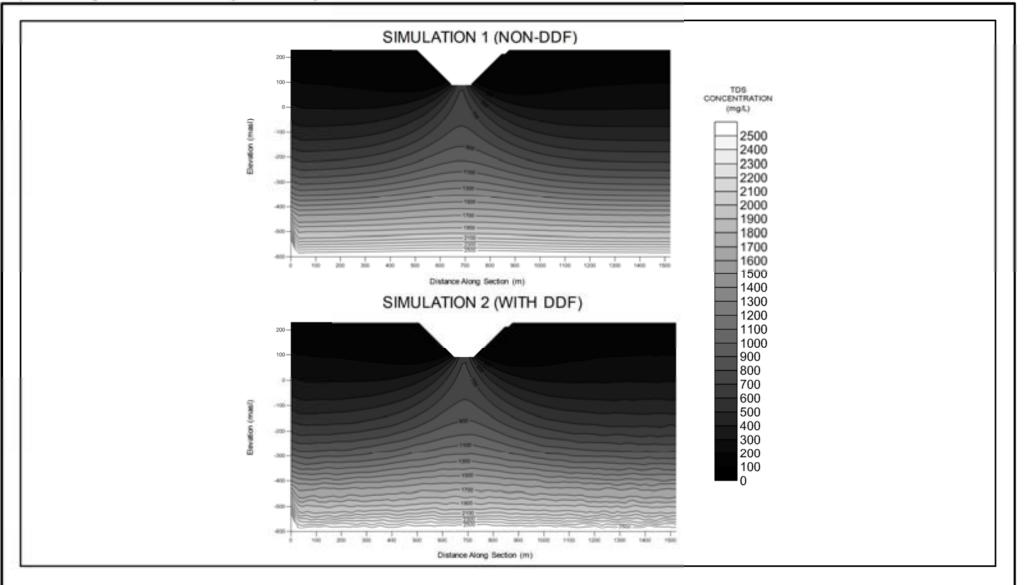








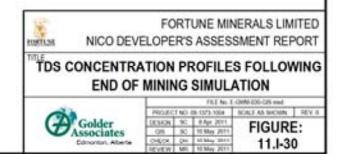


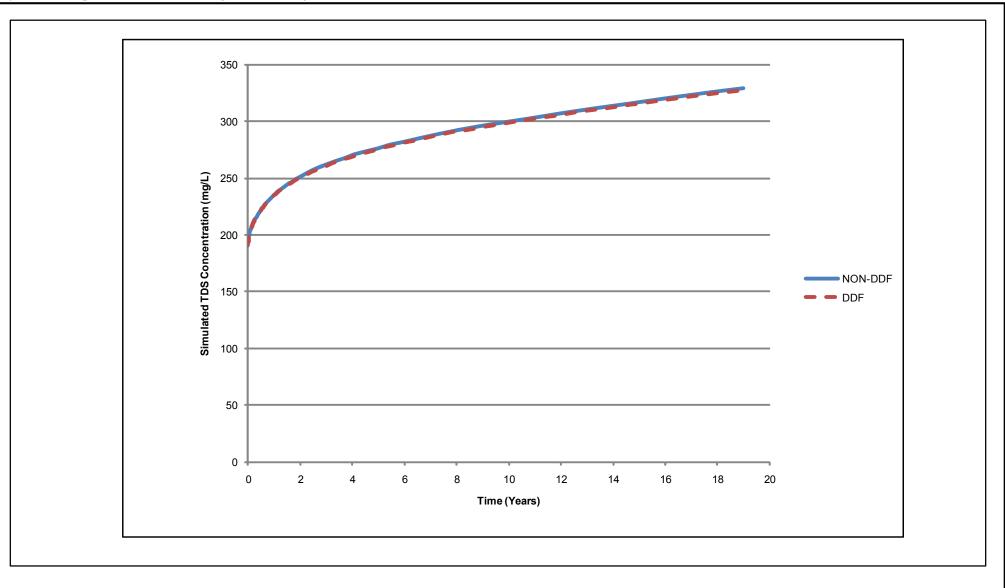


Concentration profiles are shown for the end of the 19-year transient simulations.

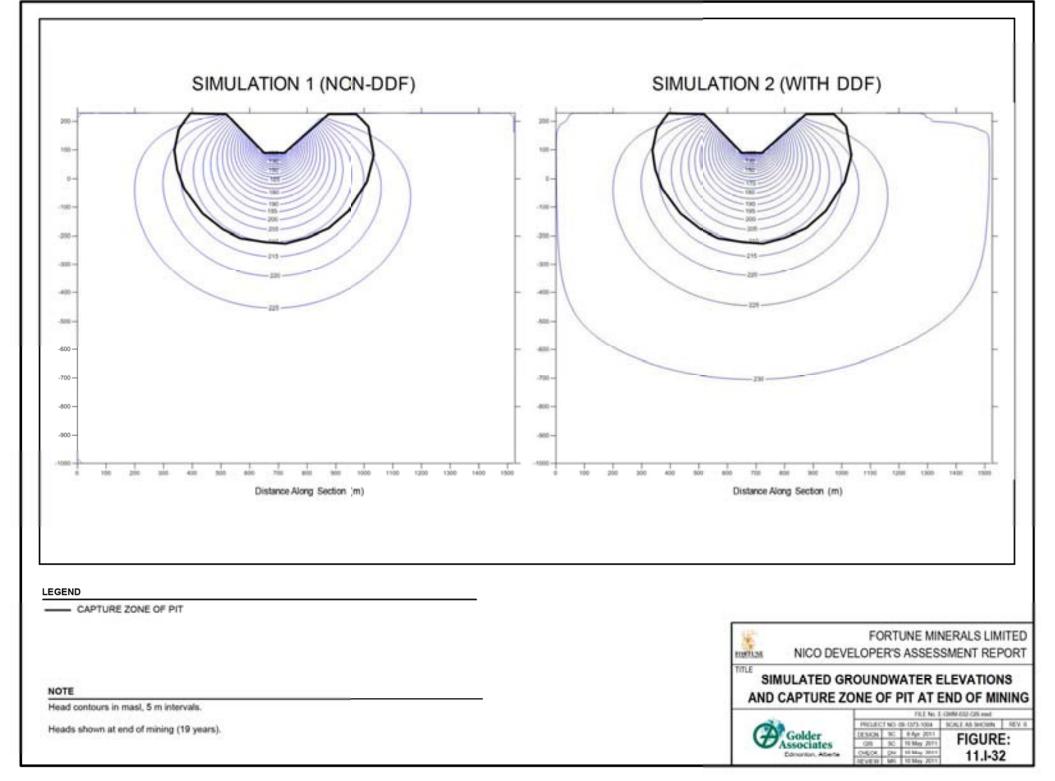
Sections only go to -600 masl, as the purpose of this Figure 11.I- is to illustrate TDS concentration profiles primarily around the pit and to compare the difference between DDF and non DDF.

Concentration contours are in 100 mg/L increments.









11.I.7.7.4 Density Dependent Flow versus Non-Density Dependent Flow

The results from the conceptual models for Simulation 1 and Simulation 2 (as illustrated on Figures 11.I-29 through 11.I-32) indicate that density dependent flow is not expected to be a significant factor in the simulation of groundwater flow and solute transport at the NICO Project site. This supports the assumption in the 3D analyses, where density effects are not included in the predictive numerical simulations using FEFLOW.

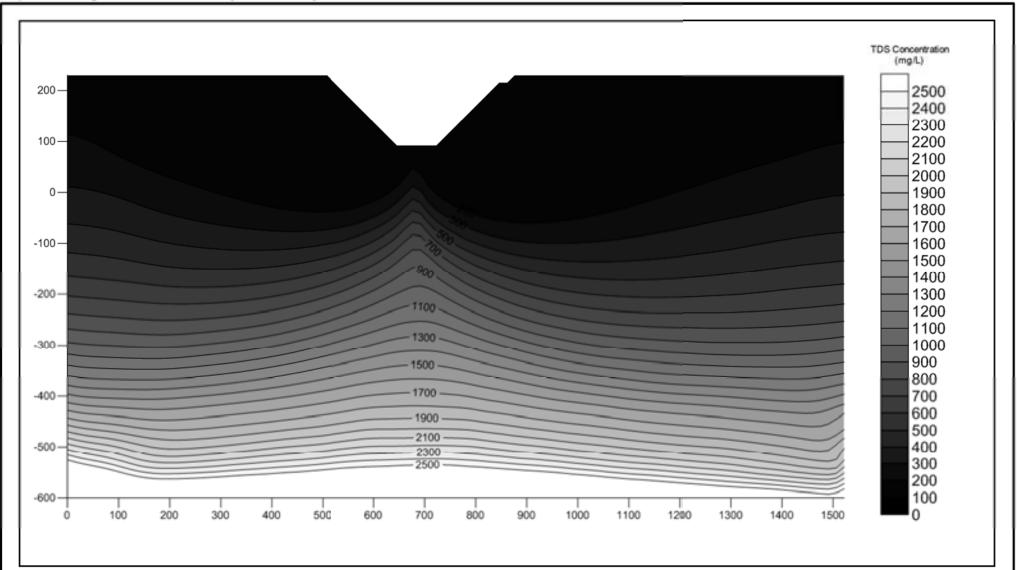
11.I.7.7.5 Potential Convection Currents

The groundwater TDS concentration contours following the end of Simulation 3, the 1000-year post mining run, are shown on Figure 11.I-33. Based on the concentration contours on Figure 11.I-32, the numerical modelling results suggest that convection currents (i.e., buoyancy effects) are unlikely to establish following closure of the mine. For reference, the simulated heads at the end of Simulation 3 are provided on Figure 11.I-34.



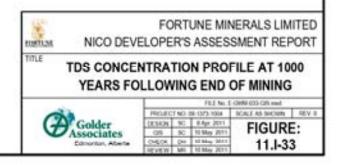




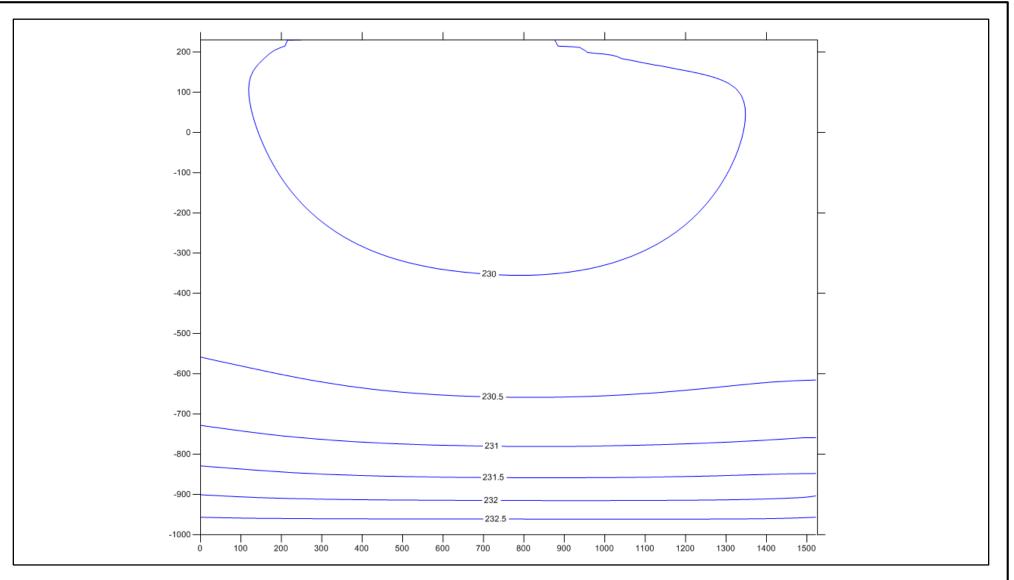


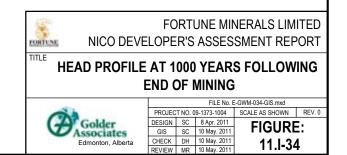
Sections only go to -600 masl, as the purpose of this figure is to illustrate TDS concentration around the pit.

Concentration contours are in 100 mg/L increments.









11.I.8 SUMMARY

Numerical groundwater modelling of the NICO Project site and regional surroundings was undertaken to estimate inflows to the NICO Project, assess potential drawdown and baseflow reduction of waterbodies to the hydrogeologic system, and evaluate the potential for saline upwelling into the mine.

A conceptual hydrogeological model was developed based on pre-existing data and reporting. The basic model conceptualization divides the study area into 2 basic regimes: 1) upland areas, and 2) lowland areas. The upland areas act as recharge zones and are comprised of fractured bedrock at surface and low permeability bedrock at depth. The lowland areas act as discharge zones and consist of silt till at surface overlying permafrost overlying low permeability bedrock at depth. The numerous lakes in the lowland areas act as discharge features, and due to thermal convection, prevent the formation of permafrost underneath them.

A 3D numerical FEFLOW model was constructed using the conceptual hydrogeological model as its framework. The numerical model utilized site and regional data to construct surfaces, apply model boundaries and input hydraulic parameters. The model was subsequently calibrated to measured water levels, surface water flows and observed tunnel inflows.

Predictive simulations were conducted to simulate the transient response of the hydrogeologic system to both underground and open pit mining throughout the 19 year operational life of the mine. The following summarizes the general findings of the predictive simulations:

- The maximum amount of groundwater seepage into the Open Pit simulated during mining is 130 m³/d. Direct precipitation on the Open Pit, overland flow and interflow (e.g., direct inputs from the freshet through local fractures in the vicinity of the workings and/or Open Pit) would be in addition to the above amount.
- The maximum drawdown simulated occurs at the end of mine life (19 years). At this time the Open Pit has reached its maximum dimensions. Vertically, the drawdown reaches 180 m in the central portion of the Open Pit. Laterally, the 1 m drawdown contour extends 100 to 510 m from the Open Pit.
- Potential baseflow loss for each sub-basin during active mining was evaluated. The largest cumulative decrease in baseflow occurs in sub-basin BL6, where a baseflow decrease of 20 to 36% is simulated. Sub-basins BL2 and LL4 have a maximum simulated cumulative baseflow loss of under 10%, while LL3, LL5, LL6, BL4, BL8, and Marian have a maximum cumulative loss of under 5%. The remaining sub-basins, LL2, BL1, BL3, and BL7 do not have any simulated baseflow loss.

In addition to the 3D model, a 2D cross-sectional model was developed to analyze issues related to saline upwelling to the mine. The following summarizes the general findings from the cross-sectional modelling:

- There was negligible difference in the results between a density-dependent flow simulation and one in which density effects were not considered. This supports the assumption in the 3D analyses, where density effects were not included in the predictive simulations.
- Average TDS concentration in groundwater entering the Open Pit were estimated to reach a maximum of 330 mg/L (the maximum loading occurs at the end of mine life).
- Convection currents are not expected post-mining.





11.I.9 REFERENCES

Diersch. 2002. WASY Software FEFLOW Reference Manual. WASY 2002.

Fortune (Fortune Minerals Limited). 2006. File: Basemapping (FML, 20060718).dwg (Eagle Mapping).

- Frape, S.K., and P. Fritz. 1987. Geochemical trends for groundwaters from the Canadian Shield; in Saline water and gasses in crystalline rocks. Editors: Fritz, P., and Frape, S.K.; Geological Association of Canada Special Paper 33, p.19 – 38.
- Freeze, R.A., and J.A. Cherry. 1979. Groundwater. Prentice-Hall Inc. Englewood Cliffs, New Jersey.
- Gascoyne, M. 2004. Hydrogeochemistry, groundwater ages and sources of salts in a granitic batholith on the Canadian Shield, southeastern Manitoba. Applied Geochemistry 19, p. 519 560.
- Golder (Golder Associates Ltd.). 2005. Factual Report On Geotechnical and Hydrogeological Investigations For The Proposed Open Pit And Underground Mine Workings, NICO Deposit, Northwest Territories. 03-1117-029. Submitted to Fortune Minerals Ltd. February 2005.
- Golder. 2006. Technical Memorandum on NICO Project bulk sample water balance. 05-1117-032. Submitted to Fortune Minerals Ltd. 23 February 2006.
- Golder. 2007a. Report on NICO tailings dams and process plant facilities 2006 geotechnical site investigation. 05-1117-032 (9100). Submitted to Fortune Minerals Ltd. 16 April 2007.
- Golder. 2007b. Final Summary Report on open pit, underground and mine waste, geotechnical engineering studies and environmental baseline data collection for NICO Project, Fortune Minerals, Northwest Territories. 05-1117-032. Submitted to Fortune Minerals Ltd. April 2007.
- Golder. 2008. Technical Memorandum Re: Monitoring Update August 2008, Thermistor Strings and Piezometers NICO Site, Northwest Territories. 05-1117-032. Submitted to Fortune Minerals Ltd. 17 October 2008.
- Golder. 2010a. Technical Memorandum Re: DOC 078 Groundwater Quality at the NICO Project Summary of Results of Groundwater Quality Monitoring Conducted in 2004 and 2009. 08-1118-0043 (4360). Submitted to Fortune Minerals Ltd. 8 February 2010.
- Golder. 2010b. Draft Report on Aquatic Baseline Report for the Proposed NICO Project. 08-1373-0011 .2000. Submitted to Fortune Minerals Ltd. September 2010.
- Golder. 2010c Technical Memorandum: Addendum, Preliminary Results of Pit Lake Water Quality Predictions (Scenarios 1 through 5). 10-1118-0046 (5400). Doc No. 119. Submitted to Fortune Minerals Ltd. 23 July 2010.
- Golder. 2010d. NICO Cobalt-Gold-Bismuth-Copper Project Canada, Factual Report On The Geotechnical Investigation for the Seepage Collection Pond and Polishing Pond Dams. Submitted to Fortune Minerals Ltd. 08-1118-0043 (3200). November 2010.
- Johnson, A.I. 1967. Specific yield compilation of specific yields for various materials. U.S. Geological Survey Water Supply Paper 1662-D. 74 p.





May 2011

Report No. 09-1373-1004

- Koshinsky, G.D. 1970. The Morphometry of Shield Lakes In Saskatchewan. Limnology and Oceanography, Vol. 15, Issue 5, p. 695-701.
- Kuchling, K., D. Chorley, and W. Zawadski. 2000. Hydrogeological Modeling of Mining Operations At The Diavik Diamonds Project. Proceedings of the Sixth International Symposium on Environmental Issues and Waste Management in Energy and Mineral Production, University of Calgary, Calgary, Alberta.
- Lim, D.H., and B. Dershowitz. 2010. Nico Derivation of Rock Mass Porosity from Packer Test on Fractured Rock. FracMan Technology Group (Golder Associates). 12 November 2010.
- Mackay, J.R. 1962. Pingos of the Pleistocene Mackenzie Delta Area. Geographic Bulletin, No. 18, p. 21-63.
- MVRB (Mackenzie Valley Review Board). 2009. Terms of Reference for the Environmental Assessment of Fortune Minerals Ltd. NICO Cobalt-Gold-Bismuth-Copper Project EA 0809-004. Yellowknife, NWT.
- Sharpe. 2010. Personal Communication, Chris Sharpe of P&E Mining Consultants Inc. to Devin Hannan of Golder (email). 26 August 2010 and 10 September 2010.
- Shepherd, R.G. 1989. Correlations of permeability and grain-size. Ground Water, Volume 27, Issue 5, p. 633–638.
- Shulz-Mackuch, D. 2005. Longitudinal Dispersivity Data and Implications for Scaling Behaviour. Ground Water, Vol. 43, No. 3, p 443 456.



